REGISTERED NO. M. 3121

PROCEEDINGS

OF THE

INDIAN ACADEMY

OF SCIENCES

VOL. XIII] *SECTION A* [NO. 5

MAY, 1941

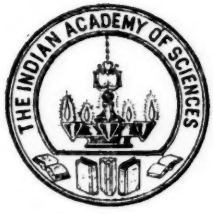

Price Rs. 2 or 3 Sh. *Annual Subscription Rs. 18*

PRINTED AT THE BANGALORE PRESS, BANGALORE CITY, BY G. SRINIVASA RAO, SUPERINTENDENT, AND PUBLISHED BY THE INDIAN ACADEMY OF SCIENCES, BANGALORE.

RECTIFICATION IN DISCHARGE TUBES—PART II

By V. T. Chiplonkar
(Department of Physics, Benares Hindu University)

Received December 14, 1940
(Communicated by Prof. Dr. R. K. Asundi)

§1. In continuation of the results reported in a previous paper[1] the following more detailed work was undertaken in order to find out the precise rôle of the electrodes, the interelectrode distance and their relative sizes, in determining the rectification effect observed. The experimental arrangement used in these investigations is the same as that described before, except for the discharge tube and the connections in its immediate neighbourhood. The discharge tube used is 3·0 cm. in diameter, 50·0 cm. in length and is provided with ground joints at both its ends, through which can be introduced the electrodes to be used. These are all of moulded aluminium, highly polished in order to eliminate secondary effects due to surface irregularities, in different sizes, with diameters 2·60, 1·80, 1·30 cm. We will designate these by the symbols E_1, E_2, E_3 respectively. The relative areas of the electrodes are $E_1/E_3 = 4·00$, $E_1/E_2 = 2·08$, $E_2/E_3 = 1·90$. For holding the electrodes in position in the centre of the discharge tube each electrode carries an aluminium rod, 10 cm. in length fixed in the centre of one of its faces. To this rod are attached two half sectors of brass (electroplated with nickel) having a diameter very nearly equal to the inner diameter of the discharge tube. These supports when they rest on the wall of the discharge tube hold the electrodes in the proper position. In order to avoid secondary effects due to the creeping of the discharge towards these supports a number of mica sheets are interposed between the electrode face and the brass support. This helps also to prevent to a great extent the passage of the discharge to the other face of the electrode, away from the discharge space. In the absence of the mica-sheets this is found to take place appreciably, especially for comparatively low pressures. Under the same conditions the discharge very often penetrates the interspace between the mica sheet and the glass wall of the discharge tube and reaches the aluminium rods supporting the electrodes. This is found to affect the rectification observed to a great extent. It is observed that the occurrence of this "creeping" is invariably accompanied by an enormous rise in the value of the rectified current. For preventing this effect, the aluminium rod is completely covered with a thin

glass tube. With these precautions the discharge occurs strictly between the exposed electrode faces. Sometimes however, in addition to a discharge glow on this exposed surface, a second glow is found hovering on the area of the curved surface which has got a width of about 0·7 cm. It has not been found possible to eliminate its occurrence which however fortunately is very infrequent being observed only in the case of very high pressures.

As in the case of the previous experiments, the evacuation obtains at one end of the discharge tube the gas being continuously streamed in from the other end. As the distance between the electrodes is varied during the course of the experiments, it is necessary to make proper arrangements to ensure that the pressure readings observed with the McLeod gauge are representative of the conditions obtaining in the discharge tube. To ensure this the McLeod gauge is connected to a point in the middle of the discharge tube, the positions of the electrodes being so adjusted that in every experiment this point is at the centre of the interelectrode distance. As it is found difficult to place both the electrodes in the required position, an arrangement is provided by means of which one of the electrodes can be moved from outside. For this purpose a piece of unspun silk is attached to the end of the aluminium rod supporting the electrode, the other being wound over the end of a ground joint, so that by rotating the ground joint the electrode can be moved back to occupy any position. The rest of the apparatus and the method of observation have already been described in detail. I will mention here, one or two points which were not described before.

§2. During this investigation the electrode with the larger area is connected to the earth through the milliammeters, the smaller one being connected to the H.T. This is done merely for ensuring uniformity in the experimental procedure. It is not unreasonable to expect that the rectification is affected to some extent by the surface charges developed by the wall of the discharge tube near the electrode connected to the H.T.; so that the rectification may be expected to be different depending on which of the electrodes is connected to the H.T. That the space charge on the walls of the discharge tube plays an important part in determining the rectification, is shown by the observation that the rectified current is affected enormously if one touches the walls of the discharge tube near the electrode connected to the H.T (the total current passing through the discharge tube remains constant). The same effect is observed if one touches the glass wall near the earthed electrode and it is remarkable that the change produced on touching, is in the same direction and sensibly of the same magnitude, as that obtained by touching the glass wall of the discharge tube near the other electrode. The order of magnitude of the change observed can be seen from

the following observation. When the rectified current is $-0{\cdot}1$ ma., on touching the glass wall of the tube near the earthed electrode the current rises to $-0{\cdot}2$ ma. The effect becomes more pronounced with lower pressures and higher voltages. In order to eliminate any doubt about the point mentioned above an actual experiment is performed in which the variation of the rectification (with pressure) is observed, first with the smaller electrode connected to the H.T. and then the larger one. The values of the rectification ratio observed under the two conditions are found to be equal in magnitude but opposite in sign showing the absence of any such effect. The rectified part of the current as will be shown in another section (§ 5) shows considerable variation with the time for which the discharge is passed. The nature of this variation is determined primarily by the pressure in the discharge tube. Accordingly, for some pressures the rectified part of the current remains unchanged while for others it either decreases or increases with the time for which the discharge is passed. It is of some importance, therefore, to ensure that in the actual method of observation these effects are eliminated as far as possible. It does not meet the difficulty if one takes the different observations after a constant time interval subsequent to initiating the discharge; the time rate of change in the three cases is widely different. The only course left is to reduce the time required for each individual observation to a minimum. With practice it is found possible to take observations within a time elapse of a few seconds. The values observed are confirmed by a number of repetitions and therefore are expected to give a fairly accurate index of the true conditions obtaining. The time for which the discharge is passed being extremely small, secondary effects due to thermal and other effects of the discharge may be said to have been automatically eliminated. Sometimes the rectified current does not show any steady value but oscillates rapidly between two well-defined limits (more often erratically than regularly), this is indicated by calling it unsteady and only the limits of oscillation are indicated in such cases. When the rectified current is stated to be positive, it means that the electrode connected to the H.T. is behaving as the anode and *vice versa*.

Observations are made on the variation of the rectification with pressure (both for low and high pressure range). The high pressure range includes pressures between $0{\cdot}1$ to $2{\cdot}1$ cm. and the low pressure range between $500\text{–}40 \times 10^{-4}$ cm. Hg (roughly) in the case of hydrogen for the following pairs of electrodes for three interelectrode distances $l = 5$, 10, 20 cm. (1) E_1E_2, (2) E_1E_3, (3) E_2E_3, (4) E_1E_2, (5) E_1E_1. In the case of air the rectification is studied for the same pressure range for the electrodes (1) E_1E_2 for $l = 20$ cm., (2) E_1E_3 for $l = 10$, 20 cm. For nitrogen it is studied for the electrodes E_1E_2 for $l = 10$, and 20 cm.

3. *Experimental Results*

(1) Electrodes E_1E_2 discharge in hydrogen

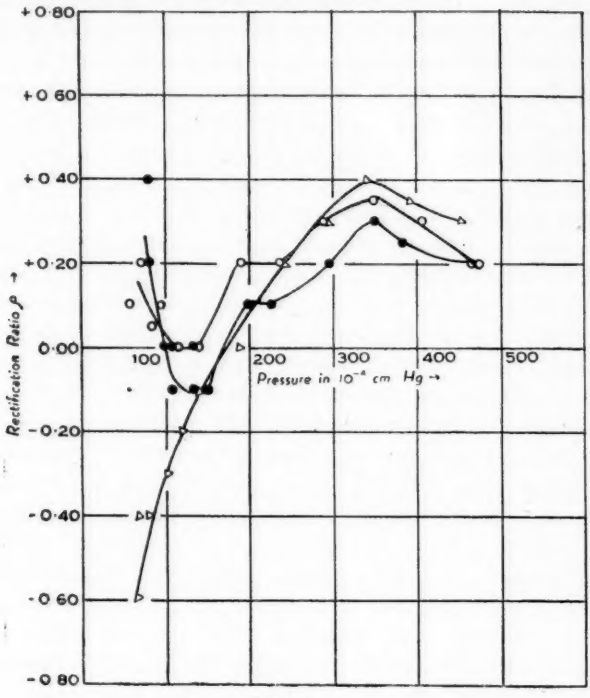

FIG. 1

Discharge in hydrogen Electrodes E_1E_2 $\sigma = 2{\cdot}08$

● $l = 20$ cm., ○ $l = 10$ cm., △ $l = 5$ cm.

Relative areas of the electrodes $\sigma = 2{\cdot}08$, $l = 5$, 10, 20 cm.

Referring to Fig. 1 we observe that generally speaking the rectification effects are more pronounced for small values of 1, the interelectrode distace than for large ones. The differences are however much smaller than might have been expected. The maximum value of ρ the rectification ratio is $+0{\cdot}40$ for $l = 5{\cdot}0$ cm., $+0{\cdot}35$ for $l = 10$ cm. and $+0{\cdot}30$ for $l = 20$ cm. The general shape of the curves for the three distances (for the low pressure stage) appear to be sensibly the same for pressures down to approximately 170×10^{-4} cm. The rectification starts with a low value for high pressures and increases more or less rapidly with decrease of pressure till it reaches a maximum. The position of the maximum in the three curves is the same at about 350×10^{-4} cm. Hg. After the maximum the curves run rather

differently from one another. The rectification ratio for $l = 5$ cm. reaches the value zero for a pressure of 180×10^{-4}, after changing sign it goes rapidly to the high value of $-0{\cdot}40$, on the negative side. As will be seen later this feature is found for all the different electrodes in the case of the curve obtained for $l = 5$ cm. In these cases the rectification always shows a final negative high value at the lowest pressures used. The curve for $l = 10$ cm. does not come on the negative side but rises rapidly after touching the zero-value at the pressure of 130×10^{-4} cm. to a second high value of $+0{\cdot}30$ at about the same pressure at which the curve for $l = 5{\cdot}0$ cm. reaches its negative high value, *viz.*, (80×10^{-4} cm.). The third curve for $l = 20$ cm. correctly reproduces the same course of changes as that obtained for the curve for $l = 10$ cm. with the exception that it goes down to $-0{\cdot}10$ on the negative side. For pressures below 100×10^{-4} cm. (approximately) the curve for $l = 5$ cm. shows a different behaviour from that obtained for $l = 10$ and 20 cm.

The curves obtained for the high pressure range appear to be far too complex for drawing any conclusions from them. This is partly due to the fact that the rectified current becomes unsteady over a considerable range of the pressures used in the case of all the different pairs of electrodes employed. In the majority of the cases there does not appear to be any correspondence between the curves obtained for the low pressure and the high pressure range.

(2) Electrodes E_1E_3 discharge in hydrogen

$\sigma = 4{\cdot}0$, $l = 5$, 10, 20 cm.

The courses of the three curves Fig. 2 are again essentially similar upto the point where they reach the maximum. The position of the maximum is slightly different in each of the three curves being 140×10^{-4} for $l = 20$, 155×10^{-4} for $l = 10$ and 190×10^{-4} for $l = 5$ cm. A rather weak secondary maximum is seen in the case of the curves for $l = 5$, 10 cm. in the neighbourhood of $290\text{–}300 \times 10^{-4}$ cm. Hg. The curve for $l = 5$ cm. shows as in the previous case a different behaviour than that shown by the others for very low pressures. It crosses the pressure axis at 50×10^{-4} cm. and goes on to the value of $-0{\cdot}40$ on the negative side. The other two curves do not reach a minimum (as obtained in the previous case) for the lowest pressures used. The maximum values for the rectification are $+0{\cdot}43$ for $l = 20$ cm., $+0{\cdot}52$ for $l = 10$ cm., $+0{\cdot}50$ for $l = 5$ cm. It will be noticed that the maximum value is greater for $l = 10$ cm. than for $l = 5$ cm. A similar result is obtained in the case of the electrodes E_2E_3.

(3) Electrodes E_2E_3 discharge in hydrogen.

$\sigma = 1{\cdot}90$, $l = 5$, 10, 20 cm.

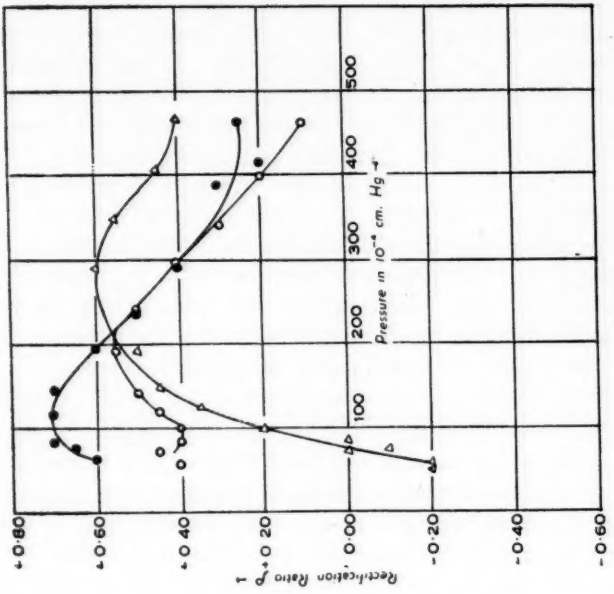

FIG. 3

Discharge in hydrogen Electrodes E_2 E_2 $\sigma = 1{\cdot}90$

● l = 20 cm., ○ l = 10 cm., △ l = 5 cm.

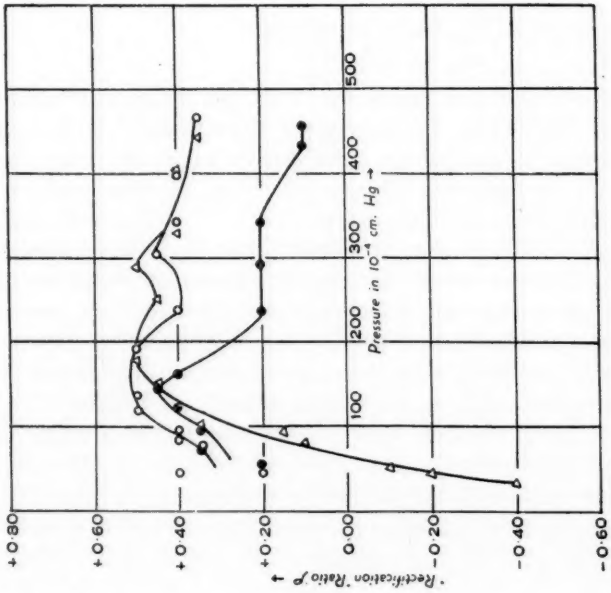

FIG. 2

Discharge in hydrogen Electrodes E_1E_3 $\sigma = 4{\cdot}00$

● l = 20 cm., ○ l = 10 cm., △ l = cm.,

The three curves now reach their maxima at three different pressures. The curve for $l = 5$ cm. reaches it at 280×10^{-4} cm., $l = 10$ cm. at about 200×10^{-4}, $l = 20$, at about 120×10^{-4} cm. It is remarkable that for pressures below 200×10^{-4} cm. the rectification is more pronounced for greater than for smaller values for l. The curves for $l = 10$ and 20 cm. do not come down to zero but at the smallest pressure used show values of $+0{\cdot}4$ and $+0{\cdot}6$. As in the previous two cases the curve for $l = 5$ cm. shows a different behaviour from that obtained for $l = 10$ cm. and 20 cm. It cuts the pressure axis at 90×10^{-4} cm. and reaches a value of $-0{\cdot}2$ on the negative side. The values of the maxima are $+0{\cdot}7$, $+0{\cdot}55$, $+0{\cdot}6$ for $l = 20$, 10 and 5 cm. respectively. For pressures above 200×10^{-4} however the rectification is more pronounced for small l than for large.

(4) Electrodes E_2E_2 discharge in hydrogen

$\sigma = 1{\cdot}00$, $l = 5$, 10, 20 cm.

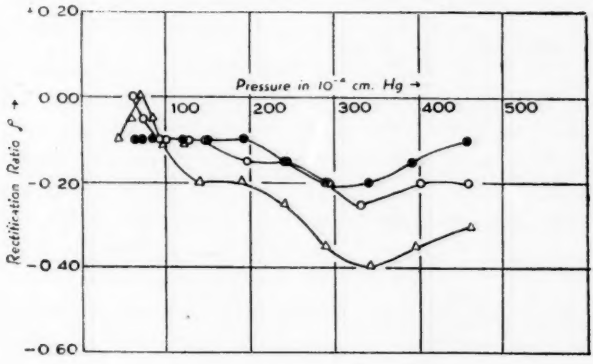

FIG. 4

Discharge in hydrogen Electrodes E_2E_2 $\sigma = 1{\cdot}00$

● $l = 20$ cm., ○ $l = 10$ cm., △ $l = 5$ cm.

All the curves (Fig. 4) show negative rectification. The rectification starts with a small value for higher pressures and reaches a maximum negative value at about 350×10^{-4} cm. in the case of all the three curves. For small pressures all the values tend to become zero. The values of the maxima are $-0{\cdot}4$, $-0{\cdot}24$, $-0{\cdot}20$ respectively for $l = 5$, 10, 20 cm. It will be noticed that all the three curves show a similar behaviour including the one obtained for $l = 5$ cm. for pressures upto 60×10^{-4} cm.

(5) Electrodes E_1E_1 discharge in hydrogen

$\sigma = 1{\cdot}00$, $l = 5$, 10, 20 cm.

The rectification starts with a small value for high pressures and reaches the maximum. The position of the maximum in the case of the three curves is however different. It is 200×10^{-4} for $l = 10$, and 20 cm. and 120×10^{-4} cm. for $l = 5$ cm. The value of the maximum in the three cases is the same, *viz.*, $-0{\cdot}20$. It is remarkable that the rectification for $l = 5$ cm. in the case of the identical electrodes E_1E_1 and E_2E_2 does not show any sensible difference from that obtained for $l = 10$, 20 cm. for pressures below say approximately 100×10^{-4} cm. Hg.

(6) Electrodes E_1E_1 discharge in air

$\sigma = 1{\cdot}00$; $l = 20$ cm.

Same general trend as in the previous case (5). There is a maximum of $-0{\cdot}20$ at 60×10^{-4} and afterwards a fall towards zero giving a value of $-0{\cdot}10$ for $p = 25 \times 10^{-4}$ cm.

(7) Electrodes E_1E_3, $l = 10$ cm.

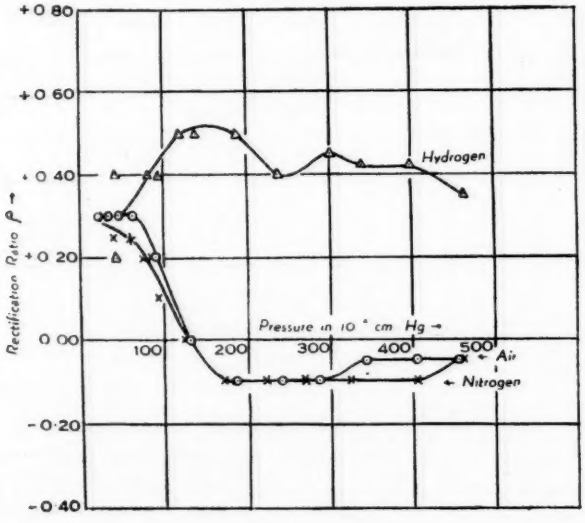

FIG. 5

Electrodes E_1E_3; $6 = 4{\cdot}00$, $l = 10$ cm.

⊙ Air, × Nitrogen △ Hydrogen

Discharge in air, hydrogen and nitrogen $\sigma = 4 \cdot 00$

Rectification in air and nitrogen (Fig. 4) is very much the same for the low pressure and the high pressure stage. The curves for air and nitrogen start with a value $-0 \cdot 04$ on the high pressure side and gradually approach the axis until they cross over at 120×10^{-4} cm. There is a rapid rise till they reach the maximum value of $+0 \cdot 3$ for pressures of about 50×10^{-4} cm.

Hydrogen on the other hand starts with a fairly high positive value on the high pressure side, rises to a somewhat low maximum at 155×10^{-4} cm. and then falls to $+0 \cdot 3$ for the lowest pressure used.

(8) Electrodes E_1E_3, $l = 20$ cm. $\sigma = 4 \cdot 00$

Discharge in air, nitrogen and hydrogen.

Rectification in air and nitrogen is again strikingly similar. It starts with a low value of $-0 \cdot 10$ on the high pressure side crosses the pressure axis at about 120×10^{-4} cm. and reaches the maximum value at 50×10^{-4} cm. at the same pressure for which a maximum was obtained in the previous case. The values of the maxima are different in this case being $+0 \cdot 40$ for nitrogen and $+0 \cdot 2$ for air.

Hydrogen shows an altogether different behaviour. It starts with the value $+0 \cdot 10$ reaches a weak maximum at about 350×10^{-4} cm. A very strong maximum is obtained further on at 130×10^{-4} cm. after which the curve falls down rapidly crossing the pressure axis at 60×10^{-4} cm. and reaches the value of only $0 \cdot 10$ cm. at 50×10^{-4}, the same pressure for which the two other curves reach their maxima on the other side of the axis.

4. Discussion

The experimental results bring out the strong dependence of the rectification on the pressure in the discharge tube. For a given gas and a pair of electrodes there exists a characteristic pressure for which the rectification is a maximum. For a given gas both the position and the value of the maximum depend on the ratio of the electrode areas, *viz.*, σ, and what appears to be less likely on the interelectrode distance as well. The evidence with regard to this latter point is somewhat conflicting as a glance at Table I will show. It appears to favour the view that the position of the maximum is independent of l rather than the opposite conclusion. The actual value of the maximum is in general greater for small than for large values of l.

TABLE I

Variation of the position and value of the maximum

Electrodes	Gas	l	Maximum value of ρ	Pressure for the max. value $\times 10^{-4}$
E_1E_2	Hydrogen	5	+0·40	350
		10	+0·35	350
		20	+0·30	350
E_1E_3	Hydrogen	5	+0·50	190
		10	+0·52	150
		20	+0·43	140
E_2E_3	Hydrogen	5	+0·60	280
		10	+0·55	190
		20	+0·71	120
E_2E_2	Hydrogen	5	−0·40	340
		10	−0·24	340
		15	−0·20	320
E_1E_3	Air	10	+0·30	62
		20	+0·20	60
E_1E_3	Nitrogen	10	Maximum not reached up to 25×10^{-4}	
		20	+0·40	63

There are however one or two exceptions to this deduction in the experimental values given in the Table II. There does not however appear to be much room for doubt for the validity of the above conclusion. For pressures higher than a certain value (the maximum itself in case, the three curves have a common maximum) the rectification shows a simple dependence on l; higher values of l correspond to lower values for the rectification ratio ρ. For pressures below this the above rule does not apply. It may happen sometimes that it is completely reversed. This is shown in the case of the electrodes E_2E_3 for the discharge in hydrogen for pressures below 200×10^{-4} cm. It has already been pointed out that the curve for $l=5$ cm. shows a characteristically different behaviour from those obtained for $l=10$, 20 cm., for pressures below a certain value in the case of the different pairs of electrodes. The value of this pressure lies roughly in the neighbourhood of 100×10^{-4} cm. For pressures above this the three curves

TABLE II

Variation of the rectification with the interelectrode distance l

Discharge in hydrogen

Pressure in 10^{-4} cm.	Rectification ratio ρ		
	$l = 5{\cdot}0$ cm.	$l = 10{\cdot}0$ cm.	$l = 20{\cdot}0$ cm.
Electrodes E_1E_2 ($\sigma = 2{\cdot}08$)			
100	$-0{\cdot}30$	$+0{\cdot}03$	$+0{\cdot}14$
200	$+0{\cdot}08$	$+0{\cdot}10$	$+0{\cdot}20$
300	$+0{\cdot}33$	$+0{\cdot}32$	$+0{\cdot}22$
400	$+0{\cdot}34$	$+0{\cdot}31$	$+0{\cdot}23$
Electrodes E_2E_3 ($\sigma = 1{\cdot}90$)			
100	$+0{\cdot}20$	$+0{\cdot}40$	$+0{\cdot}70$
200	$+0{\cdot}53$	$+0{\cdot}55$	$+0{\cdot}59$
300	$+0{\cdot}59$	$+0{\cdot}39$	$+0{\cdot}38$
400	$+0{\cdot}46$	$+0{\cdot}24$	$+0{\cdot}20$
Electrodes E_1E_2 ($\sigma = 4{\cdot}00$)			
100	$+0{\cdot}30$	$+0{\cdot}42$	$+0{\cdot}39$
200	$+0{\cdot}50$	$+0{\cdot}48$	$+0{\cdot}28$
300	$+0{\cdot}48$	$+0{\cdot}44$	$+0{\cdot}20$
400	$+0{\cdot}38$	$+0{\cdot}38$	$+0{\cdot}14$

for the different values of l have got the same general shape and nature. The curves obtained for $l = 10$ and 20 cm. retain this similarity even for pressure below this. There is some theoretical justification for the different behaviour exhibited by the curve obtained for $l = 5$ cm. It is known that in the case of a direct discharge, the condition of the discharge tube becomes sensitive when the interelectrode distance becomes very nearly equal to the length of the cathode dark space. It has been observed by Thomson[2] that in this state the discharge obtained sometimes becomes intermittent. It is particularly interesting to note here the remarks of Thomson that the current sent through the discharge tube when in this condition depends to a great

extent on the condition of the electrodes; even when they are made of the same metal and treated in the same manner the current for the same E.M.F. is different when A is the cathode and B the anode than when *vice versâ*. " It is generally possible," to quote Thomson, " to adjust the distance between the electrodes such that the current will pass in one direction but not in the other ". It is seen therefore that the rectification effects are expected to be pronounced when l becomes of the order of the length of the cathode dark space. The low pressures used in these experiments are such that the length of the cathode dark space would certainly have been equal to 5·0 cm. if not more, had the discharge been direct. The argument requires however, a certain modification on account of the fact that the voltage obtained across the discharge tube is not strictly direct. This probably is responsible for the observation that the critical pressure (100×10^{-4} cm. in the case considered here) is not as sharply defined in the case of the different pairs of electrodes as one would have expected. This is suggested by a visual observation of the discharge tube. Under most of the conditions here considered a dark space obtains at each of the electrodes. In cases where the electrodes are of different sizes these dark spaces are unequal in length. The condition of the discharge will become sensitive when the sum of the lengths of these dark spaces equals 5·0 cm. The relative lengths of the dark spaces will be determined by the relative sizes of the electrodes as well as the pressure in the discharge tube. It is understandable therefore, why the critical pressures are not the same for all the electrodes.

Visual observations reveal some interesting features about the formation and the development of the dark space between two identical electrodes. With electrodes E_2E_2 kept at a distance apart of 5·0 cm. the following course of changes are observed, in the case of a discharge in hydrogen. Starting with a high pressure of 500×10^{-4} cm., an intense discharge glow covers both the electrodes. With diminution in pressure, a dark space is formed at each of the electrodes. The lengths of the two dark spaces are identical. Each of these increases equally, with decrease in the pressure. The two dark spaces continue to approach each other till they meet at a pressure of 141×10^{-4} cm. The rectification begins to show a rapid fall in value from this point. For further decrease in the pressure, a dark space is seen to form in the middle of the discharge space, where the two previous dark spaces had met and coalesced. This second dark space widens from the centre equally on both sides for lower pressures. It is difficult to follow the course of the changes beyond this as the intensity of the light given out from the discharge space becomes very faint. The origin or the nature of this second dark space does not appear to be clear. Ordinarily speaking we

should have expected a high value for the rectification for pressures in the neighbourhood of 140×10^{-4}. The existence of this second dark space probably introduces complications. It has not been found possible to observe whether a similar phenomenon occurs in the case of electrodes unequal in area, on account of the very weak intensity of the discharge glow at the pressures involved.

The rectification is determined (as has already been mentioned) to a very great extent by the pressure in the discharge tube. The variation of the rectification with σ the ratio of the areas of the electrodes, will therefore be determined by the pressure at which the observations are made. Thus we cannot always expect the rectification to be greater for greater values for σ. For a given pressure the rectification in the case of a discharge tube with identical electrodes may actually be greater than that obtained for the highest value of σ (in these experiments 4·0). Table III illustrates this state-

TABLE III

Variation of the rectification with the relative sizes of the electrodes, σ

Pressure in 10^{-4} cm. Hg.	Rectification for the electrodes				
	E_1E_1 $\sigma = 1{\cdot}00$	E_2E_2 $\sigma = 1{\cdot}00$	E_2E_3 $\sigma = 1{\cdot}90$	E_1E_2 $\sigma = 2{\cdot}80$	E_1E_3 $\sigma = 4{\cdot}0$
l = 20 cm. discharge in hydrogen					
100	−0·20	−0·10	+0·70	0·00	+0·30
200	−0·20	−0·10	+0·60	+0·10	+0·28
300	−0·10	−0·20	+0·40	+0·20	+0·20
400	−0·06	−0·15	+0·20	+0·26	+0·14
l = 10 cm. discharge in hydrogen					
100	−0·20	−0·08	+0·40	+0·03	+0·44
200	−0·20	−0·16	+0·54	+0·20	+0·47
300	−0·19	−0·22	+0·38	+0·30	+0·42
400	−0·16	−0·20	+0·20	+0·30	+0·40
l = 5 cm. discharge in hydrogen					
100	−0·20	−0·10	+0·20	−0·30	+0·38
200	−0·12	−0·20	+0·56	+0·06	+0·28
300	−0·10	−0·36	+0·58	+0·30	+0·20
400	−0·06	−0·36	+0·45	+0·34	+0·14

ment. Here values of the rectification are collected, obtained for the same value of l and p (the pressure) but different values of σ. It will be seen that only in one case (*i.e.*, for $l = 10$ cm.) for pressure of about 400×10^{-4} cm. or more does ρ show a simple dependence on σ. For these pressures higher values of σ lead to higher values for ρ. It will be observed that the values for the rectification obtained in the case of the identical electrodes E_1E_1 and E_2E_2 are somewhat different. The divergences are not very appreciable for $l = 10$, 20 cm. but are rather marked in the case of $l = 5$ cm. This observation seems to indicate that the rectification is influenced to a certain extent by the absolute area of the electrode especially for small values of l. This probably can be explained in terms of the phenomenon of localisation[3] at high pressures the discharge makes use of the total area of the electrode whereas at low pressures such is not the case. Accordingly the area of the electrode would matter at high rather than at low pressures and the divergences would therefore be more marked under these conditions. This point however, requires further investigation.

The results obtained for hydrogen, air and nitrogen show that the rectification depends to a very great extent on the nature of the gas in the discharge tube. There is a great difference in the curves obtained for air (or nitrogen) and hydrogen, on the other hand the curves for air and nitrogen are similar.

5. Variation of the rectification with time

Fig. 5 gives the variation of the rectified part of the current with time for which the discharge is passed, in some typical cases. The observations are made in the case of the electrodes E_1E_3 for $l = 5{\cdot}0$ cm. the gas in the discharge tube being hydrogen. As has been mentioned already there are three stages of pressures for which the rectification ratio behaves differently. The first range of pressure extends from the highest pressure used (which is about 470×10^{-4}) to the point where the rectification reaches a maximum (in this case at 130×10^{-4} cm.). For this range the rectification is slowly but continuously increasing in value with diminution in pressure. The rectification is independent of the time for which the discharge is passed when the pressure in the discharge tube lies within this range. The second range comprises the pressures lying between the maximum and the point where the rectification becomes zero. For this range the rectification is extremely sensitive to the pressure and falls continuously and steeply in value with decrease in pressure. In this particular case the pressure extends from 130 to 60×10^{-4} cm. The rectification for this range of pressure falls rapidly with time. This effect cannot be explained in terms of a pressure-rise in the discharge tube on account of the heating of the tube due to the passage

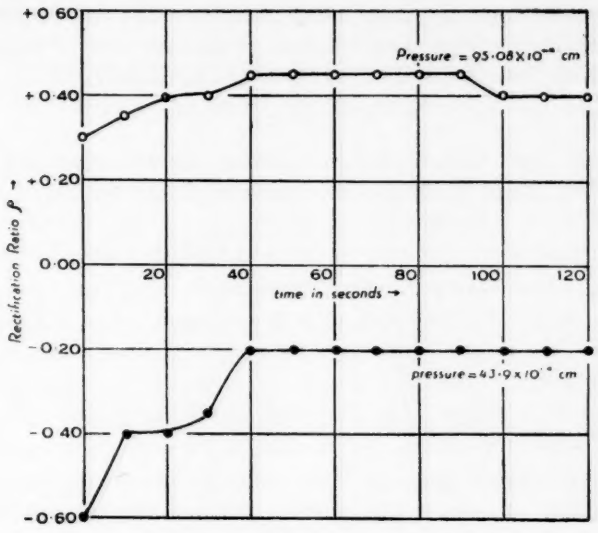

FIG. 6

Discharge in hydrogen Electrodes E_1 E_3 $\sigma = 4{\cdot}00$

$l = 5$ cm.

of the discharge. An increase in pressure as will be seen from Fig. 2 would have taken the rectified current back along the curve to a higher value. The observed finding is exactly opposite of this. Further the rectified current does not continuously decrease with time but attains a steady value after the lapse of a few minutes (ref. Fig. 5) which will not be easily explained on the basis of the above hypothesis. The third range of pressures extends from the point where the rectification curve cuts the pressure axis, down to the lowest pressures used. The rectification continuously increases in value for this range of pressures. In the particular case here considered its limits are 60 and 40×10^{-4} cm. The rectification increases in value with the time for which the discharge is passed when the pressure is within this range. As in the previous case the current reaches a steady stationary value after the lapse of a few minutes. Both these observations could be explained if we could think of any process which will reduce the pressure in the discharge tube, in a roughly exponential manner with the time for which the discharge is passed. These observations lead to a rough but quick method for finding out on which part of the characteristic of the rectification-pressure curve a given discharge tube lies at a certain pressure.

In the end I offer my grateful thanks to Prof. Dr. S. S. Joshi for giving me the facilities for work and constant encouragement. I am indebted to Prof. Dr. R. K. Asundi for advice and useful discussions.

Summary

Using the same method of observation as reported previously a detailed study has been made of the pressure variation of the rectification ratio ρ, in discharge tubes, as a function of the relative sizes of the electrodes σ, and the interelectrode distance l in the case of air, hydrogen and nitrogen.

(1) For a given gas and a pair of electrodes there exists a characteristic pressure for which the rectification is a maximum. For a given gas both the position and value of the maximum show a clear dependence on σ. Variation of l appreciably affects only the value of the maximum rectification but not its position. The maximum rectification is in general greater for smaller values of l.

(2) For pressures higher than the value for which the maximum rectification is obtained, ρ shows in general, a simple dependence on l, higher values of l corresponding to lower values for ρ. For lower pressures the above rule does not apply; it may happen sometimes that it is completely reversed. The variation of ρ with σ on the other hand is very complex and does not permit of any generalisation.

(3) The rectification obtained for values of l comparable with the length of the cathode dark space, shows a characteristically different behaviour at low pressures ($\sim 100 \times 10^{-4}$ cm. Hg.) from that obtained for higher values of l.

(4) The results obtained for hydrogen, air and nitrogen show that ρ is determined to a great extent by the nature of the gas in the discharge tube. There is great difference in the curves obtained for air and hydrogen; on the other hand the curves for air and nitrogen are similar.

REFERENCES

1. V. T. Chiplonkar .. *Proc. Ind. Acad. Sci.*, 1939, **10**, 381.
2. J. J. Thomson .. *Phil. Mag.*, 1939, **27**, 29.
3. V. T. Chiplonkar .. *Proc. Ind. Acad. Sci.*, 1940, **12**, 440.

THE INTENSITIES OF THE RAMAN LINES IN CARBON DIOXIDE

By N. S. Nagendra Nath and E. V. Chalam
(From the Department of Physics, Andhra University, Waltair)

Received January 24, 1941

§ 1. Introduction

It is well known that the Raman spectrum of carbon dioxide consists of two strong lines with frequency shifts 1285 cm.$^{-1}$ and 1388 cm.$^{-1}$. The linear symmetrical model of CO_2 has four normal vibrations, one of them being the symmetrical motion of the oxygen atoms along the axis of the molecule with the carbon atom at rest, two others being the doubly degenerate vibration of the carbon atom against the oxygen atoms in a plane perpendicular to the axis of the molecule and the remaining other being the vibration of the carbon atom against the oxygen atoms along the axis of the molecule. Fig. 1 illustrates the normal modes of vibration.

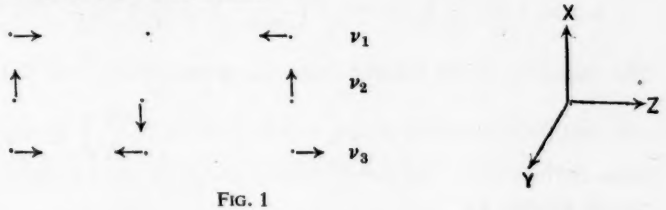

Fig. 1

Amongst the fundamental frequencies only ν_1 is active in the Raman effect, and only ν_2 and ν_3 are active in the infra-red. A simple consideration of the polarisability tensor when the molecule is vibrating with frequency ν_2 or ν_3 shows that their even harmonics only could appear in the Raman effect. Hence in addition to the fundamental frequency ν_1, we could expect $2\nu_1$, $2\nu_3$ and $2\nu_2$ to appear in the Raman spectrum. It may be remarked that the intensity of the former two overtones is mainly governed by the second differential co-efficient of the polarisability of the C–O bond with respect to the internuclear distance. As these overtones have not been reported so far in the experimental literature, we could assume that the higher derivatives of the polarisability of the C–O bond with respect to the internuclear distance are so small as not to give observable effects. But this argument does not apply to $2\nu_2$. The intensity of this line is governed by the

optical anisotropy of the molecule in the equilibrium configuration and the first derivative of the polarisability of the C–O bond with respect to the internuclear distance. To understand this clearly let us for a moment assume that the polarisabilities of the C–O bonds do not change with respect to the internuclear distance. In such a case no Raman lines will appear except those corresponding to the even harmonics of ν_2 because in the vibration ν_2, the optical anisotropy changes while it does not in the vibrations ν_2 and ν_3. Next, we can also understand the dependence of the intensity of $2\,\nu_2$ on the first differential co-efficient of the polarisability of the C–O bond with respect to the internuclear distance even without the second order coefficients. In the vibration ν_2, the change in the inter-nuclear distance of the C–O bonds is proportional to the square of the distance of the carbon atom from the line joining the oxygens, which distance corresponds to the normal co-ordinate ν_2. Hence, even though the polarisability of the C–O bonds varies linearly as a function of the bond length, it will contribute a second order polarisability in the vibration ν_2.

More generally, the polarisability tensor of a molecule as a function of the normal co-ordinates can be written as

$$a = a_0 + \sum_i \left(\frac{\partial a}{\partial q_i}\right)_0 q_i + \tfrac{1}{2} \sum_{i,j} \left(\frac{\partial^2 a}{\partial q_i\, \partial q_j}\right)_0 q_i\, q_j + \cdots \qquad (1)$$

The intensity of the Raman line corresponding to ν_i will depend on $\left(\frac{\partial a}{\partial q_i}\right)_0 q_i$ and that corresponding to $2\,\nu_i$ will depend on $\left(\frac{\partial^2 a}{\partial q_i^2}\right)_0 q_i^2$ neglecting the higher order derivatives. The polarisability tensor of the kth bond in the molecule can be written as

$$A^{(k)} = A_0{}^{(k)} + A_1{}^{(k)} \frac{\Delta r^{(k)}}{a^{(k)}} + \cdots \qquad (2)$$

where $\Delta r^{(k)}$ is the change in the internuclear distance $a^{(k)}$. Let us assume that the general expansion (1) is made up of N expansions of the type (2) where N is the number of bonds. This may be assumed to be nearly right because our procedure would be a piece-wise representation of the general expansion of the polarisability of the molecule. If such a procedure is to be adopted, it must not be thought that $\left(\frac{\partial^2 a}{\partial q_i^2}\right)_0$ will not depend on $A_1{}^{(k)}$ and $A_0{}^{(k)}$ because in certain normal modes of vibration the variations in the internuclear distances could be quadratic functions of the normal co-ordinates and the ordinary optical anisotropy of the molecule could change even though all A's other than A_0's, are zero.

In the case of CO_2 the variations in the C–O bond lengths are linear functions of the normal co-ordinates corresponding to ν_1 and ν_3 while they depend on the square of the co-ordinate corresponding to ν_2. Because the overtones of ν_1 and ν_3 are not reported so far, we could assume only A_0 and A_1 for the bonds and still account for 2 ν_2. These arguments are really very general. We could thus account for the appearance of overtones of certain modes of vibration even though the overtones of the most symmetrical vibrations are not observed (as in the case of methane and deuteromethanes).

§ 2. *The Polarisability Tensor in Terms of Normal Co-ordinates*

The axes of the molecule are chosen as shown in Fig. 1. The co-ordinates of the oxygen, carbon and oxygen atoms in the equilibrium configuration are $(0, 0, -a)$, $(0, 0, 0)$ and $(0, 0, +a)$ where a is the length of the C–O bond. The oxygen atoms are denoted by the subscripts 1 and 2 and the carbon atom by the subscript 3. Let (x_r, y_r, z_r) be the variations in the co-ordinates of the rth atom. Let m and M be the masses of the oxygen and carbon atoms respectively. Conditions of the constancy of linear and angular momenta require the following constraints among the cartesian variations:

$$\left.\begin{aligned} m(x_1+x_2)+\mathrm{M}x_3 &= 0,\\ m(y_1+y_2)+\mathrm{M}y_3 &= 0,\\ m(z_1+z_2)+\mathrm{M}z_3 &= 0,\\ x_1 &= x_2,\\ y_1 &= y_2. \end{aligned}\right\} \tag{3}$$

Following Dennison, the normal co-ordinates can be written as

$$\left.\begin{aligned} q &= z_2 - z_1,\\ x &= x_3 - \tfrac{1}{2}(x_1+x_2),\\ y &= y_3 - \tfrac{1}{2}(y_1+y_2),\\ z &= z_3 - \tfrac{1}{2}(z_1+z_2). \end{aligned}\right\} \tag{4}$$

The normal co-ordinate q refers to the vibration with frequency ν_1, the co-ordinates x and y refer to the doubly degenerate vibration with frequency ν_2 and the co-ordinate z refers to the vibration with frequency ν_3.

The variation in the (1–3) bond is given by

$$\begin{aligned} \Delta r_{13} &= \{(x_1-x_3)^2+(y_1-y_3)^2+(z_1-a-z_3)^2\}^{\frac{1}{2}} - a\\ &= \frac{1}{2a}\{(x_1-x_3)^2+(y_1-y_3)^2\} + (z_3-z_1), \end{aligned} \tag{5}$$

retaining terms of the first and second orders only. Similarly

$$\Delta r_{23} = \frac{1}{2a}\{(x_2-x_3)^2+(y_2-y_3)^2\} - (z_3-z_2). \tag{6}$$

The direction cosines of the (1 – 3) and (2 – 3) bonds are respectively given by

$$\left.\begin{aligned}(\alpha_{13}, \beta_{13}, \gamma_{13}) &= \frac{1}{a+\Delta r_{13}}(x_3-x_1, y_3-y_1, z_3-z_1+a),\\ (\alpha_{23}, \beta_{23}, \gamma_{23}) &= \frac{1}{a+\Delta r_{23}}(x_3-x_2, y_3-y_2, z_3-z_2-a).\end{aligned}\right\} \quad (7)$$

Let A, B and B be the principal polarisabilities of a C–O bond. Here A and B are functions of the internuclear distance, given by

$$\left.\begin{aligned}\mathrm{A} &= \mathrm{A}_0+\mathrm{A}_1\frac{\Delta r}{a},\\ \mathrm{B} &= \mathrm{B}_0+\mathrm{B}_1\frac{\Delta r}{a},\end{aligned}\right\} \quad (8)$$

where Δr is the variation in the inter-nuclear distance and A_0 and B_0 the polarisabilities of a C–O bond when $\Delta r = 0$. Higher order terms in (8) will of course be present but for our present discussion their presence is not necessary.

In the presence of an external electric field with components E_x, E_y and E_z, the components of the induced moment in the (1—3) bond are

$$\left.\begin{aligned}\mathrm{M}_x &= \mathrm{E}_x(\mathrm{B}+\alpha^2{}_{13}\delta_{13})+\mathrm{E}_y\alpha_{13}\beta_{13}\delta_{13}+\mathrm{E}_z\alpha_{13}\gamma_{13}\delta_{13},\\ \mathrm{M}_y &= \mathrm{E}_x\beta_{13}\alpha_{13}\delta_{13}+\mathrm{E}_y(\mathrm{B}+\beta^2{}_{13}\delta_{13})+\mathrm{E}_z\beta_{13}\gamma_{13}\delta_{13},\\ \mathrm{M}_z &= \mathrm{E}_x\gamma_{13}\alpha_{13}\delta_{13}+\mathrm{E}_y\gamma_{13}\beta_{13}\delta_{13}+\mathrm{E}_z(\mathrm{B}+\gamma^2{}_{13}\delta_{13}),\end{aligned}\right\} \quad (9)$$

where $(\alpha_{13}, \beta_{13}, \gamma_{13})$ are the direction cosines of the (1–3) bond and

$$\delta_{13} = (\mathrm{A}_0-\mathrm{B}_0)+(\mathrm{A}_1-\mathrm{B}_1)\frac{\Delta\gamma_{13}}{a} \quad (10)$$

Similar expressions hold good for the components of the induced moment in the (2—3) bond.

Using (5), (6) and (7), we get

$$\left.\begin{aligned}\gamma_{13}{}^2 &= 1-\frac{1}{a^2}\{(x_1-x_3)^2+(y_1-y_3)^2\},\\ \gamma_{23}{}^2 &= 1-\frac{1}{a^2}\{(x_2-x_3)^2+(y_2-y_3)^2\},\\ \gamma_{13}\alpha_{13} &= \frac{1}{a}(x_3-x_1)-\frac{1}{a^2}(x_3-x_1)(z_3-z_1),\\ \gamma_{23}\alpha_{23} &= -\frac{1}{a}(x_3-x_2)-\frac{1}{a^2}(x_3-x_2)(z_3-z_2),\\ \gamma_{13}\beta_{13} &= \frac{1}{a}(y_3-y_1)-\frac{1}{a^2}(y_3-y_1)(z_3-z_1),\\ \gamma_{23}\beta_{23} &= -\frac{1}{a}(y_3-y_2)-\frac{1}{a^2}(y_3-y_2)(z_3-z_2),\end{aligned}\right\} \quad (11)$$

neglecting terms of the higher order. From (9) the z-component of the total moment induced in both the bonds is

$$\begin{aligned} M_z = {} & E_x \{\alpha_{13}\gamma_{13}(\delta_0 + \delta_1 \Delta r_{13}) + \alpha_{23}\gamma_{23}(\delta_0 + \delta_1 \Delta r_{23})\} \\ & + E_y \{\beta_{13}\gamma_{13}(\delta_0 + \delta_1 \Delta r_{13}) + \beta_{23}\gamma_{23}(\delta_0 + \delta_1 \Delta r_{23})\} \\ & + E_z \{(B_0 + \frac{B_1}{a} \Delta r_{13}) + (B_0 + \frac{B_1}{a} \Delta r_{13}) \\ & + \gamma^2_{13}(\delta_0 + \delta_1 \Delta r_{13}) + \gamma_{23}{}^2(\delta_0 + \delta_1 \Delta r_{23})\}, \end{aligned} \tag{12}$$

where

$$\left.\begin{aligned} \delta_0 &= A_0 - B_0, \\ \delta_1 &= (A_1 - B_1)/a. \end{aligned}\right\} \tag{13}$$

Using (11), (5), (6) and the relation $x_1 = x_2$ and $y_1 = y_2$ given by (3) in (12), we get

$$\begin{aligned} M_z = {} & E_x (-\delta_0 + \delta_1) \frac{(x_3 - x_1)(2z_3 - z_1 - z_2)}{a^2} \\ & + E_y (-\delta_0 + \delta_1) \frac{(y_3 - y_1)(2z_3 - z_1 - z_2)}{a^2} \\ & + E_z \left\{ 2A_0 + A_1 \frac{z_2 - z_1}{a} - (2\delta_0 - A_1) \frac{\rho^2}{a^2} \right\}, \end{aligned} \tag{14}$$

where

$$\rho^2 = (x_1 - x_3)^2 + (y_1 - y_3)^2 = x^2 + y^2. \tag{15}$$

Expressing the cartesian co-ordinates (x_r, y_r, z_r) in terms of normal co-ordinates by means of (4), we get

$$\begin{aligned} M_z = {} & 2(-\delta_0 + \delta_1) \frac{zx}{a^2} E_x + 2(-\delta_0 + \delta_1) \frac{zy}{a^2} E_y \\ & + \left\{ 2A_0 + A_1 q - (2\delta_0 - A_1) \frac{\rho^2}{a^2} \right\} E_z. \end{aligned} \tag{16}$$

Similarly, we get

$$\begin{aligned} M_x = {} & \left(2B_0 + B_1 \frac{q}{a} + 2\delta_0 \frac{x^2}{a^2} + B_1 \frac{\rho^2}{a^2} \right) E_x \\ & + 2\delta_0 \frac{xy}{a^2} E_y + 2(-\delta_0 + \delta_1) \frac{xz}{a^2} E_z \end{aligned} \tag{17}$$

$$\begin{aligned} M_y = {} & 2\delta_0 \frac{yx}{a^2} + \left(2B_0 + B_1 \frac{q}{a} + 2\delta_0 \frac{y^2}{a^2} + B_1 \frac{\rho^2}{a^2} \right) E_y \\ & + 2(-\delta_0 + \delta_1) \frac{yz}{a^2} E_z. \end{aligned}$$

Hence the components of the polarisability tensor are given by

$$\left.\begin{aligned}
\alpha_{xx} &= 2\,B_0 + B_1\frac{q}{a} + 2\,\delta_0\frac{x^2}{a^2} + B_1\frac{\rho^2}{a^2},\\
\alpha_{yy} &= 2\,B_0 + B_1\frac{q}{a} + 2\,\delta_0\frac{y^2}{a^2} + B_1\frac{\rho^2}{a^2},\\
\alpha_{zz} &= 2\,A_0 + A_1\frac{q}{a} + (A_1 - 2\,\delta_0)\frac{\rho^2}{a^2}.\\
\alpha_{xy} &= \alpha_{yx} = 2\,\delta_0\frac{xy}{a^2},\\
\alpha_{yz} &= \alpha_{zy} = 2\,(\delta_1 - \delta_0)\frac{yz}{a^2},\\
\alpha_{zx} &= \alpha_{xz} = 2\,(\delta_1 - \delta_0)\frac{zx}{a^2}.
\end{aligned}\right\} \qquad (18)$$

where

$$\rho^2 = x^2 + y^2.$$

§ 3. *Matrix Elements of the Polarisability Tensor*

The normal co-ordinates of the vibrations of the CO_2 molecule are q, x, y and z as pointed out in § 1. The vibrational Hamiltonian is given by

$$H = T + V = \tfrac{1}{2}\left\{\frac{m}{2}\dot{q}^2 + \mu\,(\dot{x}^2 + \dot{y}^2 + \dot{z}^2)\right.$$
$$\left. + 4\pi^2\left(\frac{m}{2}\,\nu_1^2\,q^2 + \mu\,\nu_2^2\,\overline{x^2 + y^2} + \mu\,\nu_3^2\,z^2\right)\right\}$$

where $\mu = \dfrac{2\,m\,M}{2m + M}$. (19)

It is convenient to employ co-ordinates ρ and ϕ instead of x and y by means of the transformation

$$x = \rho\cos\phi \text{ and } y = \rho\sin\phi \qquad (20)$$

The wave function ψ of the vibrating molecule can be written as[2]

$$\psi_{V_1}(q)\,\psi_{V_2,l}(\rho)\,\psi_{V_3}(z)\,\exp(\pm\, i\,l\,\phi) \qquad (21)$$

where the functions are properly normalised and are orthogonal where V_1 and V_3 are the quantum numbers of the non-degenerate vibrations ν_1 and ν_3, and V_2 and l are the quantum numbers of the doubly degenerate vibration ν_2 with co-ordinates ρ and ϕ. By means of (21), we can calculate the matrix elements of the polarisability tensor (18) for the transitions

$$\left.\begin{aligned}
&(0, 0, 0, 0) \rightarrow (1, 0, 0, 0),\\
&\text{and } (0, 0, 0, 0) \rightarrow (0, 2, 0, 0),
\end{aligned}\right\} \qquad (22)$$

where the four quantum numbers in brackets refer to V_1, V_2, V_3 and l respectively. We will be referring to the transitions (22) simply by

$$\left.\begin{array}{l}(0,0)\rightarrow(1,0)\\(0,0)\rightarrow(0,2)\end{array}\right\} \tag{23}$$

omitting V_3 and l on the understanding that V_3 does not change and l is zero and does not change.

For the transition $(0,0)\rightarrow(1,0)$ the polarisability tensor (18) is

$$\left.\begin{array}{ccc}B_1\frac{q_1^0}{a} & 0 & 0\\ 0 & B_1\frac{q_1^0}{a} & 0\\ 0 & 0 & A_1\frac{q_1^0}{a}\end{array}\right\} \tag{24}$$

where q_1^0 is the matrix element of q for the transition $0\rightarrow 1$ in V_1. From the theory of the harmonic oscillator

$$q_1^0=\left(\frac{h}{8\pi^2\nu_1(m/2)}\right)^{\frac{1}{2}}. \tag{25}$$

Similarly for the transition $(0,0)\rightarrow(0,2)$, the tensor is

$$\left.\begin{array}{ccc}(B_1+\delta_0)\frac{(\rho^2)_2^0}{a^2} & 0 & 0\\ 0 & (B_1+\delta_0)\frac{(\rho^2)_2^0}{a^2} & 0\\ 0 & 0 & (A_1-2\delta_0)\frac{(\rho^2)_2^0}{a^2}\end{array}\right\} \tag{26}$$

where $(\rho^2)_2^0$ is the matrix element of ρ^2 for the transition $0\rightarrow 2$ in V_2. From the theory of the two dimensional oscillator

$$(\rho^2)_2^0=\left(\frac{h}{4\pi^2\nu_2\mu}\right)^{\frac{1}{2}}. \tag{27}$$

The spur and the anisotropy of the tensor (24) for the transition $(0,0)\rightarrow(1,0)$ are respectively

$$\left.\begin{array}{l}a_1=\epsilon_1\frac{q_1^0}{a},\\ \gamma_1^2=\delta_1^2\frac{(q_1^0)^2}{a^2}\end{array}\right. \tag{28}$$

where

$$\epsilon_1=(A_1+2B_1)/3 \text{ and } \delta_1=A_1-B_1. \tag{29}$$

The spur and the anisotropy of the tensor (26) for the transition $(0, 0) \rightarrow (0, 2)$ are respectively

$$\left.\begin{aligned} \alpha_2 &= \epsilon_1 \frac{(\rho^2)^0_2}{a^2}, \\ \gamma_2^2 &= (\delta_1 - 3\,\delta_0)^2 \frac{\{(\rho^2)^0_2\}^2}{a^2}. \end{aligned}\right\} \tag{30}$$

The average values of the squares of the tensor components in any fixed frame OXYZ can be calculated by standard methods.

$$\left.\begin{aligned} \overline{\{(\alpha_{zz})^{00}_{10}\}^2} &= \alpha_1^2 + \frac{4}{45}\gamma_1^2, \\ \overline{\{(\alpha_{zx})^{00}_{10}\}^2} &= \frac{1}{15}\gamma_1^2, \\ \overline{\{(\alpha_{zz})^{00}_{02}\}^2} &= \alpha_2^2 + \frac{4}{45}\gamma_2^2, \\ \overline{\{(\alpha_{zx})^{00}_{02}\}^2} &= \frac{1}{15}\gamma_2^2. \end{aligned}\right\} \tag{31}$$

Also

$$\overline{(\alpha_{zz})^{00}_{10} \cdot (\alpha_{zz})^{00}_{02}}$$

$$= \text{average of the product}$$

$$\{B_1 \cos^2(xZ) + B_1 \cos^2(yZ) + A_1 \cos^2(zZ)\}\ \{(B_1 + \delta_0)\cos^2(xZ)$$

$$+ (B_1 + \delta_0)\cos^2(yZ) + (A_1 - 2\,\delta_0)\cos^2(zZ)\}\frac{q_1^0}{a} \cdot \frac{(\rho^2)^0_2}{a^2}$$

$$= \alpha_1\alpha_2 + \frac{4}{45}\gamma_1\gamma_2 \tag{32}$$

where

$$\gamma_1 = \delta_1 \frac{q_1^0}{a}, \quad \gamma_2 = (\delta_1 - 3\,\delta_0)\frac{(\rho^2)^0_2}{a^2} \tag{33}$$

Similarly

$$\overline{(\alpha_{zx})^{00}_{10} \cdot (\alpha_{zx})^{00}_{02}} = \frac{1}{15}\gamma_1\gamma_2. \tag{34}$$

§ 4. *Calculation of the Intensities of the Fermi Split Lines*

The appearance of a doublet of comparable intensities instead of a strong line corresponding to ν_1 and a faint line corresponding to $2\nu_2$ in the Raman spectrum of CO_2, has been explained by Fermi[3] as due to the accidental degeneracy $\nu_1 \backsimeq 2\nu_2$.

Denoting $\nu_1 - 2\,\nu_2$ by Δ, the matrix elements of the polarisability for the observed split lines are, following Placzek,[4]

$$\left.\begin{aligned}[a]^{00}_{10} &= \frac{1}{\sqrt{2x}}\left\{\sqrt{x+|\Delta|}\;(a)^{00}_{10} \pm \sqrt{x-|\Delta|}\;(a)^{00}_{02}\right\}\\ [a]^{00}_{02} &= \frac{1}{\sqrt{2x}}\left\{\sqrt{x-|\Delta|}\;(a)^{00}_{10} \mp \sqrt{x+|\Delta|}\;(a)^{00}_{02}\right\}\end{aligned}\right\} \tag{35}$$

where

$$x = \sqrt{(\Delta^2 + 16\,P^2)} \tag{36}$$

where

$$P = \frac{\beta_{12}}{4\pi^3}\sqrt{\frac{h}{(\nu_1 + 2\,\nu_2)^3}}, \tag{37}$$

β_{12} being the anharmonic constant coupling the vibrations with frquencies ν_1 and ν_2. For $\Delta^2 << P^2$ the matrix elements are :

$$\left.\begin{aligned}[a]^{00}_{10} &= \frac{1}{\sqrt{2}}\{(a)^{00}_{10} + (a)^{00}_{02}\}\\ [a]^{00}_{02} &- \frac{1}{\sqrt{2}}\{(a)^{00}_{10} - (a)^{00}_{02}\}\end{aligned}\right\} \tag{38}$$

the former corresponding to the higher energy split state and the latter to the lower energy split state. The numbers following square brackets must not be thought of as the quantum numbers because the split states are obtained by linear combinations of the states (1, 0) and (0, 2) obtained when the anharmonicity P is zero.

Using 31 in 38, we have

$$\overline{\{[a_{zz}]^{00}_{10}\}^2} = \tfrac{1}{2}\left[\overline{\{(a_{zz})^{00}_{10}\}^2} + \overline{\{(a_{zz})^{00}_{02}\}^2} + 2\,\overline{\{(a_{zz})^{00}_{10}\}\,(a_{zz})^{00}_{02}\}}\right]$$

$$= \tfrac{1}{2}\left[(a_1 + a_2)^2 + \frac{4}{45}(\gamma_1 + \gamma_2)^2\right] \tag{39}$$

$$\overline{\{(a_{zx})^{00}_{10}\}^2} = \tfrac{1}{2}\cdot\frac{2}{15}(\gamma_1 + \gamma_2)^2 \tag{40}$$

For unpolarized incident light, the intensity of parallel component of the transversely scattered light is

$$\tfrac{1}{2}\left[(a_1 + a_2)^2 + \frac{7}{45}(\gamma_1 + \gamma_2)^2\right] \tag{41}$$

and that of the perpendicular component is

$$\tfrac{1}{2}\cdot\frac{2}{15}(\gamma_1 + \gamma_2)^2. \tag{42}$$

These intensities are the total intensities of the P, Q and R branches of the vibrational line. If we are interested in the purely vibrational state (*i.e.*,) the

Q branch, the anisotropic scattering in the Q-branch is approximately $\frac{1}{4}$ that of the total anisotropic scattering at ordinary temperatures while the spur scattering has no P and R branches. The intensities of the parallel and perpendicular components of the Q-branch are

$$\left.\begin{aligned}[I_{\parallel}]_{10}^{00} &= \tfrac{1}{2}\left[(\alpha_1+\alpha_2)^2+\frac{7}{180}(\gamma_1+\gamma_2)^2\right],\\ [I_{\perp}]_{10}^{00} &= \tfrac{1}{2}\cdot\frac{1}{30}(\gamma_1+\gamma_2)^2\end{aligned}\right\} \tag{43}$$

The aggregate intensity and the depolarisation are respectively given by

$$\left.\begin{aligned}I_1 &= \tfrac{1}{2}\left[(\alpha_1+\alpha_2)^2+\frac{13}{180}(\gamma_1+\gamma_2)^2\right]\\ \rho_1 &= \frac{6(\gamma_1+\gamma_2)^2}{180(\alpha_1+\alpha_2)^2+7(\gamma_1+\gamma_1)^2}\end{aligned}\right\} \tag{44}$$

Similarly the aggregate intensity and the depolarisation of the other split line are

$$\left.\begin{aligned}I_2 &= \tfrac{1}{2}\left[(\alpha_1-\alpha_2)^2+\frac{13}{180}(\gamma_1-\gamma_2)^2\right]\\ \rho_2 &= \frac{6(\gamma_1-\gamma_2)^2}{180(\alpha_1-\alpha_2)^2+7(\gamma_1-\gamma_2)^2}\end{aligned}\right\} \tag{45}$$

From (44) and (45)

$$\frac{I_2}{I_1}=\frac{\rho_1}{\rho_2}\cdot\frac{(1+\rho_2)}{(1+\rho_1)}\cdot\frac{(\gamma_1-\gamma_2)^2}{(\gamma_1+\gamma_2)^2} \tag{46}$$

$$(\gamma_1+\gamma_2)^2=\frac{180\,\rho_1}{6-7\,\rho_1}(\alpha_1+\alpha_2)^2 \tag{47}$$

$$(\gamma_1-\gamma_2)^2=\frac{180\,\rho_2}{6-7\,\rho_2}(\alpha_1-\alpha_2)^2 \tag{48}$$

Using (47) and (48) in (46), we get

$$\frac{I_2}{I_1}=\frac{(1+\rho_2)(6-7\,\rho_1)}{(1+\rho_1)(6-7\,\rho_2)}\left(\frac{\alpha_1-\alpha_2}{\alpha_1+\alpha_2}\right)^2 \tag{49}$$

From (28) and 30)

$$\alpha_1=\epsilon_1\sigma_1,\quad \alpha_2=\epsilon_1\sigma_2 \tag{50}$$

where

$$\sigma_1=q_1^0/a.\quad \sigma_2=(\rho^2)_2^0/a^2 \tag{51}$$

Hence

$$\frac{I_2}{I_1}=\frac{(1+\rho_2)(6-7\,\rho_1)}{(1+\rho_1)(6-7\,\rho_2)}\left(\frac{\sigma_1-\sigma_2}{\sigma_1+\sigma_2}\right)^2 \tag{52}$$

Defining

$$\theta = \frac{\sigma_2}{\sigma_1 + \sigma_2} \text{ and } \phi = \frac{\sigma_2}{\sigma_1 - \sigma_2} \tag{53}$$

and using (50), (51) and (33), we can write the expressions for the depolarisations

$$\rho_1 = \frac{6}{\frac{180\ \epsilon_1^2}{(\delta_1 + 3\,\delta_0\,\theta)^2} + 7},\quad \rho_2 = \frac{6}{\frac{180\ \epsilon_1^2}{(\delta_1 + 3\,\delta_0\,\phi)^2} + 7} \tag{54}$$

From (52) and (54), we see that the intensity ratio of the split Raman lines and their depolarisations are expressed in terms of σ_1 and σ_2 which are the matrix elements of q and ρ^2 for the required transitions and in terms of δ_0, ϵ_1 and δ_1 where δ_0 is the optical anisotropy of the undisturbed C–O bond, ϵ_1 and δ_1 are respectively the changes in the spur and anisotropy of the bond for doubling the internuclear distance. The expressions (52) and (54) have been derived assuming Δ $(= \nu_1 - 2\,\nu_2)$ to be very small. In case Δ is not small and P and Δ are of the same sign

$$\left.\begin{aligned} &\frac{I_2}{I_1} = \frac{(1+\rho_2)\,(6-7\,\rho_1)}{(1+\rho_1)\,(6-7\,\rho_2)}\left(\frac{c_1\,\sigma_1 - c_2\,\sigma_2}{c_2\,\sigma_1 + c_1\,\sigma_2}\right)^2, \\ &\rho_1 = \frac{6}{\frac{180\ \epsilon_1^2}{(\delta_1 - 3\,\delta_0\,\Theta)^2} + 7},\quad \rho_2 = \frac{6}{\frac{180\ \epsilon_1^2}{(\delta_1 + 3\,\delta_0\,\Phi)^2} + 7} \end{aligned}\right\} \tag{55}$$

where

$$\left.\begin{aligned} &c_1 = \sqrt{x - |\,\Delta\,|},\ c_2 = \sqrt{x + |\,\Delta\,|}, \\ &\Theta = \frac{c_1\sigma_2}{c_2\sigma_1 + c_1\sigma_2},\quad \Phi = \frac{c_2\sigma_2}{c_2\sigma_1 - c_1\sigma_2}\,. \end{aligned}\right\} \tag{56}$$

Assuming $\Delta^2 \ll P^2$ we will now compute the intensity ratio given by (52). We will first estimate σ_1 and σ_2. They are

$$\sigma_1 = \frac{1}{a}\left(\frac{h}{4\,\pi^2\,\nu_1 m}\right)^{\frac{1}{2}} \tag{57}$$

$$= 0\cdot03408,$$

$$\sigma_2 = \frac{1}{a^2}\left(\frac{h}{4\,\pi^2\,\nu_2}\cdot\frac{2m+M}{2mM}\right) \tag{58}$$

$$= 0\cdot004266$$

assuming $a = 1\cdot16$Å, $\nu_1 = 1336$ cm.$^{-1}$

$\nu_2 = 667$ cm.$^{-1}$ Hence

$$\frac{\sigma_1}{\sigma_2} = 7\cdot987 \tag{59}$$

Thus

$$\frac{I_2}{I_1}=\frac{(1+\rho_2)(6-7\rho_1)}{(1+\rho_1)(6-7\rho_2)}\times\cdot 6045 \tag{60}$$

If $\rho_1, \rho_2 \ll 1$ or $\rho_1 \approx \rho_2$, then

$$\frac{I_2}{I_1} \approx 0\cdot 6 \tag{61}$$

Bhagavantam's[5] experimental determination gives both ρ_1 and ρ_2 to be nearly equal to 0·2. In this case the intensity ratio would be nearly 0·6. On the other hand taking ρ_1 and ρ_2 to be respectively 0·14 and 0·18 given by Langseth and Nielsen,[6] the intensity ratio would be 0·66 still not far from 0·6 though their depolarisation values are rather different from those determined by Bhagavantam. This is natural since our intensity expression (60) is not very sensitive to ρ_1 and ρ_2 so long as they are nearly equal or both small compared to unity, the former alternative being more plausible. The intensity ratio 0·6 calculated by us is in very good accord with the observed ratios 0·57 by I. Hansen[7] and 0·61 by Langseth and Nielsen and ·5 by Bhagavantam.

We can solve for δ_1 δ_0 and ϵ_1/δ_0 by means of equations in (54). The solutions are

$$\left.\begin{aligned}\frac{\delta_1}{\delta_0}&=\frac{3(\theta+k\phi)}{1-k},\\ \frac{\epsilon_1}{\delta_0}&=\pm 3\left(\frac{6-7\rho_1}{180\rho_1}\right)^{\frac{1}{2}}\frac{k\phi}{1-k}\end{aligned}\right\} \tag{62}$$

where

$$k=\pm\left[\frac{\rho_1(6-7\rho_2)}{\rho_2(6-7\rho_1)}\right]^{\frac{1}{2}} \tag{63}$$

$$\theta=\frac{\sigma_2}{\sigma_1+\sigma_2}=0\cdot 112,\ \phi=\frac{\sigma_2}{\sigma_1-\sigma_2}=0\cdot 1443$$

It may thus be expected that we could determine δ_1 and ϵ_1 and consequently the constants A_1 and B_1 by knowing the experimental values of ρ_1, ρ_2 and δ_0. But it may be seen from our expressions that the determination will be very sensitive to the values of ρ_1 and ρ_2. It has not been found possible to arrive at any definite conclusion about these constants from the available experimental data.

We are thankful to Prof. S. Bhagavantam for his interest in this work.

Summary

The polarisability of a molecule is assumed to be made up of the bond polarisabilities as functions of the inter-nuclear distances. It is pointed out that certain normal co-oridnates could be quadratic functions of some of the variations in the inter-nuclear distances which fact accounts for the appearance of overtone Raman lines assuming only first order variations in the bond polarisabilities. These ideas have been applied to the case of CO_2 and the intensity ratio of the Fermi split lines has been calculated which is in good accord wih experimental observations.

REFERENCES

1. Dennison .. *Rev. Mod. Phy.*, 1941, **3**, 280.
2. ———————. .. *Phy. Rev.*, 1932, **41**, 304.
3. Fermi .. *Zeits. f. Phy.*, 1931, **71**, 250.
4. Placzek .. *Handbuch der Radiologie*, **6** (2), 323.
5. Bhagavantam .. *Ind. Jour. Phy.*, 1931, **6**, 319.
6. Langseth and Nielsen .. *Phy. Rev.*, 1934, **46**, 1057.
7. Hansen .. *Ibid.*, 1934, **46**, 122.

ERRATA

Page 343, second line of equation (16)—

for $+\left\{2\,A_0 + A_1\,q - (2\delta_0 - A_1)\,\frac{\rho^2}{a^2}\right\} E_z.$

read $+\left\{2\,A_0 + A_1\,\frac{q}{a} - (2\delta_0 - A_1)\,\frac{\rho^2}{a^2}\right\} E_z.$

Page 350, second line of equation (62)—

for $\frac{\epsilon_1}{\delta_0} = \pm 3\left(\frac{6-7\,\rho_1}{180\,\rho_1}\right)^{\frac{1}{2}} \frac{k\,\phi}{1-k}$

read $\frac{\epsilon_1}{\delta_0} = \pm 3\left(\frac{6-7\,\rho_1}{180\,\rho_1}\right)^{\frac{1}{2}} \frac{k\,(\phi+\theta)}{1-k}$

ALUMINIUM CHLORIDE, A NEW REAGENT FOR THE CONDENSATION OF β-KETONIC ESTERS WITH PHENOLS

Part V. The Condensation of Substituted Resacetophenones with Ethyl Acetoacetate

By C. V. Deliwala and N. M. Shah

(From the Department of Chemistry, M. R. Science Institute, Gujerat College, Ahmedabad)

Received January 31, 1941
(Communicated by Dr. M. S. Shah)

In Part I of this series, one of the present authors (N. M. S.) with Sethna and Shah, R. C.,[1] has shown that resacetophenone condensed with ethyl acetoacetate in presence of anhydrous aluminium chloride with the formation of otherwise difficultly accessible 5-hydroxy-6-acetyl-4-methyl coumarin in good yield. In the subsequent parts, the investigation was extended to the similar condensation of other di-hydroxy- and tri-hydroxy-phenyl-ketones and also to various 4-acyl-resorcinols with ethyl acetoacetate; in all cases, whenever the reaction took place, the product obtained was found to be 5-hydroxy-6-acyl-coumarin derivative (Shah, N. M., and Shah, R. C.[2]; Deliwala and Shah, N. M.[3]).

Recently Desai and Ekhlas[4] have studied the condensation of some substituted resacetophenones with ethyl acetoacetate in presence of phosphorus oxychloride as the condensing agent.

The work described in this paper was undertaken with a view to ascertain the influence of constitutional factors in resacetophenone molecule on the course of the reaction with ethyl acetoacetate in presence of anhydrous aluminium chloride.

In this communication, the condensation of (1) 5-ethyl-, (2) 5-bromo-, (3) 5-nitro-, (4) 5-benzyl-, (5) ω-methoxy-resacetophenones, (6) methyl β-resacetophenone carboxylate, (7) 2 : 4-diacetyl-resorcinol, and (8) 4 : 6-diacetyl-resorcinol with ethyl acetoacetate with aluminium chloride as the condensing agent has been investigated.

5-Ethyl-resacetophenone (2 : 4-dihydroxy-5-ethyl-acetophenone) condenses with ethyl acetoacetate in presence of aluminium chloride in dry nitro-benzene solution at about 115°, giving 5-hydroxy-6-acetyl-8-ethyl-4-methyl coumarin

(I; X = C_2H_5). The constitution (I; X = C_2H_5) has been assigned to it as (*a*) it gives ferric chloride colour reaction, and dissolves in alkali with non-fluorescent yellow colour, characteristic of a 5-hydroxy-coumarin derivative[5]; (*b*) on Clemmensen reduction, it gives 5-hydroxy-6: 8-di-ethyl-4-methyl-coumarin (III) identical with that of Mehta and Shah[6]; (*c*) it is identical with 5-hydroxy-6-acetyl-8-ethyl-4-methyl coumarin obtained by Desai and Ekhlas,[4] and (*d*) it gives on Kostanecki acetylation, the coumarino-chromone, 4: 2′-di-methyl-3′-acetyl-6′-ethyl-chromono-7′: 8′: 6: 5-α-pyrone (II; X = C_2H_5; R = CO·Me) identical with that of Desai and Ekhlas.[4] It may be mentioned here that 5-ethyl-resacetophenone does not condense with acetoacetic ester in presence of sulphuric acid.

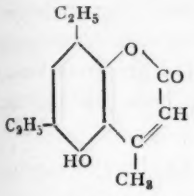

(III)

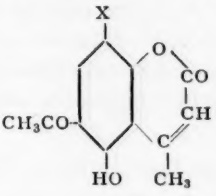

(I)

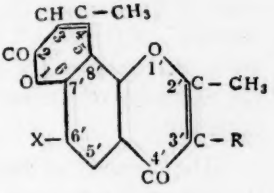

(II)

5-Bromo-resacetophenone on condensation with acetoacetic ester in presence of anhydrous aluminium chloride gave 5-hydroxy-6-acetyl-8-bromo-4-methylcoumarin (I; X = Br); its constitution rests on the following grounds: (i) it gives a positive ferric chloride test and dissolves in alkali giving non-fluorescent yellow colour characteristic of a 5-hydroxy-coumarin derivative, and (ii) it gives on Kostanecki acetylation, 4: 2′-dimethyl-6′-bromo-chromono-7′: 8′: 6: 5-α-pyrone (II; X = Br, R = H). 5-Bromo-resacetophenone does not condense either in presence of phosphorus oxychloride or sulphuric acid.

5-Benzyl-, 5-nitro-, ω-methoxy-resacetophenones as well as methyl β-resacetophenone carboxylate did not condense in spite of several attempts.

Owing to the close resemblance between α-naphthol and resorcinol in undergoing the Pechmann reaction, the condensation of 4-acetyl- and 4-propionyl-α-naphthols was studied in presence of aluminium chloride, but instead of the expected acyl-coumarin derivative, 4-methyl-1: 2-α-naphthapyrone was obtained in both the cases, the acyl group being split off during the reaction. Desai and Ekhlas have found that the acyl group is eliminated even in presence of phosphorus oxychloride.

From the above results and those of Chakravarty,[7] Desai,[8] Limaye[9] and their co-workers and Sethna, Shah, N. M., and Shah, R. C.,[1] and Deliwala

and Shah,[3] it can be safely concluded that the condensing agents so far found efficient for effecting the condensation of 4-substituted resorcinol and derivatives are phosphorus oxychloride and aluminium chloride. Both are characteristic in their behaviour as condensing agents. Phosphorus oxychloride, if the reaction takes place, produces mainly 7-hydroxy-6-acyl-coumarins. It is a good substitute for sulphuric acid in cases where the acid fails. Aluminium chloride entirely changes the course of the condensation with the production of 5-hydroxy-6-acyl-coumarin derivatives, difficultly accessible by the hitherto-known methods.

It has been already pointed out by Shah, N. M., and Shah, R. C.,[2] that the above reactivity in 2-position of the resorcinol nucleus is explicable on the view of the fixation of double bonds of the benzene nucleus, the chelation between $-OH$ and $-CO.R$ (R = Me, Et, etc.) in 4-acyl-resorcinols bringing about that state in the presence of aluminium chloride. On the same view, the reactivity of the substituted resacetophenones studied here can also be explained.

The presence of negative groups like $-NO_2$, $-CO-Me$, $-COOMe$ in the resacetophenone molecule has de-activating effect and therefore hinder the condensation; moreover, they introduce an additional chelating factor, which may also be responsible for the de-activation of the molecule:

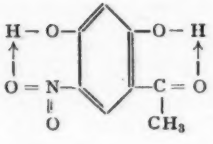

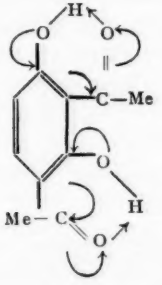

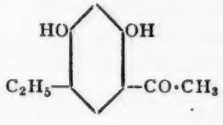

But the introduction of the positive groups like $-CH_3$, $-C_2H_5$ has no such effect; hence the condensation in case of 5-ethyl-resacetophenone easily takes place. The introduction of ethyl group in 5-position of the resacetophenone molecule excludes the possibility of the 7-hydroxy-coumarin-formation. This also explains the formation of 5-hydroxy-coumarin even in presence of phosphorus oxychloride (Desai and Ekhlas).

5-Bromo-resacetophenone does not condense in presence of phosphorus oxychloride (Desai and Ekhlas) or sulphuric acid; while in presence of aluminium chloride, 5-hydroxy-6-acyl-coumarin derivative was obtained.

Phosphorus oxychloride has a little or no tendency to promote chelation; the possibility of 7-hydroxy-coumarin-formation is excluded as both 4- and 6-positions (considered as resorcinol molecule) are already substituted. In presence of aluminium chloride, the chelation between —OH and —COMe stabilises one of the Kekule forms by the fixation of double bonds. 4-Halogeno-resorcinols are feebly chelated (Sidgwick[10]) but such chelation cannot be dependent upon the electromeric transfer as halogen cannot increase number of its electrons, hence the reactivity in 2-position of the resorcinol molecule brings about the condensation with the subsequent 5-hydroxy-coumarin ring-formation.

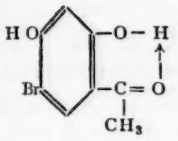

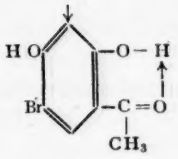

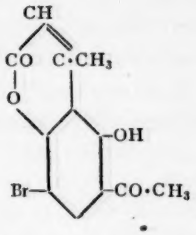

Experimental

Condensation of 5-ethyl-resacetophenone with ethyl acetoacetate in presence of aluminium chloride: Formation of 5-hydroxy-6-acetyl-8-ethyl-4-methyl-coumarin.—5-Ethyl-resacetophenone (3·8 g.: 1 mol.) prepared according to Shah, R. C., and Mehta (*J. Univ. Bom.*, 1935, **4**, 110) and ethyl acetoacetate (2·6 g.: 1 mol.) were added to the solution of aluminium chloride (5·6 g.: 2 mols.) dissolved in dry nitro-benzene (25 c.c.) and heated for one hour at 110–15°, keeping the temperature at 90° in the beginning. (Calcium chloride guard-tube.) HCl fumes were evolved. After HCl evolution was negligible, the reaction-mixture was cooled, ice and conc. HCl (10 c.c.) added and nitro-benzene steam-distilled off. The brown residue on crystallisation from alcohol gave needles, m.p. 168–69° (yield, 2 g.). Desai and Ekhlas also give the same melting point, which was not depressed on mixture with the above sample.

5-Hydroxy-6-acetyl-8-ethyl-4-methylcoumarin was reduced according to Clemmensen: the reduction product, 5-hydroxy-6: 8-di-ethyl-4-methyl-coumarin obtained melted at 171°, after crystallisation from alcohol. It did not give any colour with alcoholic ferric chloride; it dissolved in alkali with deep yellow colour. It was identical in all respects with an authentic sample prepared by the Pechmann condensation of 4: 6-di-ethyl-resorcinol with ethyl acetoacetate in presence of sulphuric acid, according to the method of Shah and Mehta.[6]

5-Hydroxy-6-acetyl-8-ethyl-4-methylcoumarin (1 g.) was subjected to the Kostanecki reaction with acetic anhydride (8 c.c.) and fused sodium acetate (2 g.) by heating the mixture at 170–80° for ten hours. The chromono-coumarin obtained on working up the reaction-mixture in the usual manner crystallised from alcohol, needles, m.p. 173°, identical with the sample of Desai and Ekhlas.[4]

Condensation of 5-bromo-resacetophenone with ethyl acetoacetate in presence of aluminium chloride: Formation of 5-hydroxy-6-acetyl-8-bromo-4-methyl coumarin.—5-Bromo-resacetophenone (5 g. : 1 mol.) prepared according to Desai and Ekhlas,[4] and ethyl acetoacetate (3 g. : 1 mol.) were added to aluminium chloride (5–5 g. : 2 mols.) in nitrobenzene (30 c.c.). The mixture protected from moisture ($CaCl_2$ guard-tube) was heated on oil-bath at 115–20° for one hour and finally to 130° till the evolution of HCl gas was negligible. After removal of nitro-benzene as before, the residue on crystallisation from alcohol gave needles, m.p. 208–10°; yield 1 g. (Found: Br, 27·17; $C_{12}H_9O_4Br$ requires Br, 26·9 per cent.) The coumarin dissolves in alkali with deep yellow colour without any fluorescence and gives with ferric chloride deep cherry-red colour in alcoholic solution.

The *acetyl* derivative prepared by acetic anhydride in pyridine solution by heating for about 6 hours on water-bath crystallised from dilute alcohol, m.p. 150°. (Found: Br, 23·32; $C_{14}H_{11}O_5Br$ requires Br, 23·6 per cent.)

The *oxime* crystallised from nitro-benzene in needles unmelted below 250°.

Kostanecki acetylation of 5-hydroxy-6-acetyl-8-bromo-4-methyl-coumarin: Formation of 4: 2′-dimethyl-6′-bromo-chromono-7′: 8′: 6: 5-α-pyrone.—The coumarin (1 g.), acetic anhydride (20 c.c.) and sodium acetate (2 g.) were reflexed at 170–80° for 10 hours. The cooled reaction-mixture was poured into water; the solid that separated was treated with Na_2CO_3 (5%) solution, washed with water and collected, and crystallised from dil. alcohol, granular crystals, m.p. 240–41° after shrinking. (Found: Br, 25·3.; $C_{14}H_9O_4Br$ requires Br, 24·92 per cent.) The chromono-α-pyrone did not give colouration with ferric chloride in alcoholic solution. It is sparingly soluble in dilute alkali solution.

Attempted condensation of 4-acyl-α-naphthol and other substituted resacetophenone derivatives.—We are thankful to Dr. R. D. Desai for the detailed information regarding the preparation of 4-acetyl-α-naphthol, recently published in these *Proceedings*.[11]

4-Acetyl-α-naphthol (3·5 g.) and ethyl acetoacetate (2·5 g.) were added to aluminium chloride (5·5 g.) in dry nitro-benzene (30 c.c.) and the mixture protected from moisture was heated at 100° for an hour. On working it up as in previous cases, the purified product obtained melted at 172°, the mixed melting point with an authentic sample of 4-methyl-1 : 2-α-naphtha-pyrone being undepressed. 4-Propionyl-α-naphthol on similar condensation also gave 4-methyl-1 : 2-α-naphtha-pyrone, the propionyl group being eliminated.

5-Nitro-resacetophenone,[12] 5-benzyl-resacetophenone,[13] ω-methoxy-resacetophenone,[14] methyl-β-resacetophenone-carboxylate,[15] 4 : 6-diacetyl-resorcinol and 2 : 4-diacetyl-resorcinol[16] were tried but the condensation could not be affected, either the original ketone being recovered or tarry material being formed.

The work on the effect of α-substituent in acetoacetic ester on the course of the reaction is in progress.

We thank Dr. M. S. Shah for his interest and facilities for the work. We are also grateful to Dr. R. C. Shah for his useful criticism and interest in the investigation.

Summary

The condensation of acetoacetic ester with substituted resacetophenones in the presence of aluminium chloride has been investigated. 5-Ethyl-resacetophenone, 5-bromo-resacetophenone underwent the condensation giving the expected 5-hydroxy-6-acetyl-coumarin derivatives. 4-Acetyl-α-naphthol and 4-propionyl-α- naphthol underwent the condensation but the product obtained was found to be 4-methyl-1 : 2-α-naphtha-pyrone, the acyl group being split off during the condensation. Negative results were obtained with 5-nitro-resacetophenone, 5-benzyl-resacetophenone, ω-methoxy-resacetophenone, methyl-β-resacetophenone carboxylate, 4 : 6-diacetyl-resorcinol and 2 : 4-diacetyl-resorcinol. The results obtained have been explained; negative groups like $-NO_2$, $-CO.Me$, etc., hinder the reaction, while positive groups like $-C_2H_5$ have no de-activating effect on the course of the reaction.

REFERENCES

1. Sethna, S. M., Shah, N. M., and Shah, R. C. — *J.*, 1938, 228.
2. Shah, N. M. and Shah, R. C. — *Ibid.*, 1938, 1424.
3. Deliwala, C. V., and Shah, N. M. — *Ibid.*, 1939, 1250.
4. Desai, R. D., and Ekhlas, M. — *Proc. Ind. Acad. Sci.*, 1938, **8**, 567.
5. Collie and Chrystall .. *J.*, 1907, **91**, 1804.
   Dey .. *Ibid.*, 1915, **107**, 1614, 1621.
6. Mehta and Shah, R. C. .. *J. Univ. Bom.*, 1935, **4**, 113.
7. Chakravarty and co-workers — *J. Ind. C. S.*, 1935, **12**, 622; 1937, **14**, 37, 725.
8. Desai and Hamid .. *Proc. Ind. Acad. Sci.*, 1937, **6**, 185.
9. Limaye .. *Rasayanam*, 1937, **1**, 99.
10. Sidgwick .. *J.*, 1920, 389.
    ——— and Turner .. *Ibid.*, 1922, 2256.
11. Akram and Desai .. *Proc. Ind. Acad. Sci.*, 1940, **11**, 149.
12. Baker .. *J.*, 1934, 1690.
13. Venkataraman and co-workers — *Proc. Ind. Acad. Sci.*, 1936, **3**, 206.
14. Stephen .. *J.*, 1920, 312.
15. Desai and Ekhlas .. *Proc. Ind. Acad. Sci.*, 1938, **8**, 199.
16. Baker .. *J.*, 1934, 1690; 1933, 1885.

MAGNETISM AND MOLECULAR STRUCTURE OF SULPHUR COMPOUNDS

By S. S. Dharmatti

(*Chemical Laboratories, Royal Institute of Science, Bombay*)

Received December 23, 1940

(Communicated by Dr. Mata Prasad, D.Sc., F.I.C., F.A.Sc.)

In previous communications[1] molecular structure of some of the selenium and tellurium compounds have been discussed from the magnetic standpoint, using Langevin equation and Slater's and Angus's methods for the calculation of $\Sigma\overline{r^2}$. Sulphur belongs to the same group of elements as selenium and tellurium and, like them, presents an interesting study on account of its variable valency. The study of the magnetic properties of sulphur compounds was initiated by Pascal[2] and was followed by Farquharson[3] who determined the susceptibilities of a series of these compounds with a view to test some of the modern theories of magnetism.

Recently Varadachari and Subramaniam[4] have measured and theoretically calculated the molecular susceptibilities of a number of sulphur compounds and they find that in some cases there is a wide divergence in their experimental and calculated values. Perhaps this is due to the fact that they used Kido's values for the constitutive constants. Nevgi[5] has also measured the magnetic susceptibilities of some of the sulphur compounds and has arrived at the conclusion that Pascal's susceptibility constants are in good agreement for sulphur in various valency states.

The present paper deals with the calculations of (i) the values of $\Sigma\overline{r^2}$ according to Slater's and Angus's methods as well as with the slight changes mentioned in the previous papers (*loc. cit.*) and hence (ii) the ionic susceptibilities for sulphur in various valency states. These values, given in Table I, have been made use of in calculating theoretically the magnetic susceptibilities of several compounds of sulphur for which the experimental values are known. The symbols used in this paper are the same as given in the previous publications (*loc. cit.*).

TABLE I

Diamagnetic Susceptibilities of S in Various Valency States Calculated from Various Methods

Valency states	Σr^2 Calculated by Slater's method	$\chi \times 10^6$ Calculated by Slater's method	Σr^2 Calculated by modification in Slater's method	$\chi \times 10^6$ Calculated by modification in Slater's method using constant ·790 instead of 0·807	Σr^2 Calculated by Angus's method	$\chi \times 10^6$ Calculated by Angus's method	Σr^2 Calculated by modification in Angus's method	$\chi \times 10^6$ Calculated by modification in Angus's method using constant 0·790 instead of 0·807
S divalent	15·05	−12·14	15·05	−11·890	13·65	−11·02	13·65	−10·78
S tetravalent	7·10	− 5·732	7·10	− 5·61	6·98	− 5·636	6·98	− 5·517
S hexavalent	1·73	− 1·397	1·73	− 1·367	1·61	− 1·302	1·61	− 1·275

Discussion of Results

(*a*) *Sulphur monochloride* (S_2Cl_2).—Like selenium monochloride (Se_2Cl_2) this compound also may have two different constitutions—the symmetrical Cl-S-S-Cl and the unsymmetrical $S = S\begin{matrix}Cl\\Cl\end{matrix}$. Susceptibilities calculated for both these formulæ are given in Table II.

The values calculated by the author for the constitution $S = S\begin{matrix}Cl\\Cl\end{matrix}$ are in better agreement with those experimentally obtained by Varadachari and Subramaniam than those calculated by the author. The experimental values obtained by Nevgi do not agree with any of the calculated values.

The above remarks show that Slater's and Angus's values for ionic susceptibilities are more correct than Kido's values employed by Varadachari and Subramaniam. Further the above results point out that the constitution of the sulphur monochlorides is represented by the Formula II and not I. This structure is also supported by the results of Meyer (*Z. Anorg. Allm. Chem.*, 1931, **146,** 203) who studied the smekel-Raman effect of Me_2S_2 and Et_2S_2 and found that the structural formula of the monochloride is $S = S\begin{matrix}Cl\\Cl\end{matrix}$ (II) and not Cl-S-S-Cl (I). Matossi and Aderhold (*Z. physik*, 1931, **683,** 683) also arrived at the same constitution (II) from the measurement of

TABLE II

Constitution	Cl-S-S-Cl (I)	$S=S\begin{matrix}Cl\\Cl\end{matrix}$ (II)
$(\chi_a)_1$	-0.5088×10^{-6}	-0.4613×10^{-6}
$(\chi_m)_1$	-68.68×10^{-6}	-62.272×10^{-6}
$(\chi_a)_2$	-0.5051×10^{-6}	-0.4585×10^{-6}
$(\chi_m)_2$	-68.18×10^{-6}	-61.90×10^{-6}
$(\chi_a)_3$	-0.4922×10^{-6}	-0.4523×10^{-6}
$(\chi_m)_3$	-66.44×10^{-6}	-61.05×10^{-6}
$(\chi_a)_4$	-0.4887×10^{-6}	-0.4496×10^{-6}
$(\chi_m)_4$	-65.96×10^{-6}	-60.697×10^{-6}
$(\chi_a)0_1$	..	-0.461×10^{-6}
$(\chi_m)0_1$	..	-62.2×10^{-6}
$(\chi_a)0_2$	..	-0.4964×10^{-6}
$(\chi_m)0_2$	..	-67.0×10^{-6}
$(\chi_a)0_3$	..	-0.405×10^{-6}
$(\chi_m)0_3$	..	-54.7×10^{-6}

0_1 Refers to the values observed by Varadachari and Subramaniam (*loc. cit.*).

0_2 Refers to the values calculated by Varadachari and Subramaniam (*loc. cit.*).

0_3 Refers to the values observed by Nevgi (*loc. cit.*).

Raman spectra of various sulphur compounds including the monochloride. This formula is also expected from the analogy of the monochloride with thionyl chloride.

However, Spong (*J.C.S.*, 1934, 485) who investigated the Raman spectrum, parachor and dielectric constant of sulphur monochloride concluded that the monochloride consists of a mixture of the two forms $S=S\begin{matrix}Cl\\Cl\end{matrix}$ and Cl-S-S-Cl. These results are not supported by the magnetic data.

In the case of selenium monochloride and monobromide (*loc. cit.*) the magnetic method definitely supports the constitution -Se-Se-, in which Se is divalent. Compounds of this type with tellurium are not known. It may therefore, be inferred that the affinity for halides decreases from Te to S in this group of elements and in S the union is of the most feeble kind.

(*b*) *Sulphur monoiodide* (S_2I_2).—The existence of a compound between iodine and sulphur has been the subject of great controversy for a long time. It is only recently that sulphur mono-iodide has been prepared in a pure state (*cf.* Rao, *Proc. Ind. Acad. Sci.*, 1939, **10,** 423 ; Rao, *Ibid.*, 1940, **11,** 162). Susceptibilities calculated according to the plan followed in this paper for the two possible constitutions for the monoiodide along with the values obtained by Varadachari and Subramaniam are given in Table III.

TABLE III

Constitution	I-S-S-I (I)	$S=S\begin{matrix}I\\I\end{matrix}$ (II)
$(\chi_a)_1$	$-\ 0{\cdot}3633\times 10^{-6}$	$-\ 0{\cdot}3430\times 10^{-6}$
$(\chi_m)_1$	$-\ 115{\cdot}48\ \times 10^{-6}$	$-\ 109{\cdot}072\ \times 10^{-6}$
$(\chi_a)_2$	$-\ 0{\cdot}3616\times 10^{-6}$	$-\ 0{\cdot}3418\times 10^{-6}$
$(\chi_m)_2$	$-\ 114{\cdot}98\ \times 10^{-6}$	$-\ 108{\cdot}7\ \times 10^{-6}$
$(\chi_a)_3$	$-\ 0{\cdot}3560\times 10^{-6}$	$-\ 0{\cdot}3393\times 10^{-6}$
$(\chi_m)_3$	$-\ 113{\cdot}24\ \times 10^{-6}$	$-\ 107{\cdot}856\ \times 10^{-6}$
$(\chi_a)_4$	$-\ 0{\cdot}3546\times 10^{-6}$	$-\ 0{\cdot}3381\times 10^{-6}$
$(\chi_m)_4$	$-\ 112{\cdot}76\ \times 10^{-6}$	$-\ 107{\cdot}497\ \times 10^{-6}$
$(\chi_a)0_1$		$-\ 0{\cdot}329\ \times 10^{-6}$
$(\chi_m)0_1$		$-\ 104{\cdot}6\ \times 10^{-6}$
$(\chi_a)0_2$		$-\ 0{\cdot}4064\times 10^{-6}$
$(\chi_m)0_2$		$-\ 129{\cdot}2\ \times 10^{-6}$

0_1 refers to the values observed by Varadachari and Subramaniam.

0_2 refers to the values calculated by Varadachari and Subramaniam using Kido's values for the constitution $S=S\begin{matrix}I\\I\end{matrix}$

The agreement between the calculated and the observed results shows that the constitution of the iodide is represented by the formula II which is analogus to that of the monochloride.

Using Kido's values Varadachari and Subramaniam conclude that it is merely a mixture of sulphur and iodine. These authors refer to Mellor (*Inorganic Chemistry*, Vol. X, p. 653) in support of their conclusion but the same literature mentions definitely the formation of this compound (*cf.* also Caven Lander, *Inorganic Chemistry*, p. 281). This conclusion does not also seem to be satisfactory on account of the unreliability of Kido's constants and the isolation of the iodide (*loc. cit.*).

(*c*) *Sulphur dichloride* (SCl_2).—Sulphur dichloride cannot have any other constitution excepting $S\begin{matrix}Cl\\Cl\end{matrix}$. It has been found in the case of $TeCl_2$ and $TeBr_2$ that the agreement between the theoretically calculated and the experimental values is not good and the divergence is assigned to the unstable nature of the compounds which makes it difficult to obtain the correct experimental values. Since sulphur dichloride is also an unstable compound, it is of interest to find if any disagreement exists in this case also. The theoretical values calculated according to Slater's and Angus's methods for this constitution are given in Table IV.

TABLE IV

Constitution	$S\begin{matrix}Cl\\Cl\end{matrix}$
$(\chi_a)_1$	$-0{\cdot}5489\times10^{-6}$
$(\chi_m)_1$	$-56{\cdot}54\times10^{-6}$
$(\chi_a)_2$	$-0{\cdot}5466\times10^{-6}$
$(\chi_m)_2$	$-56{\cdot}29\times10^{-6}$
$(\chi_a)_3$	$-0{\cdot}5381\times10^{-6}$
$(\chi_m)_3$	$-55{\cdot}42\times10^{-6}$
$(\chi_a)_4$	$-0{\cdot}5358\times10^{-6}$
$(\chi_m)_4$	$-55{\cdot}18\times10^{-6}$
$(\chi_a)0_1$	$-0{\cdot}467\times10^{-6}$
$(\chi_m)0_1$	$-48{\cdot}1\times10^{-6}$
$(\chi_a)0_2$	$-0{\cdot}478\times10^{-6}$
$(\chi_m)0_2$	$-49{\cdot}4\times10^{-6}$
$(\chi_a)0_3$	$-0{\cdot}478\times10^{-6}$
$(\chi_m)0_3$	$-49{\cdot}2\times10^{-6}$
$(\chi_a)0_4$	$-0{\cdot}4796\times10^{-6}$
$(\chi_m)0_4$	$-49{\cdot}4\times10^{-6}$

0_1 refers to the experimental values of Varadachari and Subramaniam.
0_2 refers to the experimental values of Kido.
0_3 refers to the experimental values of Nevgi.
0_4 refers to the values calculated by Varadachari and Subramaniam.

The Table above shows that although the experimental values of all the workers agree well with each other the calculated values are rather high. This difference is, as mentioned above, due to the unstable nature of the compound.

(*d*) *Thionyl chloride* ($SOCl_2$).—Judged by the formation of sulphonides (Stecker, *Ber.*, 1910, **43**, 1131; Grignard and Zorn, *Compt. rend.*, 1910, **150**, 1177; Oddo, *Gazetta*, 1911, **41**, 1, 11) such as diphenyl sulphoxide $O=S\langle^{C_5H_6}_{C_5H_6}$ and di-ethyl sulphite $O=S\langle^{OC_2H_5}_{OC_2H_5}$, the constitution of thionyl chloride can only be represented as $O=S\langle^{Cl}_{Cl}$. The calculations of the magnetic susceptibilities were, however, made from the point of view of oxygen atom which, due to strong binding has been shown to exhibit a peculiar behaviour in the case of $SeOCl_2$. The values calculated with the dia- and paramagnetic constants of oxygen are given in Table V.

TABLE V

Constitution $O=S\langle^{Cl}_{Cl}$	χ_a and χ_m obtained by using Pascal's value for $O(-3{\cdot}36\times10^{-6})$	χ_a and χ_m obtained by using the value of $O(+1{\cdot}8\times10^{-6})$
$(\chi_a)_1$	$-0{\cdot}4494\times10^{-6}$	$-0{\cdot}4061\times10^{-6}$
$(\chi_m)_1$	$-53{\cdot}492\times10^{-6}$	$-48{\cdot}332\times10^{-6}$
$(\chi_a)_2$	$-0{\cdot}4485\times10^{-6}$	$-0{\cdot}4052\times10^{-6}$
$(\chi_m)_2$	$-53{\cdot}37\times10^{-6}$	$-48{\cdot}21\times10^{-6}$
$(\chi_a)_3$	$-0{\cdot}4487\times10^{-6}$	$-0{\cdot}4053\times10^{-6}$
$(\chi_m)_3$	$-53{\cdot}396\times10^{-6}$	$-48{\cdot}23\times10^{-6}$
$(\chi_a)_4$	$-0{\cdot}4477\times10^{-6}$	$-0{\cdot}4043\times10^{-6}$
$(\chi_m)_4$	$-53{\cdot}277\times10^{-6}$	$-48{\cdot}117\times10^{-6}$
$(\chi_a)0_1$		$-0{\cdot}372\times10^{-6}$
$(\chi_m)0_1$		$-44{\cdot}3\times10^{-6}$
$(\chi_a)0_2$		$-0{\cdot}4479\times10^{-6}$
$(\chi_m)0_2$		$-53{\cdot}3\times10^{-6}$
$(\chi_a)0_3$		$-0{\cdot}451\times10^{-6}$
$(\chi_m)0_3$		$-53{\cdot}2\times10^{-6}$
$(\chi_a)0_4$		$-0{\cdot}380\times10^{-6}$
$(\chi_m)0_4$		$-45{\cdot}2\times10^{-6}$

0_1 refers to the values observed by Varadachari and Subramaniam.
0_2 refers to the values calculated by Varadachari and Subramaniam.
0_3 refers to the values observed by Kido.
0_4 refers to the values observed by Nevgi.

The above Table clearly shows that the values calculated using Slater's and Angus's values and the paramagnetic value for O are in better agreement with the observed values of Varadachari and Subramaniam and Nevgi. Kido's values are, however, in good agreement with the values calculated from the diamagnetic values of O. It is not possible at this stage to decide whether O in $SOCl_2$ is para- or dia-magnetic. However, if the analogy of this compound with $SeOCl_2$ is taken into consideration it will appear that O is paramagnetic and Varadachari and Nevgi's experimental values are correct. The small differences in the calculated and experimental values can be attributed to the strong binding of oxygen atom as has been pointed out in the case of $SeOCl_2$.

(*e*) *Sulphuryl chloride* (*SO_2Cl_2*).—On the basis of the physical and chemical properties of this substance its constitution has been accepted as 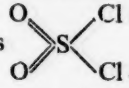
in which S is hexavalent. Values calculated for this constitution are given in Table VI.

Author's calculated values are in close agreement with those observed by Nevgi and Kido while those calculated by Varadachari and Subramaniam are rather high.

(*f*) *Chlorosulphonic acid* (*SO_3HCl*).—Chlorosulphonic acid forms with aromatic hydrocarbons sulphonic acids of the structure R-SO_2OH and sulphones of the structure , where R represents an aromatic radical such as phynyl (C_6H_5) (*cf.* Muller, *Ber.*, 1873, **6**, 227; de Purgold, *Ber.*, 1873, **6**, 602; Claesson, *J. Pract. Chem.*, 1879, (ii) **19**, 231). From these and other reactions it is believed that in chlorosulphonic acid the chlorine atom is directly attached to sulphur and its constitution is represented

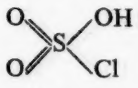

The compound SO_2Cl_2 (discussed in the previous paragraphs) is obtained by replacing OH by Cl in SO_3HCl. The constitutions of the compounds SO_2Cl_2 and SO_3HCl being the same, the difference between their molecular susceptibilities ought to be the difference in the susceptibilities of OH and Cl group which according to Pascal is 12·5. According to Nevgi's and

TABLE VI

Constitution	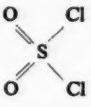
$(\chi_a)_1$	$-0{\cdot}3891 \times 10^{-6}$
$(\chi_m)_1$	$-52{\cdot}517 \times 10^{-6}$
$(\chi_a)_2$	$-0{\cdot}3888 \times 10^{-6}$
$(\chi_m)_2$	$-52{\cdot}487 \times 10^{-6}$
$(\chi_a)_3$	$-0{\cdot}3884 \times 10^{-6}$
$(\chi_m)_3$	$-52{\cdot}422 \times 10^{-6}$
$(\chi_a)_4$	$-0{\cdot}3820 \times 10^{-6}$
$(\chi_m)_4$	$-52{\cdot}365 \times 10^{-6}$
$(\chi_a)0_1$	$-0{\cdot}365 \times 10^{-6}$
$(\chi_m)0_1$	$-49{\cdot}3 \times 10^{-6}$
$(\chi_a)0_2$	$-0{\cdot}4193 \times 10^{-6}$
$(\chi_m)0_2$	$-56{\cdot}6 \times 10^{-6}$
$(\chi_a)0_3$	$-0{\cdot}397 \times 10^{-6}$
$(\chi_m)0_3$	$-53{\cdot}6 \times 10^{-6}$
$(\chi_a)0_4$	$-0{\cdot}402 \times 10^{-6}$
$(\chi_m)0_4$	$-54{\cdot}6 \times 10^{-6}$

0_1 refers to the experimental values of Varadachari and Subramaniam.
0_2 refers to the calculated values of Varadachari and Subramaniam.
0_3 refers to the experimental value of Nevgi.
0_4 refers to the experimental value of Kido.

Kido's data this difference is 6·7 and 8·0, respectively. Values calculated according to Slater's and Angus's values are given in Table VII.

The values observed by Nevgi and Kido are much higher than the calculated values. Since in the case of sulphuryl chloride there is a very close agreement between the calculated and experimental values of Nevgi and Kido, they can be taken as correct. The difference between the molecular susceptibility of SO_2Cl_2 (53·6) as observed by Nevgi and the molecular susceptibility of SO_3HCl (37·86) calculated above is 15·7. This is in close agreement with the value expected from Pascal's data (12·5).

TABLE VII

$(\chi_a)_1$	$-0{\cdot}3249\times10^{-6}$
$(\chi_m)_1$	$-37{\cdot}86\times10^{-6}$
$(\chi_a)_2$	$-0{\cdot}3246\times10^{-6}$
$(\chi_m)_2$	$-37{\cdot}287\times10^{-6}$
$(\chi_a)_3$	$-0{\cdot}3241\times10^{-6}$
$(\chi_m)_3$	$-37{\cdot}762\times10^{-6}$
$(\chi_a)_4$	$-0{\cdot}3239\times10^{-6}$
$(\chi_m)_4$	$-37{\cdot}735\times10^{-6}$
$(\chi_a)0_1$	$-0{\cdot}402\times10^{-6}$
$(\chi_m)0_1$	$-46{\cdot}9\times10^{-6}$
$(\chi_a)0_2$	$-0{\cdot}400\times10^{-6}$
$(\chi_m)0_2$	$-46{\cdot}6\times10^{-6}$

0_1 refers to the values observed by Nevgi.
0_2 refers to the values observed by Kido.

Conclusion

Table VIII gives at a glance the experimental and the calculated values for the constitution of the sulphur compounds found according to the plan employed in this investigation. Wide differences between the calculated and the observed values are observed only in the case of compounds (*c*) and (*f*). This may be due either to the want of purity of the substances used or to their instability.

In the case of sulphur compounds also as in the case of Se and Te compounds, the magnetic method seems to be of great value in fixing the correct molecular constitution and the magnetic susceptibilities calculated by Slater's and Angus's method seem to be in better agreement with the experimental ones.

Further work on compounds of this group is in progress.

TABLE VIII

Sulphur Compounds

Compound	Constitution	$-\chi_a \times 10^6$ & $-\chi_m \times 10^6$ observed by other authors	$-\chi_a \times 10^6$ & $-\chi_m \times 10^6$ calculated by Slater's method	$-\chi_a \times 10^6$ & $-\chi_m \times 10^6$ calculated by the modification of Slater's method	$-\chi_a \times 10^6$ & $-\chi_m \times 10^6$ calculated by Angus's method	$-\chi_a \times 10^6$ & $-\chi_m \times 10^6$ calculated by the modification of Angus's method
S_2Cl_2	$S=S\begin{matrix}Cl\\Cl\end{matrix}$	(χ_a) 0·461 (χ_m) 62·2	0·4613 Varadachari and Subramaniam 62·272	0·4585 61·90	0·4523 61·05	0·4496 60·697
		(χ_a) 0·405 (χ_m) 64·7	Nevgi			
S_2I_2	$S=S\begin{matrix}I\\I\end{matrix}$	(χ_a) 0·329 (χ_m) 104·6	0·3430 Varadachari and Subramaniam 109·072	0·3418 108·7	0·3393 107·856	0·3381 107·497
SCl_2	$S\begin{matrix}Cl\\Cl\end{matrix}$	(χ_a) 0·467 (χ_m) 48·1	Varadachari and Subramaniam			
		(χ_a) 0·478 (χ_m) 49·4	0·5489 Kido 56·54	0·5466 56·29	0·5381 55·42	0·5358 55·18
		(χ_a) 0·478 (χ_m) 49·2	Nevgi			

$SOCl_2$		(χ_a) 0·372 (χ_m) 44·3	0·4061 Varadachari and Subramaniam 48·332	0·4052 48·21	0·4053 48·23	0·4043 48·117
		(χ_a) 0·451 (χ_m) 53·2	Kido			
		(χ_a) 0·380 (χ_m) 45·2	Nevgi			
SO_2Cl_2	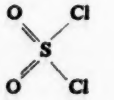	(χ_a) 0·365 (χ_m) 49·5	0·3891 Varadachari and Subramaniam 52·517	0·3888 52·487	0·3884 52·422	0·3820 52·395
		(χ_a) 0·397 (χ_m) 53·6	Nevgi			
		(χ_a) 0·402 (χ_m) 54·6	Kido			
SO_2HCl	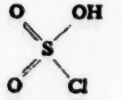	(χ_a) 0·402 (χ_m) 46·9	0·3249 Nevgi 37·86	0·3246 37·827	0·3241 37·762	0·3239 37·735
		(χ_a) 0·400 (χ_m) 46·6	Kido			

The author takes this opportunity to express his sincere thanks to Dr. Mata Prasad, D.Sc., F.I.C., F.N.I., for his keen interest and guidance throughout the work. He is also thankful to Professor Sir S. S. Bhatnagar, O.B.E., D.Sc., for his helpful criticisms and suggestions.

REFERENCES

1. Mata Prasad and Dharmatti .. *Curr. Sci.*, 1940, **9**, 175.
   ———— .. *Proc. Ind. Acad. Sci.*, 1940, **12**, 185.
   S. S. Dharmatti .. *Ibid.*, 1940, **12**, 211.
2. Pascal .. *Compt. rend.*, 1921, **3**, 45.
3. Farquharson .. *Phil. Mag.*, 1932, **14**, 1003.
4. Varadachari and Subramaniam *Proc. Ind. Acad. Sci.* (A), 1936, **3**, 428.
5. Nevgi .. *J. Univ. Bombay*, 1938, 7, 82.

STUDIES IN CHLORAL AMIDES

Part X. Reactivity of α-Halogen in α-Halogeno chloral-methoxy nitro-, and bromo-benzamides

By (Late) N. W. Hirwe, Miss. K. D. Gavankar and B. V. Patil
(Chemical Laboratories, Royal Institute of Science, Bombay)

Received January 5, 1941
(Communicated by Dr. Mata Prasad, D.Sc., F.A.Sc.)

In continuation of the work on chloral nitro salicylamides, chloral-bromo salicylamides and their methyl ethers the action of phosphorus pentachloride and of phosphorus tribromide on the methyl ethers only has been studied and the expected reactivity of α-halogen atom has also been shown by various reactions.[1]

Chloral 3 : 5 dinitro 2-methoxy benzamide reacts differently with phosphorus pentachloride. It gives a compound whose analysis points to the following imidochloride formula. It is however more stable to moisture than the ordinary imidochlorides.

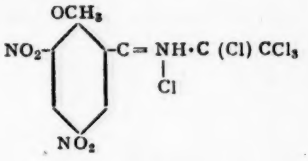

Experimental

All the experimental methods are the same as usual by the previous workers (Ch. ref. No. 1).

[1] Rana and Hirwe, *J. Ind. Chem. Soc.*, 1940, 481; Hirwe and Deshpande (Studies in Chloral Amides, Part IX).

Compound	Solvent	Crystalline nature	M.P.	Molecular formulæ	Found %		Required %
α-Chloro chloral-5-nitro-2-methoxy benzamide	acetone	needles	149–50°	$C_{10}H_6O_4N_2Cl_4$	Cl	38·9	39·2
α-Methoxy chloral-5-nitro-2-methoxy benzamide	methyl alcohol	cubes	144°	$C_{11}H_{11}O_5N_2Cl_3$	Cl N	29·8 7·6	29·8 7·8
α-Ethoxy chloral-5-nitro-2-methoxy benzamide	alcohol	prisms	146–47°	$C_{12}H_{13}O_5N_2Cl_3$	Cl	28·8	28·7
α-Anilino chloral-5-nitro-2-methoxy benzamide	,,	needles	168–69°	$C_{16}H_{14}O_4N_3Cl_3$	Cl	25·3	25·5
α-(*o*-toluidino)-chloral-5-nitro-2-methoxy benzamide	,,	,,	151–52°	$C_{17}H_{16}O_4N_3Cl_3$	Cl	24·9	24·6
α-(*p*-toluidino)-chloral-5-nitro-2-methoxy benzamide	,,	greenish needles	171–72°	$C_{17}H_{16}O_4N_3Cl_3$	Cl	24·4	24·6
α-Methoxy chloral-3-nitro-2-methoxy benzamide	methyl alcohol	rectangular plates	104–05°	$C_{11}H_{11}O_5N_2Cl_3$	Cl	29·5	29·8
2-Methoxy-3 : 5-dinitro benzamide chloro-β-trichloro ethyl imino chloride	alcohol	plates	91°	$C_{10}H_6O_5N_3Cl_5$	Cl C H N	41·8 28·6 1·5 9·8	41·7 28·2 1·4 9·8
α-Chloro chloral-5-bromo-2-methoxy benzamide	acetone	rectangular plates	150–51°	$C_{10}H_6O_2NCl_4Br$	halide N	192·2 3·4	192·4 3·5
α-Bromo chloral-5-bromo-2-methoxy benzamide	,,	square plates	140°	$C_{10}H_6O_2NCl_3Br_2$	halide	178·9	183·1
α-Ethoxy chloral-5-bromo-2-methoxy benzamide	alcohol	cubes	147–49°	$C_{12}H_{13}O_3NCl_3Br$	halide N	151·8 3·3	152·5 3·5
α-Anilino chloral-5-bromo-2-methoxy benzamide	,,	needles	168–69°	$C_{16}H_{14}O_2N_2Cl_3Br$	halide	136·2	136·8
α-(*o*-toluidino)-chloral-5-bromo-2-methoxy benzamide	,,	cubes	166–67°	$C_{17}H_{16}O_2N_2Cl_3Br$	halide N	132·7 5·9	132·6 6·0

α-(*p*-toluidino)-chloral-5-bromo-2-methoxy benzamide	acetone	needles	175–77°	$C_{17}H_{16}O_3N_2Cl_3Br$	halide	131·7	132·6
α-Phenoxy chloral-5-bromo-2-methoxy benzamide	alcohol	parallelograms	191–92°	$C_{16}G_{13}O_3NCl_3Br$	halide	134·7	136·4
α-Chloro chloral-3 : 5-dibromo-2-methoxy benzamide	acetone	plates	109–10°	$C_{10}H_7O_2NCl_4Br_2$	halide	201·6	200·0
α-Anilino chloral-3 : 5-dibromo-2-methoxy benzamide	alcohol	needles	166–67°	$C_{16}H_{13}O_2N_2Cl_3Br_2$	halide	151·0	151·7
α-(*o*-toluidino)-chloral-3 : 5-dibromo-2-methoxy benzamide	,,	,,	166–67°	$C_{17}H_{15}O_2N_2Cl_3Br_2$	halide	148·6	147·9
α-(*p*-toluidino)-chloral-3 : 5-dibromo-2-methoxy benzamide	acetone	plates	173–74°	$C_{17}H_{15}O_2N_2Cl_3Br_2$	halide	148·7	147·9

STUDIES ON THERMAL REPULSION

By L. A. Ramdas and S. Y. Joglekar
Meteorological Office, Poona.

Received March 4, 1941

1. *Introduction*

In a series of papers[1, 2, 3, 4, 5] published during the last few years the subject of the dust-free or dark layer of air surrounding a hot body in relation to the convective movements in its neighbourhood was discussed in the light of experimental work carried out at Poona. It was shown by Ramdas and Paranjpe[3, 4] that the dark space may undergo variations in its extent under the influence of convection but that when care was taken to eliminate all convective movements in the interspace between a hot and a cold surface by bringing them sufficiently close to each other, the whole interspace is filled by the dark or dust-free layer. The above result was very significant because the phenomenon of thermal repulsion could be observed in its *true simplicity* for the first time without the element of confusion introduced by the convective movements which were always present in the experiments made by earlier workers.[6, 7, 8, 9, 10] *In all our subsequent investigations on this problem, we have worked with convection-free air cells.*

For example, in the work referred to above,[3, 4] when a *horizontal* cold surface was brought to within 3 mm. of a *horizontal* hot surface, the convective movements present at larger separations, all stopped. Under these conditions if some smoke or dust particles entered the interspace, the particles were seen to be repelled *vertically downwards towards the cold surface.* The movement of the particles was *normal* to the hot surface and without any trace of a horizontal component. The velocity was also shown to be proportional to the temperature gradient. By an interferometric method[5] it was found that the temperature gradient between the hot and the cold surface was *uniform* as soon as the thickness of the horizontal air cell was made less than 4 mm.

In the earlier experiments at Poona the observations of the velocity of the particles in the interspace were made by introducing a layer of smoke very gently and noting the time taken by the upper edge of the smoke to move to the cold surface. The particles here moved downwards under the joint influence of gravity and of the force of thermal repulsion. Knowing

the average size of particles and applying Stokes's law, an estimate of the force of thermal repulsion was made. Since then a considerable amount of work has been done on individual particles moving under the joint influence of gravity (*vertical*) and a horizontal thermal gradient between vertical hot and cold surfaces placed parallel to each other. The thermal repulsion could also be observed when the free particle was replaced by a thin flake of mica suspended in the space between the hot and cold surfaces by means of a fine quartz fibre. Some instruments have also been designed for making air or water free from dust by passing the fluid through the interspace between hot and cold surfaces kept sufficiently close to each other to prevent convection.

In the present paper the authors intend to give a brief outline of some of the main results to indicate the scope of these investigations. A detailed account of the different experiments including those with the suspended mica piece using (1) various thicknesses of mica piece, (2) different gases, (3) mica pieces coated with silver and lamp black, and (4) different air pressures ranging from a few millimetres of mercury to one atmosphere is being given in a thesis under preparation by the junior author of this paper. An explanation of the phenomenon of thermal repulsion on the basis of the kinetic theory of gases will be discussed in a later paper.

2. *Measurements of the Velocity of Individual Particles in a Thermal Field and the Estimation of the Force of Thermal Repulsion*

(*a*) *Description of experimental arrangements.*—Fig. 1 shows the horizontal section of the experimental arrangement. A and B are two rectangular

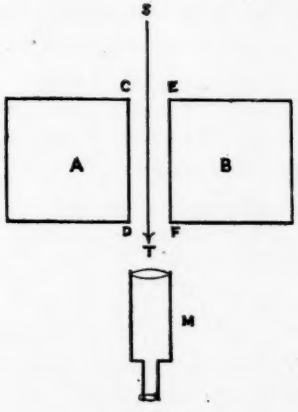

FIG. 1

vessels, the sides CD and EF of which enclose a thin film of air through which oil drops sprayed from above fall vertically (perpendicular to the plane of the paper). To eliminate stray air currents the ends CE and DF are covered by glass plates. Hot water of the required temperature is circulated in A and cold water in B. Oil drops sprayed above and entering the space CEFD are illuminated at a slight angle by the pencil of light ST. The illuminated drops are viewed through a low power microscope M into which the direct beam ST does not enter, but light scattered or reflected by the falling drops can enter. Under the influence of gravity alone an oil drop falls vertically; the thermal gradient repels it from A to B. The distance from CD to EF is decreased sufficiently to eliminate convection in the air cell. Careful observations of the movements of particles let into the vertical air cell showed that when the distance between the hot and cold surfaces is 1 mm. or less, convection is absent. Under these circumstances the oil drops are observed to travel in straight lines inclined downwards from the hot towards the cold surface in a plane perpendicular to the direction of observation. The eye-piece of the microscope M is provided with a square graticule with the help of which the number of divisions through which a droplet moves vertically and horizontally in a given time interval can be measured. In the arrangement used 1 mm. was equal to 3·5 divisions of the graticule and the time intervals were measured with a stop-watch reading correct to 1/20th of a second. The advantage of this experiment is obvious. The vertical component of the velocity of a droplet can be used to calculate its radius r by using Stokes's law

$$6\pi r \eta v = \tfrac{4}{3}\pi r^3 (\rho - \rho') g$$

where η is the viscosity of air [η at temperature $t°$ C.

$$= 1715 \cdot 5 \times 10^{-7} (1 + \cdot 00275\, t - \cdot 00000034\, t^2)],$$

v is the vertical velocity of the droplet,

ρ is the density of the droplet (0·92 gr. per c.c.)

ρ' is the density of air, and

g is the acceleration due to gravity.

Neglecting ρ' which is small compared to ρ, we have

$$r = \sqrt{\frac{9}{2} \cdot \frac{\eta v}{\rho g}}.$$

The size of droplet and the horizontal component of its velocity are thus obtained simultaneously by observation on the same droplet in a single measurement.

Table I gives the values of r and v_h the horizontal velocity for a set of nine droplets observed one after the other in a single experiment when the hot surface was at 51·5° C. and the cold one at 23·4° C., the separation between them being 0·0572 cm. The temperature gradient was 409° C. per cm.

TABLE I

Droplet No.	Horizontal distance travelled by droplet in cm.	Vertical distance travelled by droplet in cm.	Time taken in seconds	Vertical velocity in cm./sec.	Radius in cm. × 10^4	Horizontal velocity in cm./sec.
1	·0143	·0629	0·55	·1143	3·293	·0260
2	·0357	·1510	1·25	·1208	3·385	·0286
3	·0143	·0692	0·45	·1537	3·818	·0318
4	·0215	·1258	0·75	·1677	3·987	·0287
5	·0143	·1133	0·55	·2060	4·420	·0260
6	·0215	·2831	1·15	·2461	4·831	·0187
7	·0257	·2831	1·20	·2359	4·731	·0214
8	·0172	·0787	0·55	·1431	3·684	·0313
9	·0143	·0787	0·65	·1211	3·388	·0220

More than a thousand measurements with individual drops like those given in Table I were made with different temperature gradients. It may be remarked that with the arrangement described in Fig. 1 it was quite easy to make measurements on droplets varying in radius from 2×10^{-4} to 5×10^{-4} cm. Droplets smaller than 2×10^{-4} cm. moved too early from the hot to the cold surface for observations to be made on them while those larger than 5×10^{-4} cm. moved vertically too fast for their velocities to be measured. We are thus left with only a small range of size. A wider range of size can be brought under observation only if a more elaborate time-measuring device and photographic methods of recording the tracks of the droplets are used.

(*b*) *Discussion of measurements made with oil drops.*—In this section we shall focus our attention on the variation of the horizontal component of the velocity of a droplet with the horizontal thermal gradient. Any possibls influence of drop-size is restricted by picking out observations on drops within the small range $2 \cdot 8 \times 10^{-4}$ to $3 \cdot 2 \times 10^{-4}$ cm. out of the very large number of available observations. These observations were then grouped under small intervals of temperature gradient, *viz.*, 50–69° C. per cm.,

70–89° C. per cm., and so on up to 450° C. per cm. The mean values of v_h the horizontal velocity are plotted against the mean values of temperature gradient (*viz.*, 60, 80, 100 · · · 420° C. per cm.) in Fig. 2. The dots in the diagram cluster about a straight line drawn through the origin indicating that the velocity of a particle under the influence of a force acting in the direction of the thermal gradient is proportional to the thermal gradient. From the slope of the straight line in Fig. 2 it is found that the horizontal velocity due to unit temperature gradient (1° C. per cm.) is of the order of $8 \cdot 17 \times 10^{-5}$ cm. per second.

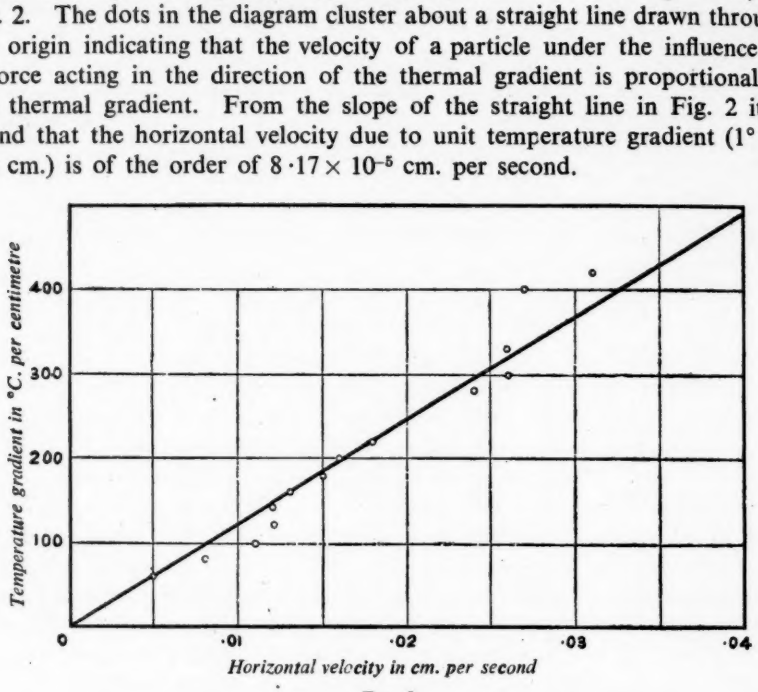

FIG. 2

Variation of horizontal velocity of particles ($2 \cdot 8$ to $3 \cdot 2 \times 10^{-4}$ cm.) with temperature gradient (between two vertical surfaces ·6 to ·7 mm. apart)

Velocity due to a temperature gradient of 1° C. per cm. $= 8 \cdot 17 \times 10^{-5}$ cm./sec.

As discussed in previous papers[3,4] the uniform velocity of the droplet should be looked upon as being due to an extra pressure or force acting on a droplet moving through a viscous medium, *viz.*, air, under the influence of the temperature gradient. We may apply Stokes's law to this case also. Neglecting the density of air as compared to that of the droplet we have,

$$6 \pi \eta r v_h = \tfrac{4}{3} \pi r^3 \rho \alpha$$

where v_h is the horizontal component of the velocity of the droplet and α is the acceleration due to the thermal gradient. Then,

$$\alpha = \frac{6 \pi \eta r v_h}{\tfrac{4}{3} \pi r^3 \rho} = \frac{9 \eta v_h}{2 r^2 \rho}.$$

Substituting the value $\eta = 1 \cdot 9 \times 10^{-4}$,

$v_k = 8 \cdot 17 \times 10^{-5}$ cm. per second for a unit temperature gradient (1° C. per cm.), $r = 3 \times 10^{-4}$ and $\rho = \cdot 92$, we have $a = \cdot 8437$ per unit temperature gradient.

The value of a for a temperature gradient of 400° C. per cm. is equal to 337. This is slightly more than 1/3 the value of g, the acceleration due to gravity.

The force per unit area or the extra pressure P exerted on the droplet, when expressed per unit area of the cross-section of the droplet through its centre and normal to the direction of its movement, under the influence of temperature gradient of 400° C. per cm. is given by

$$P = \frac{F}{\pi r^2} = \frac{m a}{\pi r^2} = \frac{\frac{4}{3} \pi r^3 \rho a}{\pi r^2} = \frac{4}{3} r \rho a = \cdot 124 \text{ dyne/cm.}^2$$

Again $P = 3 \cdot 1 \times 10^{-4}$ dyne/cm.^{2} per unit temperature gradient.

3. *Measurements with Thin Pieces of Mica Suspended in the Space between Vertical Hot and Cold Surfaces*

In the previous pages we have attempted to estimate the force acting on a free drop or particle when it is in a thermal field from the uniform velocity with which it moves against the viscous resistance of air. This led us to investigate whether this force can be measured directly by suspending a light object like a piece of thin mica in a horizontal thermal field by means of a long and very fine quartz fibre and observing the steady displacement from the vertical experienced by it as soon as the thermal field is put on. Preliminary observations showed that the mica piece does undergo a visible displacement in a thermal field.

A suitable apparatus was constructed immediately for carrying out the measurements with precision. Fig. 3 shows a vertical cross-section of the apparatus. The temperature gradient is maintained between the faces GH and KL of the vessels A and B which are maintained at the desired temperatures by circulating hot and cold water respectively through the tubes C_1, C_2 and C_3, C_4. Thermometers T_1 and T_2 for measuring the temperatures of the water in A and B are inserted through apertures provided for the purpose. The vessels A and B slide in the outer piece CEFD so that the distance between GH and KL may be adjusted as desired. The joints at C, D, E and F can be made air-tight by means of modeller's clay or a mixture of bees-wax and rosin. The mica piece M is suspended by means of a quartz fibre, the upper end of which is attached to the end of the moveable rod R. The rod R can be fixed in position as desired by

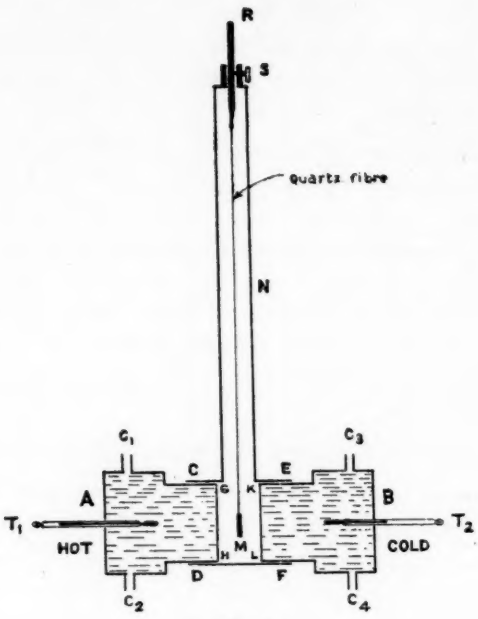

FIG. 3

means of the screw S. The tube N is screwed on to an aperture in the upper surface CE. The joints at both ends of the tube N can also be made air-tight. The mica piece kept parallel to the surfaces GH and KL is seen edge-wise in Fig. 3, its thickness being shown exaggerated. The pieces used in the experiments were square or rectangular (dimensions 2 or 3 mm. by 4 or 5 mm.) weighing 20 mg. or less. A low power microscope with a graticule is used to view the edge of the mica piece which is visible through a circular glass window on the front side of the apparatus. The mica piece is illuminated by sending a beam of light through another glass window at the back. The position of the quartz fibre where it meets the edge of the mica piece can be read off from the vertical lines in the graticule. The magnification was 6 divisions in the graticule equal to 1 mm. When the temperatures in A and B are the same, the quartz fibre hangs vertically. When hot water is circulated through A, the mica is displaced towards the cold surface KL. If cold water at the same temperature as in B is again circulated through A, the mica piece comes back to its original position.

From the displacement of the lower end of the quartz fibre where it meets the mica piece and knowing the length of the quartz fibre we know

θ the angle by which the suspended system is displaced from the vertical. If M is the mass of the mica, A its area, then the total horizontal force on the mica piece due to the temperature gradient is given by $F = Mg\,\theta$, for small values of θ. The pressure P on the mica or the force per unit area is given by

$$P = \frac{F}{A} = \frac{Mg\,\theta}{A} = mg\,\theta,$$

where m is the mass per unit area of mica.

To give one example, in one of the experiments the mass of the mica piece was ·00198 gr., its area being 0·09 sq. cm. The length of the quartz fibre was 20 cm. The deflection corresponding to a difference of temperature of 44·8° C. between the faces GH and KL (Fig. 4) when separated by 0·108 cm. was 0·8 of a scale division in the graticule, *i.e.*, $\frac{0\cdot8}{60}$ cm. The value of θ is equal to $\frac{0\cdot8}{60\times20}$ radian and the temperature gradient is equal to $\frac{44\cdot8}{0\cdot108}$ or 414·1° C. per cm.

The force F on an area ·09 sq. cm. $= Mg\,\theta$

$$= \cdot00198 \times 981 \times \frac{0\cdot8}{60\times20}$$

$$= 1\cdot295 \times 10^{-3} \text{ dyne.}$$

The pressure P per sq. cm. for a temperature gradient of 414·1° C. per cm. .. $= 1\cdot439 \times 10^{-2}$ dyne per cm.^{2}

Using the same piece of mica, quartz fibre, etc., the pressure per unit area has been measured for different temperature gradients. Some typical values are given in Table II.

TABLE II

Temperature gradient in ° C. per cm.	P, pressure in dynes per sq. cm. × 10^2
89	·36
144	·54
170	·72
243	1·08
331	1·25
385	1·43

From the above values it is estimated that the mean pressure per unit area for unit temperature gradient is of the order of $3 \cdot 8 \times 10^{-5}$ dyne per cm.^{2}

A number of experiments were performed using mica sheets of the same thickness but different shapes and areas. They show that the pressure per unit area due to a given thermal gradient is constant, the actual force on the mica being proportional to the area.

Thermal pressure and radiation pressure.—Before concluding this section we may compare the pressure due to the thermal gradient with the radiation pressure exerted by the temperature radiation from the two surfaces on either side of the mica piece in the above experiments.

It can be shown that the pressure of radiation on a small surface facing another plane surface parallel to it but infinite in extent is given by $\frac{4R}{5V}$, where R is the black body radiation falling on the small element (equal to σT^4, where σ is the Stefan-Boltzmann's constant and T is the absolute temperature of the infinite plane) and V is the velocity of radiation. The difference of pressure due to radiation from two infinite plane surfaces on a surface of unit area suspended between them will be

$$4\sigma \frac{(T_1^4 - T_2^4)}{5V},$$

where T_1 and T_2 are the temperatures of the hot and the cold surfaces. Putting $T_1 = 70°$ C. and $T_2 = 30°$ C. we have a difference in the pressure of radiation of the order of $8 \cdot 3 \times 10^{-6}$ which is roughly $\frac{1}{1000}$ of the thermal pressure when the two surfaces are separated by a distance of 1 mm. *We thus see that we are dealing with a phenomenon which is very much more conspicuous than radiation pressure.*

4. An Apparatus for the Filtration of Dusty Air or Water

It is obvious that the *greater efficiency* with which a particle is repelled in the presence of a temperature gradient *when convection is eliminated* than when convection is present can be utilised for the rapid removal of dust in ordinary air. A thermal filter based on the above principle has been designed. A vertical cross-section of the apparatus is shown in Fig. 4, where EFGH is maintained at ordinary temperature by circulating cold water through the tubes T_3 and T_4 in the outer chamber ABCD, and KLMN is maintained at a high temperature by heating water contained in the inner vessel. The separation between the surfaces EF and KL is of the order of 1/5 mm. A large temperature gradient is thus maintained between KLMN and EFGH.

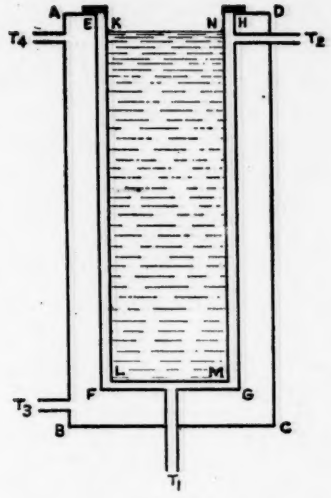

FIG. 4

Thermal filter for dusty air or water

Dusty air can be admitted through the tube T_1 into the interspace between the hot and cold surfaces, and when it comes out through the tube T_2 it is quite free from dust as all the particles are repelled towards the cold surface before the air stream leaves the apparatus. The efficiency of this filter has been tested by passing air heavily laden with smoke into the apparatus and verifying that when the air, after passing through the thermal filter, is allowed to enter another chamber illuminated by a condensed beam of light, not a single particle can be seen in the track of the beam of light. An attempt was made to see whether particles suspended in water can be removed by passing water through the above apparatus. The movement of the particles through water which is a very much more viscous medium, must be correspondingly slower, so that for the complete elimination of the suspended particles, the apparatus will have to be correspondingly longer.* With the present apparatus, therefore, one can only expect a partial elimination of the dust particles in water. Our experiments made with a number of soil suspensions, fully justify the above expectation. A comparison between the number of particles present before and after filtration can be made by examining corresponding samples of water kept in rectangular glass vessels in a condensed beam of light. In Fig. 5 photographs of the tracks of the

* Such an apparatus is being made.

FIG. 5

Photographs of the track of a beam of light in water containing clay particles in suspension (*a*) before and (*b*) after passing through the thermal filter

beam of light in (*a*) unfiltered water and (*b*) water after filtration through the apparatus are shown. The intensity of the Tyndall cone is seen to be very much weaker in the case of filtered water. It may be remarked that the current of water through the apparatus has to be passed sufficiently slowly to attain maximum efficiency with the given size of the apparatus.

5. *A Simple Dust Counter*

The same principle was used for the design of a simple dust counter. A vertical section of this apparatus is shown in Fig. 6. The hot surface is

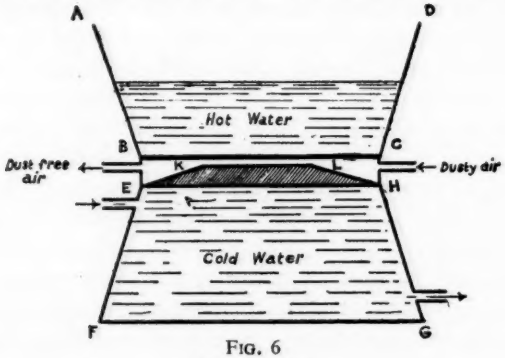

FIG. 6

Dust counter.

the bottom of the vessel ABCD in which water is maintained at a higher temperature. The cold surface below is formed by the upper surface of the lower vessel EFGH through which cold water is circulated. The interspace between the two surfaces is covered at the two ends by means of metal plates of suitable shape, to which the tubes for the admission of the

dusty air and for its exit are attached. The interspace is wide at the beginning and end so that dust particles will not be affected in these regions. As soon, however, as the air enters the narrow region KL which is about 1/5 mm. in thickness the particles are repelled and they stick to a microscope slide kept above the cold surface. In fact, the size of the cold surface is exactly that of the standard microscope slide. Preliminary observations with air heavily laden with smoke show that all the particles are deposited on the microscope slide if the air is aspirated through the apparatus at a rate of 1 c.c. per second or less.

Precise measurements using the instrument described in Sections 4 and 5 above are in progress and the results obtained will be discussed in due course.

6. *Conclusion*

In the present paper work done on the phenomenon of thermal repulsion of particles or objects placed in a thermal field (where convection has been eliminated by bringing the hot and cold surfaces sufficiently close to each other) has been described. Observations have been made with (*a*) drops falling freely under the joint influence of gravity and a horizontal thermal gradient and (*b*) objects like thin mica pieces suspended in the thermal field by means of a fine quartz fibre. The pressure due to the thermal field is verified in both cases and estimates have been given. The pressure is about 1000 times as large as radiation pressure. A thermal filter and a dust counter utilising the above phenomenon have been designed by the authors. These are described.

In conclusion, the authors have great pleasure in thanking the Director-General of Observatories for the facilities given at the Meteorological Office for these investigations.

REFERENCES

1. Ramdas, L. A., and Malurkar, S. L. — *Indian Journal of Physics*, 1932, 7, Pt. I, p. 1.
2. ———— .. *Nature*, Feb. 1932, 6, p. 201.
3. Ramdas, L. A. .. *The Journal of the University of Bombay*, Sep. 1937, 6, Pt. II, p. 18.
4. Paranjpe, M. K. .. *Proceedings of the Indian Academy of Sciences*, 1936, 4A, No. 4, 423.
5. ———— .. *Ibid.*, 1936, 4, No. 6, 639.
6. Tyndall .. *Proceedings of the Royal Institute, London*, 1870, 6, 1.
7. Rayleigh .. *Proceedings of the Royal Society, December* 1882, 32.
8. Aitken .. *Transactions of the Royal Society, Edinburgh*, 1884, 32.
9. Lodge, O. J., and Clark, J. W. — *Philosophical Magazine*, 1884, 17.
10. Hooper, W. J. .. *Physics*, 1931, 1, No. 1.

CHEMOTHERAPY OF BACTERIAL INFECTIONS

Part IV. Synthesis of (N^1)-sulphonamide substituted heterocyclic derivatives of Sulphanilamide

By K. Ganapathi

(From the Haffkine Institute, Parel, Bombay)

Received March 3, 1941

(Communicated by Lieut.-Col. S. S. Sokhey, M.A., M.D., I.M.S.)

The results of our testing many typical sulphanilamide derivatives for anti-bacterial activity having convinced us that the compounds more active and more polyvalent in therapeutic action than sulphanilamide should be searched for amongst its (N^1)-sulphonamide substituted derivatives,[1] the synthesis of such a class of compounds was undertaken. As suitable substituents for this purpose, we chose the significant radicals or ring systems present in the reputed antiseptics, chemotherapeuticals of undoubted value in the treatment of the protozoal infections and also the compounds with vital biochemical functions such as the vitamins, coenzymes, nucleic acids, etc. After a trial of the various radicals and ring systems (the results obtained are being published), success was met with in the thiazole derivatives and the very impressive results obtained by us with one of them, 2–N^1-sulphanilamidothiazole (sulphathiazole) in some experimental infections[2] and clinical trials in plague[3] have already been published. This paper presents the list of compounds further synthesised in accordance with our scheme (a preliminary report of which has already been published[4]). Since the immediate programme at hand is a preliminary survey of the various ring systems for anti-bacterial activity and we had to reap the maximum benefit of the very limited stock of chemicals available, only typical representatives of each group were prepared and tested to trace the direction in which further elaboration would be expected to be profitable. As is inevitable and is also becoming a rather common experience in this field wherein a large number of investigators are rushing for new and more potent compounds, there is much overlapping of work. Thus, some of the compounds prepared and tested here have been reported by other researchers also.[5,6,7] Though in our synthesis of sulphanilamidothiazole with substituents at the positions 4 or 5 or both in the thiazole ring, we were anticipated by a patent of Messrs. May and Baker,[8] we are still continuing our studies because the therapeutic properties of most of them have not yet been reported.

The compounds synthesised are given in the table that follows :—

Compound	Melting point (degrees)	Molecular formula	Percentage of nitrogen	
			Found	Required
Sulphanilylguanidine	188–89	$C_7H_{10}N_4O_2S$	25·8	26·2
Acetsulphanilylguanidine	266	$C_9H_{12}N_4O_3S$	21·8	21·9
N^4-Sulphanilylsulphanilylguanidine ..	155–60	$C_{13}H_{15}N_5O_4S_2$	19·2	19·0
N^4-Acetsulphanilylsulphanilylguanidine ..	143–45 (Dec.)	$C_{15}H_{17}N_5O_5S_2$	17·0	17·0
4-N^1-Sulphanilamidouracil	..	$C_{10}H_{10}N_4O_4S$	20·6	19·9
5-N^1-Sulphanilamidobarbituric acid ..	..	$C_{10}H_{10}N_4O_5S$	19·4	18·8
2-N^1-Sulphanilamido (1 : 3 : 4) thiodiazole	216–18	$C_6H_6N_4O_2S_2$	21·7	21·9
2-N^1-Sulphanilamido-5-methyl (1 : 3 : 4) thiodiazole	190–92	$C_9H_{10}N_4O_2S_2$	20·9	20·7
2-N^1-Sulphanilamidopyrimidine	240–42	$C_{10}H_{10}N_4O_2S$	22·0	22·4
2-N^1-Sulphanilamido-4-methyl pyrimidine..	236–38	$C_{11}H_{12}N_4O_2S$	21·0	21·2
2-N^1-Sulphanilamido-4 : 6-dimethyl-pyrimidine	235–40	$C_{12}H_{14}N_4O_2S$	19·6	20·1
2:N^1-Sulphanilamido-4-methyl-6 : 6-dimethyl dihydropyrimidine ..	230–32	$C_{13}H_{18}N_4O_2S$	18·9	19·0
7-N^1-Sulphanilamidoalloxazine	..	$C_{16}H_{12}N_6O_4S$	22·5	21·9

For sulphanilylguanidine two structures (I) and (II) are possible; Marshall *et al.*,[5] who also prepared this compound, do not choose one in preference to the other. But this compound being insoluble in alkali indicating the absence of a hydrogen atom attached to the nitrogen of the sulphonamide group, we prefer to represent it as (I). Our interest in this compound

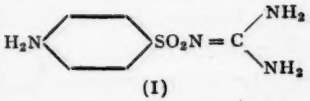

(I)

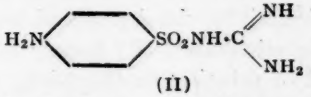

(II)

as well as its acetyl derivative is also as an intermediate for the construction of the pyrimidine derivatives with the guanidine residue. In sharp contrast to the free guanidine or amidine derivatives, these compounds are very reluctant to condense with β-diketones, β-ketonic esters and $\alpha : \beta$-unsaturated ketones under the usual conditions. Other conditions are being tried and the results will be reported in a subsequent communication.

When sulphanilylguanidine (I) is condensed with *para*acetaminobenzene sulphochloride, a compound insoluble in dilute hydrochloric acid is formed ; hence for the product obtained by hydrolysis, the structure of N^4-sulphanilyl-sulphanilylguanidine (III) has been assigned. Acetsulphanilylguanidine,

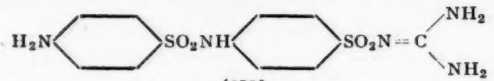

(III)

however, under the above conditions did not condense with *para*acetamino-benzenesulphochloride, indicating the comparative inertness of the two amino groups in the former. Since 2-N^1-sulphanilamido-4-methylpyrimidine, tested by us as a representative of the pyrimidines, shows interesting therapeutic properties,[6] a series of 4 : 5- and 4 : 6-dialkyl derivatives of this group are being synthesised by obvious methods. The synthesis of the 4 : 6-derivatives are of special interest to us because the condensation of β-diketones with guanidine in one step yields the starting 2-aminopyrimidine derivative. In the place of the aminopyrimidine in the above condensations, the corresponding pyrimidones and chloropyrimidines have also been tried, but herein the condensations so far tried have not been so smooth. These are being further studied.

Most of the compounds reported here have been tested in experimental *β-hæmolytic streptococcal* and *pneumococcal* (type I) infections in mice and those worthwhile among them in plague infection also. The results obtained will be reported elsewhere in detail. The uracil, barbituric acid and alloxazine derivatives were inactive, while none of the rest surpassed sulphathiazole in therapeutic activity.

The knowledge so far obtained by testing hundreds of sulphanilamide derivatives of diverse structures by us and other workers can be summed up as follows : The grouping is essential for the therapeutic activity, the *degree* and *range* of which being governed by the nature of the substitutent (R) present at the sulphonamide radical. Of the various types of substituents (R) tried, only the heterocyclic compounds, the ring structure of which are present in products of vital biochemical functions (as vitamins, coenzymes), yield sulphanilamide derivatives of outstanding value. Among these heterocycles themselves, the groups or atoms present therein and also the position of their attachment to the sulphonamide radical do govern the activity. It looks as though some specific spatial configuration of the whole molecule is essential for intense therapeutic activity.

Experimental

The methods of synthesis of these compounds being so much standardised, the details of their preparation are omitted to save space. The starting amines were all prepared by methods described in literature. In the condensations of the sulphochlorides with the amines, pyridine or alkali (sodium bicarbonate) was used as the condensing agent and acetone as the diluent. Hydrolysis of the acetylderivatives was always carried out with (4-6 N) hydrochloric acid since this was much quicker and the end point could be seen. Since our interest in these compounds is frankly only for testing their antibacterial properties, the intermediate acetyl derivatives (known to be very little active) were not isolated. The meltings of many of the compounds were not at all sharp even though they gave correct analytical figures and possessed the unmistakable properties of the sulphanilamides.

My grateful thanks are due to Lieut.-Col. S. S. Sokhey, Director, Haffkine Institute, Bombay, for his keen interest in this investigation and also to the Lady Tata Memorial Trust for the extension of the Scholarship for the fourth year to continue these researches.

Summary

In an attempt to assess the antibacterial effect of sulphanilamides with various heterocyclic rings introduced into the (N^1)-sulphonamide radical, typical derivatives, of guanidine, thiodiazole, uracil, barbituric and pyrimidine have been synthesised and are reported here.

REFERENCES

1. Ganapathi, K. .. *Proc. Indian Acad. Sci.*, 1940, **11A**, 298; **12A**, 277.
Current Sci., 1940, **9**, 314.
Indian Jour. Med. Res., 1940, **27**, 975.
2. Sokhey, S. S., and Dikshit, B. B. *Lancet*, 1940, **1**, 1040.
Rao, R. S., and Ganapathi, K. *Indian Med. Gaz.*, 1940, **75**, 674.
Ibid., 1941, **76**, 78.
Dikshit, B. B., and Ganapathi, K. *Jour. Malaria Inst. India*, 1940, **3**, 525.
3. Wagle, P. M., Sokhey, S. S., Dikshit, B. B., and Ganapathi, K. *Indian Med. Gaz.*, 1941, **76**, 29.
4. Ganapathi, K. .. *Current Sci.*, 1940, **9**, 417.
5. Marshall, E. K., Jr., Bratton, A. C., White, H. J., and Litchfield, J. T. *Bull. John. Hop. Hosp.*, 1940, **67**, 163.
6. Roblin, R. O., Williams, J. A., Winneck, P. S., and English, J. P. *Jour. Amer. Chem. Soc.*, 1940, **62**, 2002.
7. Northey, E. H. .. *Chemical Rev.*, 1940, **27**, 85.
8. Messrs. May & Baker .. *Indian Patent*, 26850.

ON THE GRAVEST MODE OF SOME VIBRATING SYSTEMS

By B. R. Seth

(From the Department of Mathematics, Hindu College, Delhi)

Received November 9, 1940

The gravest mode of any vibrating system should be devoid of internal nodal lines. In some well-known cases only the symmetrical solutions have been obtained, and hence the gravest mode remains undetermined. The following are some examples :

(*a*) Transverse oscillations of water contained in a canal (*i*) with sides inclined at an angle of 60° to the vertical, (*ii*) whose section is a hyperbola of eccentricity 2.

If we take the axes of x and y respectively horizontal and vertical, the solution due to Greenhill for (*i*) is given by the stream function[1]

$$\psi = Ax\,(x^2 - 3y^2)\cos(\sigma t + \epsilon),\ \sigma^2 = g/h, \tag{1}$$

h being the depth of water in the canal. The slowest mode, as Lamb remarks, is asymmetrical and has not yet been determined.

For (*ii*) we find[2]

$$\psi = Ax\,(y^2 - \tfrac{1}{3}x^2 - a^2)\cos(\sigma t + \epsilon),\ \sigma^2 = g/h, \tag{2}$$

which again gives a symmetrical type.

(*b*) Standing waves between two transverse partitions in a canal with sides inclined at 60° to the vertical.

If the x-axis be parallel to the length of the canal, the z-axis drawn vertically upwards, the y-axis horizontal and transverse to the canal, and (π/k) be the distance between the transverse partitions, Macdonald[3] finds that the velocity potential of the motion is given by

$$\phi = A\left[\cosh k\,(z-h) + \frac{\sigma^2}{gk}\sinh k\,(z-h) + 2\cosh\frac{k\,y\sqrt{3}}{2}\left\{\cosh k\left(\frac{z}{2}+h\right) - \frac{\sigma^2}{gk}\sinh k\left(\frac{z}{2}+h\right)\right\}\right]\cos kx, \tag{3}$$

[1] Lamb, *Hydrodynamics*, 5th Ed., 1930, p. 419.

[2] Seth, *Phil. Mag.*, Ser. 7, 1937, **23**, 113–14.

[3] Macdonald, *Proc. Lond. Math. Soc.*, 1894, **25**, 101.

where

$$2\left(\frac{\sigma^2}{gk}\right)^2 - 3\frac{\sigma^2}{gk}\coth\frac{3kh}{2} + 1 = 0,$$

omitting the time-factor $\cos(\sigma t + \epsilon)$.

The motion is symmetrical about the z-axis, and hence (3) cannot give the gravest mode.

(*c*) Transverse vibrations of an isosceles triangular membrane containing an angle of 120°.

If the sides are given by $x = a$, $y = x\sqrt{3}$, $y + x\sqrt{3} = 2a/\sqrt{3}$, it is given in a recent paper[4] that the displacement z should be

$$\begin{aligned} z &= 2\sin\frac{(m-n)\pi x}{a}\sin\frac{(m+n+1)\pi y\sqrt{3}}{a} \\ &\quad - 2\cos\left(2m+1+\frac{2n+1}{2}\right)\frac{\pi x}{a}\cos\frac{(2n+1)\pi y\sqrt{3}}{2a} \\ &\quad + 2\cos\left(2n+1+\frac{2m+1}{2}\right)\frac{\pi x}{a}\cos\frac{(2m+1)\pi y\sqrt{3}}{2a}, \qquad (4) \\ \frac{\sigma}{2\pi} &= \frac{1}{2}\frac{c}{a}\left\{(2m+1)^2+(2n+1)^2+(2m+1)(2n+1)\right\}^{\frac{1}{2}}, \end{aligned}$$

m and n being integers.

This is again symmetrical about the median bisecting 120°.

(*d*) Transverse vibrations of a rhombus containing an angle of 120°[4] and those of a regular hexagon.[5]

If we take the sides as $x = 0$, $x = a$, $y = x/\sqrt{3}$, $y = x/\sqrt{3} + 2a/\sqrt{3}$, in the first case, and as $x = \pm a$, $y = \pm x/\sqrt{3} \pm 2a/\sqrt{3}$ in the second case, it is found that the displacement z is given by

$$\begin{aligned} z &= 2\sin\frac{(m-n)\pi x}{a}\cos\frac{(m+n)\pi y\sqrt{3}}{a} \\ &\quad - 2\sin\frac{(2m+n)\pi x}{a}\cos\frac{n\pi y\sqrt{3}}{a} \\ &\quad + 2\sin\frac{(2n+m)\pi x}{a}\cos\frac{m\pi y\sqrt{3}}{a}, \qquad (5) \\ \frac{\sigma}{2\pi} &= \frac{c}{a}(m^2+n^2+mn)^{\frac{1}{2}}, \end{aligned}$$

m and n being integers as before.

---

[4] Seth, *Proc. Ind. Acad. Sci.* (A), 1940, **5**.

[5] D. G. Christopherson, *Quart. J. of Math.*, 1940, **11**, 65.

The solution is symmetrical about the diagonal bisecting 120° in the first case, and about all the three diagonals in the second.

In all the above cases we see that whenever there is symmetry about the bisector of the angle 120° the modes are also symmetrical about the same line.

The determination of the asymmetrical types in each of the above cases, and hence that of the gravest mode, yields an infinite determinant for the frequency. Rayleigh's method can be used to get an approximate value of the gravest mode. We shall illustrate this by discussing in detail the case of transverse oscillations of water contained in a canal with its sides inclined at 60° to the vertical.

We take the x-axis vertically downwards, and the sides given by $\theta = \frac{2}{3}\pi$ and $\theta = \frac{4}{3}\pi$. Let the free surface be given by $x = -h$. Omitting the time factor we see that the asymmetrical modes are given by

$$\phi = \sum_1^\infty A_n r^{\frac{3}{2}(2n-1)} \cos \tfrac{3}{2}(2n-1)\theta, \tag{6·1}$$

$$\psi = \sum_1^\infty A_n r^{\frac{3}{2}(2n-1)} \sin \tfrac{3}{2}(2n-1)\theta. \tag{6·2}$$

This value of ψ vanishes over $\theta = \frac{2}{3}\pi$ and $\theta = \frac{4}{3}\pi$, but does not do so over $\theta = \pi$, which is the line of symmetry.

The condition at the free surface, $r \cos\theta = -h$, is

$$\sigma^2\phi = -g\frac{\partial\phi}{\partial x}, \tag{7}$$

and since

$$\frac{\partial\phi}{\partial x} = \cos\theta \frac{\partial\phi}{\partial r} - \sin\theta \frac{\partial\phi}{r\partial\theta},$$

we get

$$g\left[\tfrac{3}{2}A_1 r^{\frac{1}{2}} \cos\tfrac{1}{2}\theta + \tfrac{9}{2}A_2 r^{\frac{7}{2}} \cos\tfrac{7}{2}\theta + \tfrac{15}{2}A_3 r^{\frac{13}{2}} \cos\tfrac{13}{2}\theta + \ldots\right]$$
$$= -\sigma^2\left[A_1 r^{\frac{3}{2}} \cos\tfrac{3}{2}\theta + A_2 r^{\frac{9}{2}} \cos\tfrac{9}{2}\theta + A_3 r^{\frac{15}{2}} \cos\tfrac{15}{2}\theta + \ldots\ldots\right]. \tag{8·1}$$

Multiplying both sides by $r^{\frac{1}{2}} \cos\frac{1}{2}\theta$ we get

$$g\left[\tfrac{3}{2}A_1 r(1+\cos\theta) + \tfrac{9}{2}A_2 r^4(\cos 4\theta + \cos 3\theta) + \tfrac{15}{2}A_3 r^7(\cos 7\theta + \cos 6\theta) + \ldots\right]$$
$$= -\sigma^2\left[A_1 r^2(\cos 2\theta + \cos\theta) + A_2 r^5(\cos 5\theta + \cos 4\theta) + A_3 r^8(\cos 8\theta + \cos 7\theta) + \ldots\ldots\right].$$

Expanding the cosines in powers of $\cos\theta$ and putting $r\cos\theta = -h$, we get

$$g\left[\tfrac{3}{2}A_1(r-h) + \tfrac{9}{2}A_2(r^4 - 8r^2h^2 + 8h^4 + 3r^3h - 4rh^3) + \ldots\ldots\right]$$
$$= -\sigma^2\left[A_1(2h^2 - r^2 - rh) + A_2(-5r^4h + 20r^2h^3 - 16h^5 + r^5 - 8r^3h^2 + 8rh^4) + \ldots\ldots\right]. \tag{8·2}$$

Putting $t = \sigma^2 h/g$, and equating the coefficients of like powers of r, we get the following set of infinite equations:—

$$A_1(2t - \tfrac{3}{2}) - A_2h^3(2^4t - \tfrac{9}{2}\cdot 2^3) + A_3h^6(2^7t - \tfrac{15}{2}\cdot 2^6) - A_4h^9(2^{10}t - \tfrac{21}{2}\cdot 2^9) + \ldots\ldots = 0,$$

$$A_1(t - \tfrac{3}{2}) - A_2h^3(2^3t - \tfrac{9}{2}\cdot 2^2) + A_3h^6(2^6t - \tfrac{15}{2}\cdot 2^5) - A_4h^9(2^9t - \tfrac{21}{2}\cdot 2^8) + \ldots\ldots = 0,$$

$$A_1t - A_2h^3(\tfrac{5}{11}2^2t - \tfrac{9}{2}\cdot\tfrac{4}{11}\cdot 2) + A_3h^6(\tfrac{8}{11}2^5t - \tfrac{15}{2}\cdot 2^4\cdot\tfrac{7}{11}) - A_4h^9(\tfrac{11}{11}2^8t - \tfrac{21}{2}\cdot\tfrac{10}{11}\cdot 2^7) + \ldots = 0,$$

$$A_2h^3(\tfrac{4}{11}2t - \tfrac{9}{2}\cdot\tfrac{3}{11}) - A_3h^6(\tfrac{7}{11}2^4t - \tfrac{15}{2}\cdot\tfrac{6}{11}\cdot 2^3) + A_4h^9(\tfrac{10}{11}2^7t - \tfrac{21}{2}\cdot\tfrac{9}{11}\cdot 2^6) + \ldots = 0,$$

$$A_2h^3(\tfrac{5\cdot 2}{21}t - \tfrac{9}{2}) - A_3h^6(\tfrac{8\cdot 5}{21}2^3t - \tfrac{15}{2}\cdot\tfrac{7\cdot 4}{21}2^2) + A_4h^9(\tfrac{11\cdot 8}{21}2^6t - \tfrac{15}{2}\cdot\tfrac{10\cdot 7}{21}\cdot 2^5) + = 0, \qquad (9)$$

.. ..

Eliminating the A's we get an infinite determinant for t.

To get an approximate value of the frequency of the gravest mode we take

$$\phi = A_1 r^{\frac{3}{2}} \cos\tfrac{3}{2}\theta \cos(\sigma t + \epsilon) \qquad (10)$$

as a constrained type. If T and V represent the kinetic and potential energies respectively, we find

$$T = \tfrac{1}{2}\rho \int_{\frac{2}{3}\pi}^{\frac{4}{3}\pi} \int_0^{-h\sec\theta} \tfrac{9}{4} A_1^2 \cos^2(\sigma t + \epsilon)\, r^2\, dr\, d\theta$$

$$= \tfrac{3}{8} A_1^2 \rho h^3 [2\sqrt{3} + \log(2 + \sqrt{3})] \cos^2(\sigma t + \epsilon),$$

$$V = \tfrac{1}{2}\rho g \int_{-h\sqrt{3}}^{h\sqrt{3}} \frac{\sigma^2 A_1^2}{g^2} \sin^2(\sigma t + \epsilon)\, r^3 \cos^2\tfrac{3}{2}\theta\, dy, \qquad (y = -h\tan\theta)$$

$$= \frac{1}{16}\frac{\rho A_1^2 \sigma^2}{g} h^4 [38\sqrt{3} + 3\log(2 + \sqrt{3})] \sin^2(\sigma t + \epsilon).$$

Hence

$$\sigma^2 = \frac{g}{h}\cdot\frac{6[2\sqrt{3} + \log(2 + \sqrt{3})]}{38\sqrt{3} + 3\log(2 + \sqrt{3})} = \frac{g}{h}\cdot(0{\cdot}4112)$$

$$\therefore \sigma = (0{\cdot}641)\sqrt{\frac{g}{h}}. \qquad (11)$$

The lowest symmetrical mode is, of course, $\sigma = \sqrt{g/h}$.

For a hyperbola with eccentsicity 2 we should take

$$\phi = \sum_1^\infty A_n \cosh \tfrac{3}{2}(2n-1)\,\xi \cos \tfrac{3}{2}(2n-1)\,\eta, \tag{12·1}$$

$$\psi = \sum_1^\infty A_n \sinh \tfrac{3}{2}(2n-1)\,\xi \sin \tfrac{3}{2}(2n-1)\,\eta, \tag{12·2}$$

where (ξ, η) are the elliptic co-ordinates, and the hyperbola is given by $\eta = \frac{3}{8}\pi$.

The first term may be taken as a constrained type to get an approximate value of the frequency of the gravest mode.

In the case of (b) we should take

$$\phi = \sum_1^\infty A_n I_{\frac{3}{2}(2n-1)}(kr) \cos \tfrac{3}{2}(2n-1)\,\theta, \tag{13}$$

$I_{\frac{3}{2}(2n-1)}$ which are Bessel's function of fractional order with an imaginary argument, can be expressed in finite terms. If we take the first term for the constrained type, we get

$$\phi = A_1 I_{\frac{3}{2}}(kr) \cos \tfrac{3}{2}(2-1)\,\theta$$

$$= \frac{A}{\sqrt{kr}}\left[\frac{\sinh kr}{kr} - \cosh kr\right] \cos \tfrac{3}{2}(2n-1)\,\theta. \tag{13·1}$$

To give an example from the vibrations of membranes we can take (c), and, in this case we easily see that the displacement should be taken as

$$z = \sum_1^\infty A_n J_{\frac{3}{2}(2n-1)}(kr) \sin \tfrac{3}{2}(2n-1)\,\theta, \tag{14}$$

where $k = \sigma/c$. $J_{\frac{3}{2}(2n-1)}(kr)$ can again be expressed in finite terms.

For the constrained mode we have

$$z = \frac{A_1}{\sqrt{kr}}\left[\frac{\sin kr}{kr} - \cos kr\right] \sin \tfrac{3}{2}\theta. \tag{14·1}$$

THE GLYCOSIDIC COMPONENTS OF THE FLOWERS OF *BUTEA FRONDOSA*

By P. Bhaskara Rama Murti and T. R. Seshadri

(From the Department of Chemical Technology, Andhra University, Waltair)

Received March 24, 1941

The flowers of *Butea frondosa* find use in fairly large quantities even at the present time. In the course of a detailed study of the chemical composition it has been found necessary to separate the different types of components carefully. By an initial extraction with petrol the flower wax was isolated and its chemical composition was described.[1] The de-fatted material was extracted with alcohol and by subsequent treatment of the concentrated extract with water and ether, butin and butein were isolated.[2] Continuing the work it has now been possible to obtain butrin in a high state of purity and in high yield without the difficulty that is experienced when employing the method of the previous workers.[3] This is obviously due to the removal of interfering impurities in the earlier stages.

Hydrolysis of this glucoside with dilute sulphuric acid has been stated to yield the flavanone, butin. Similar statements have been made regarding other flavanone glycosides such as naringin, hesperidin, etc. Carefully purified butrin has now been hydrolysed with dilute sulphuric acid and the product examined using the method that has been already described for the separation of the two isomeric compounds, the flavanone and the chalkone. As the result it is noticed that along with butin which is the major part some quantity of butein is also produced. Since particular care has been taken to employ a pure sample of butrin which is free from chalkone derivatives, the formation of butein during the hydrolysis is definite. This conclusion is further supported by other (unpublished) results relating to this group of compounds. It therefore becomes necessary to look for two isomeric products whenever flavanone glycosides are subjected to hydrolysis with acids.

Further in the course of this work two colourless crystalline compounds have also been isolated one of which is a phytosterolin and the other an unidentified heteroside. They were obtained in very small amounts. The former yields on hydrolysis a phytosterol, $C_{28}H_{40}O$ and glucose. The heteroside has the formula $C_{23}H_{40}O_{10}$ and yields on hydrolysis glucose and an aglucone melting at 220°. Both the heteroside and its aglucone do not give

the usual colour reactions of flavanones or chalkones. Further work on these glucosides is in progress.

Experimental

The dry flower powder was extracted first with petroleum ether and subsequently with alcohol as already described.[2] The concentrate of the alcoholic extract was poured into a large excess of water and the orange yellow solution was repeatedly extracted with small quantities of ether to remove the aglucones. The extracts were separated (A) and preserved for examination. The aqueous solution (2 litres from 3 kg. of the flowers) was allowed to stand saturated with ether. In the course of a few days a pale yellow solid separated out in the form of thin flakes (B). It did not give any of the colour reactions of flavanones or chalkones and it is described later in this paper. After the separation of the above solid the solution was again allowed to stand with the addition of some more ether in order to keep it saturated. In the course of a week about 1·5% yield of butrin separated out in a crystalline condition. More was obtained on longer standing and on concentrating the solution at the ordinary temperature and subsequently saturating it with ether. The solid was pale yellow in colour and contained a small amount of mineral matter. It was further purified by one re-crystallisation from hot rectified spirits when it was obtained as colourless long needles melting at 194–95° (decomp.). When crystallised from water however, the crystals take the form of aggregates of micacious plates. Though the yield of crude butrin obtained by the method of Lal and Dutt is considerably high (about 2·5%), after passing through the several stages of purification the yield of the pure product becomes less than 0·4%. The glycoside is fairly soluble in water and when impure its solubility is markedly high. The highly soluble impure sample has been said to contain metallic salts of the pigment.[3] But there seems to be no definite support for this view and all data point towards the colloidal condition of the substances as the cause of solubility (compare Seshadri[4]). The presence of a little mineral matter is nothing unusual in crude substances isolated from plant materials.

Butrin (1·2 g.) was treated with 7% aqueous sulphuric acid (50 c.c.) and the mixture boiled for about 2 hours. The clear solution deposited on cooling a brown precipitate in a crystalline condition. After filtering and washing with water it gave reactions for butin, a green colour with alcoholic ferric chloride and violet colour with magnesium and alcoholic hydrochloric acid. Close examination of the solid indicated that it was a mixture. A small quantity of more highly coloured crystals could be picked out and these gave tests for butein. Complete separation was however effected using boiling water (20 c.c.) and filtering hot. The less soluble portion on the filter was

repeatedly washed with small quantities of hot water and finally crystallised from dilute alcohol. It was found to be identical with butein in all respects. It gave an olive brown colour with alcoholic ferric chloride, an orange red solution with alkali and it did not respond to the anthocyanin test using magnesium and alcoholic hydrochloric acid. It melted at 215° and the melting point was not depressed by admixture with an authentic sample of butein. The yield of this chalkone amounted to 6% of the aglucone mixture. From the aqueous filtrate pale yellow crystals of butin dihydrate were isolated. Longer heating during the course of hydrolysis did not produce any difference in the yield of the two isomeric aglucones nor did the substitution of 7% hydrochloric acid for sulphuric acid for purposes of hydrolysis make any change in the result. An estimation of the products of hydrolysis (aglucone mixture and glucose) was made with a view to confirm the composition of butrin as diglucoside. The aglucones were extracted repeatedly with ether and weighed after evaporating the solvent and air-drying. For purposes of calculation the product was taken to be butin dihydrate. The sugar was estimated by titration with Fehlings solution. (Found: aglucone 45·0, glucose 55·3; $C_{27}H_{32}O_{15}$, $2H_2O$ requires aglucone 48·7 and glucose 57·0%.)

Isolation of a phytosterolin.—The ether extract (A) was shaken with aqueous sodium bicarbonate with a view to extract the butin-butein mixture from it. During this operation a colourless solid separated out being insoluble in both the aqueous and ether layers. It was ordinarily found suspended at the bottom of the ether layer. It was filtered and washed with more ether. It was sparingly soluble in ether, chloroform, ethyl acetate and even in alcohol. But it was easily soluble in glacial acetic acid and in pyridine. It was therefore purified by successive treatment with boiling ether and alcohol to remove impurities and by a final crystallisation from dilute pyridine. The pure substance appeared as colourless hexagonal plates and melted at 260–62° (decomp.). It yields a blood red colour with chloroform and sulphuric acid (Hesse's reagent) and a display of colours, pink—blue—green with the Liebermann–Burchard reagent. Thus it gives the typical sterol reactions. (Found in the sample dried at 120° for 2 hours: C, 71·7; H, 11·5; $C_{34}H_{62}O_6$ requires C, 72·1; H, 11·0%.) The substance was hydrolysed with amyl alcoholic hydrochloric acid and the amyl alcohol was removed by steam distillation. By ether extracting the residual aqueous mixture was obtained sitosterol melting at 145–46°. The aqueous solution was found to contain glucose. The yield of the phytosterolin was very small being about 0·02% of the flowers taken.

Heteroside (*B*).—The pale yellow solid, as it was first obtained, melted at about 212°. It was purified by dissolving in excess of alcohol and allowing to cool slowly when it separated out as a colourless crystalline solid. This

was filtered and repeatedly washed with small quantities of warm water. In order to get more of the substance the alcoholic mother liquor was concentrated to small bulk, treated with water till it became just turbid and the mixture allowed to stand. Shining colourless crystals were thereby obtained and the final aqueous mother liquor contained a small quantity of butrin. The purified heteroside was insoluble in water, ether and chloroform, and moderately easily soluble in hot alcohol. It was however readily soluble in glacial acetic acid and pyridine and it was obtained in the form of colourless hexagonal plates by crystallising from a mixture of water and pyridine. It melted at 236–37° with decomposition. It was insoluble in aqueous sodium carbonate or hydroxide and gave no colour with alcoholic ferric chloride or with magnesium and alcoholic hydrochloric acid. The last reaction could be employed as a sensitive test for the existence of butrin as an impurity since even a small quantity of it gives a noticeable pink colour. The heteroside dissolved in concentrated sulphuric acid to produce a bright orange red solution the colour of which deepened on standing and changed to deep purple in the course of about 12 hours. With chloroform and concentrated sulphuric acid (Hesse's reagent) it formed a pale yellow solution whereas with chloroform, acetic anhydride and a drop of concentrated sulphuric acid (Liebermann-Burchard reagent) a pink solution was produced which slowly changed to brown on standing. These reactions indicate that the substance does not belong to the group of sterols but may be related to the resinols. (Found in the sample dried at 120°: C, 57·4; H, 8·6; $C_{23}H_{40}O_{10}$ requires C, 57·9; H, 8·4%.) When hydrolysed with amyl alcoholic hydrochloric acid it yielded glucose and a colourless aglucone melting at 220° C. The aglucone gave reactions very similar to those of the heteroside but dissolved easily in alcohol, chloroform and ether. Further work on this substance is in progress.

Our thanks are due to Mr. G. V. L. Narasimha Murty for some of the micro-analyses.

Summary

Butrin has been obtained by a simple method and in good yield from the flowers of *Butea frondosa*. On hydrolysis with acids it gives a mixture of butin and butein. Two colourless crystalline compounds have also been isolated, one of which is a phytosterolin and the other an unidentified heteroside.

REFERENCES

1. P. B. R. Murti and H. Krishnaswamy .. *Proc. Ind. Acad. Sci.*, 1940, **12**, 472.
2. ———, and T. R. Seshadri .. *Ibid.*, 1940, **12**, 477.
3. J. B. Lal and S. Dutt .. *J.I.C.S.*, 1935, 262.
4. T. R. Seshadri .. *Curr. Sci.*, 1934, 343.

A STUDY OF THE CHEMICAL COMPONENTS OF THE ROOTS OF *DECALEPIS HAMILTONII*

Part III. Comparison with *Hemidesmus indicus* (Indian Sarsaparilla)

BY P. BHASKARA RAMA MURTI AND T. R. SESHADRI

(From the Department of Chemical Technology, Andhra University, Waltair)

Received March 24, 1941

THE general chemical composition of the roots of *Decalepis Hamiltonii* has been described in Part I.[1] Since *Hemidesmus indicus* belongs to the same family (Asclepiadaceæ) and resembles the *Decalepis* in smell and in taste it has been felt necessary to examine this root also on the same lines and compare the nature of the various components. The only systematic work done so far on this drug is that of Dutta, Ghosh and Chopra.[2] According to them the chief constituents of the root are (1) an essential oil 0·225% on the weight of the air-dried root consisting of *para*-methoxysalicylicaldehyde, (2) two sterols, Hemidesterol melting at 182–84° having the formula $C_{34}H_{60}O$ and Hemidesmol melting at 161° and having the formula $C_{33}H_{58}O$, (3) two amorphous resin acids one melting at 155–58° and the other at 128–30°, and (4) a small amount of an indefinite glucoside melting at 133–36° besides tannins and resins.

When we examined the roots of *Hemidesmus indicus* on the same lines as we have adopted for *Decalepis Hamiltonii* the results indicated that both the roots are very similar in the nature of the components ; this is brought out in the accompanying table. It may be stated in general that in the case of *Hemidesmus indicus* the yields are much poorer as compared with *Decalepis Hamiltonii*. For example *p*-methoxysalicylicaldehyde exists in the latter to the extent of 0·8% on the weight of the dried roots whereas in the former it forms only 0·12%. Consequently the *Decalepis* should be more serviceable for the purposes for which the *Hemidesmus* is employed.

In regard to the differences in the findings of Dutta, Ghosh and Chopra and those recorded in this paper, it seems probable that what the previous workers considered to be sterols were really mixtures of the resinols with smaller quantities of phytosterols. In an experiment carried out by us following their method of extraction it was found possible to isolate the various non-sterol fractions already mentioned. These do not give the correct reactions of sterols but give positive tests for resinols.

TABLE I

D. Hamiltonii			*Hemidesmus indicus*		
Nature of the fractions and melting point	Liebermann-Burchard reaction	Derivatives melting point	Nature of the fractions and melting point	Liebermann-Burchard reaction	Derivatives melting point
Petroleum Ether Extract—			*Petroleum Ether Extract—*		
1. Resinols			Resinols		
(*a*) 235°	Pink	No acetate	235°	Pink	No acetate
(*b*) 175–85°	,,	Acetate 212–18°	175–85°	,,	Acetate 210–15°
(*c*) 160–65°	,,		165–70°	,,	
(*d*) 155–57°	,,		155–65°	,,	
(*e*) 151–53°	,,		150–54°	,,	
(*f*) 135–45°	,,		135–40°	,,	
2. Sterols 105–10°	Pink-blue-green	Acetate 130–60°	105–10°	Pink-blue-green	Acetate 130–60°
3. Ketone 83°	Nil	Oxime 68°	Ketone 83°	Nil	Oxime 68°
4. Aldehyde 42°			Aldehyde 42°		
5. Fatty acids (solid) 80–82°	(Sap. equivalent 360)		Fatty acids (solid) 80–82°	(Sap. equivalent 352)	
Alcohol Extract—			*Alcohol Eextract–*		
1. Inositol 221°					
2. Crystalline resin acid 245°					
3. Amorphous resin acid 180°			Amorphous resin acid 160°		
4. Saponins			Saponins		
5. Tannins			Tannins		

Experimental

Fresh material (*Hemidesmus* roots) for the examination was obtained locally. The roots were small in size when compared with those of *Decalepis Hamiltonii*. As ordinarily employed, portions of the stem are also mixed up with the roots. Four kilograms of the air-dried powdered material were

extracted just in the same way as in the case of *Decalepis Hamiltonii* and the extracts examined. Here too the petroleum ether and alcohol extracts formed the most prominent bulk and hence these solvents only were used.

The petroleum ether extract contained a little chlorophyll in addition to other substances. Though it could be separated into the four fractions as in the case of the *Decalepis Hamiltonii* by the treatment of the semi-solid residue with alcohol and subsequent careful concentration, fractions (W) and (A) were mixed together for the sake of convenience and thus division into three main fractions was made for detailed study. The first fraction (48 g.) corresponded to the wax (W) and fraction (A) of *Decalepis Hamiltonii*. This was subjected to saponification and the unsaponifiable matter fractionated as before. The other two fractions corresponded to (B) and (C). The following table sums up the results of the study of the fractions.

TABLE II

Fractions melting point	Yield	Colour reactions	
		Liebermann-Burchard	Hesse
From (W + A)			
1. 83° (Ketone)	0·5 g.	Nil	Nil
2. 175–85° (Resinols)	1·5 g. (acetate, m.p. 210–15°)		
3. 165–70° ,,	2·0 g.		
4. 155–65° ,,	4·0 g.	Pink	Yellow
5. 150–54° ,,	2·5 g.		
6. 135–40° ,,	2·5 g.		
7. 105–110° (Sterols)	1 g. (acetate, m.p. 130–60°)	Pink-blue-green	Red
From (B) and (C)			
8. 235° (Resinols)	0·3 g.	Pink	Yellow
210–22° ,,			
9. Aldehyde			

The unsaponifiable matter from fraction (W + A) gave only a deep pink colour when the mixture was tested with the Liebermann-Burchard reagent. This can be explained as due to the predominant presence of resinols in the

mixture. When this was fractionated just as in the case of *Decalepis Hamiltonii*, the ketone melting at 83° separated out. Then the resinols melting between 135–185° were systematically fractionated and they all gave the pink colour with the Liebermann-Burchard reagent and yellow colour with Hesse's reagent. The final mother liquor, after careful manipulation as described already, gave a very small quantity of a colourless solid which gave the play of colours, pink-blue-green and a blood red colour with the Hesse's reagent characteristic of sterols. The final yellow residue was acetylated as before and a sterol acetate mixture melting at 130–60° was obtained and is under study. The above fractions were found to be very similar to the corresponding fractions of *Decalepis Hamiltonii*.

From the fraction (B) of the petrol extract the compound melting at 235° was isolated by adopting the same procedure as described under *Decalepis Hamiltonii*. The samples from the two sources were found to be identical since they gave the same colour reactions and the mixed melting point was undepressed.

As a typical member of the group the fraction melting at 175–85° was acetylated with acetic anhydride and sodium acetate in the usual way. The separated solid was recrystallised from alcohol-acetone mixture when a needle-shaped crystalline substance melting at 210–15° was obtained. This was found to be similar with the acetate (m.p. 212–15°) obtained from the fraction melting at 170–85° of *Decalepis Hamiltonii*. The mother liquor after the separation of the acetate melting at 212–15°, yielded another fraction melting at 175–80°.

The soap obtained from the saponificatin of the (W + A) fraction was decomposed and studied just as before. The aggregate of the mixed fatty acids obtained weighed 10·5 g. of which the solid acids amounted to 7 g. They melted at about 80° and had a saponification equivalent equal to 352.

Fraction (C) yielded about 8 g. of an essential oil. The *para*-methoxysalicylicaldehyde in this case was best obtained by steam distillation since the presence of chlorophyll rendered purification by recrystallization very difficult. The yield of the aldehyde was about 6 g. (0·12%).

After petrol extraction, the residue (root powder) was extracted in the same apparatus with alcohol exhaustively. A detailed study of the alcoholic extract revealed the presence of saponin, and tannin in much smaller amounts along with the resin acid melting at about 160°. The presence of the crystalline acid melting at 245° (cf. *Decalepis Hamiltonii*) and of inactive inositol could not be detected.

A separate experiment employing direct hot alcoholic extraction of the dry root powder was made. On concentrating the extract to half the bulk and cooling, a colourless solid mixed with chlorophyll was obtained. This was found to consist mostly of wax very similar in properties and composition to the wax obtained by petroleum extraction. By further fractionation of the mother liquor the crystalline solid melting at 235° along with the related lower fractions found in (B) were obtained. A small quantity of the resinols melting above 130° corresponding to fraction (A) could also be isolated.

Summary

The roots of the *Hemidesmus indicus* were studied on the lines adopted for *Decalepis Hamiltonii* and were found to have a similar composition particularly with regard to the petrol extract. Since the *Decalepis* roots contain much higher percentages of the various chemical components they are more suitable for use as drug.

REFERENCES

1. Murti and Seshadri .. *Proc. Ind. Acad. Sci.* (A), 1941, **13**, No. 2, 221.
2. Dutta, Ghosh and Chopra *Arch. Pharm.*, 1938, **276**, 333–40.

SYNTHETIC EXPERIMENTS IN THE BENZO-PYRONE SERIES

Part IV. Synthesis of Karanjin

By T. R. Seshadri and V. Venkateswarlu

(From the Department of Chemistry, Andhra University, Waltair)

Received March 31, 1941

The constitution of karanjin as 3-methoxy-flavono-7 : 8-furan (IV) was proposed by Limaye[1] after a study of its properties and reactions and it has been supported by the work of Manjunath, Seetharamaiah and Siddappa.[2] Amongst the attempts to synthesise this compound may be mentioned the preparation of karanjin-α-carboxylic acid (I) by Rangaswami and Seshadri[3]; the final decarboxylation has not so far been successful. In this method 3-methoxy-7-hydroxy-flavone is the starting point and the furan ring is built up. The alternative method proceeds through karanjol or 4-hydroxy coumarone (II), the ω-methoxy ketone (III) and the subsequent synthesis of the flavone ring system to produce karanjin (IV). Karanjol could be prepared by the method of Reichstein[4] or by that of Limaye.[1] The conversion of the ketone (III) into karanjin has been effected by Manjunath, Seetharamaiah and Siddappa.[2] Consequently, the stage that has not yet been realised in the complete synthesis of karanjin is the preparation of the ketone (III) from karanjol (II). This could not be accomplished by the action of methoxy-acetonitrile with the hydroxy coumarone (II) since no condensation takes place under the conditions of Hoesh's reaction.[2] Amongst other possible methods may be mentioned those proceeding through the intermediate stage of karanjic acid (V), the preparation of which from karanjol has been carried out by Limaye.[1] One of the possible routes has now been successfully explored and the results are presented in this paper.

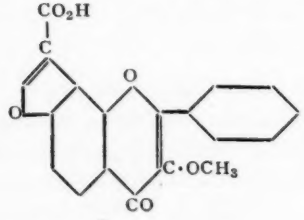

I

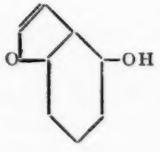

II

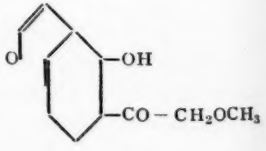

III

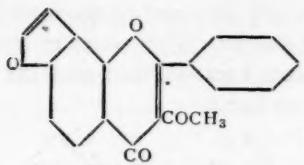

IV

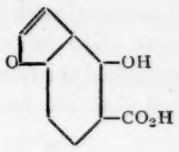

V

Karanjic acid is acetylated by means of acetyl chloride in the presence of pyridine and the acetyl derivative (VI) is converted into the acid chloride (VII) by the action of phosphorus pentachloride in carbon tetrachloride solution. The acid chloride is subsequently condensed with the mono-sodium salt of α-γ-dimethoxy-ethylacetoacetate. The condensation product is directly hydrolysed with methyl alcoholic potash and as one of the products of hydrolysis 5-ω-methoxyacetyl-4-hydroxy-coumarone (III) is obtained. In the course of the hydrolysis which should be expected to take place in different ways, some karanjic acid is also produced. When aqueous potash is employed for the hydrolysis, mostly the acid is produced, whereas with alcoholic potash, the desired ketone is the main product. It may be pointed out that a similar effect of the reagents is noticed in the decomposition of karanjin. The synthetic ketone has been found to be identical with the sample obtained by the degradation of karanjin.

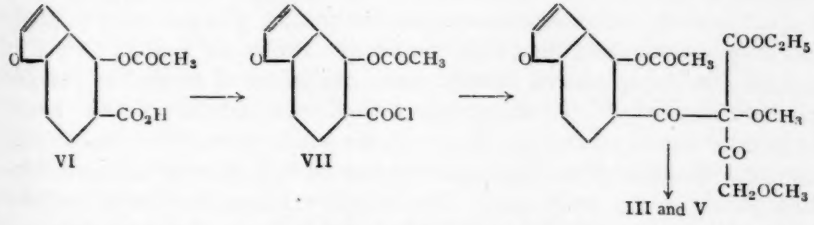

With a view to explore the feasibility of the several transformations involved in the above synthetic procedure and also to make a preliminary study of the correct conditions, pilot experiments were carried out using the methyl ether of karanjic acid (VIII) which is simpler to deal with. It was obtained from karanjic acid through the intermediate formation of the ether-ester (IX) by the action of methyl iodide and potassium carbonate and by subsequent ester hydrolysis. The ether acid smoothly underwent conversion to the acid chloride (X) which was condensed with the mono-sodium salt of α-γ-dimethoxy-ethylacetoacetate and the product finally hydrolysed. In this case, the conditions of hydrolysis were not so difficult to manipulate and even aqueous potash gave rise to a fairly good yield of the dimethyl ether, 5-ω-methoxyacetyl-4-methoxy coumarone (XI). The synthetic product was

found to be identical with the compound obtained by the methylation of the hydroxy ketone (III) derived from karanjin. This series of transformations not only established the relation between karanjic acid and the ketone, but also indicated that the method is workable.

When the ketone (III) was heated with benzoic anhydride and sodium benzoate,[2] it yielded karanjin. Thus, as a result of the present work, the synthesis of karanjin in all its stages, as outlined in the scheme, may be said to have been accomplished.

Experimental

Ether-ester of Karanjic Acid—

Method 1 (*a*): *Methyl ester of karanjic acid.*—Karanjic acid (1 g.) was dissolved in anhydrous methyl alcohol (12 c.c.) and concentrated sulphuric acid (2·2 c.c.) slowly added with cooling under the tap. The mixture was gently boiled on a water-bath for about five hours. Prolonged heating should be avoided, since it produced resinification. As much of alcohol as possible was then distilled off and the residue treated with 100 c.c. of cold water. A crystalline solid separated. However, the whole mixture was shaken with ether and the clear ether solution washed twice with aqueous sodium bicarbonate using 20 c.c. each time. The solvent was then evaporated and the solid residue recrystallised from dilute alcohol. The methyl ester came out in colourless rectangular plates, melting at 105–106°, the yield of the pure substance being 0·9 g. (Found : C, 62·5; H, 4·2; $C_{10}H_8O_4$ requires C, 62·5; H, 4·2%.)

(*b*) *Methylation of the methyl ester.*—The use of dimethyl sulphate and sodium hydroxide for this methylation was not found to be suitable, since the ester was highly sensitive to aqueous alkali. Hence the following method was adopted. The methyl ester (2 g.) was dissolved in acetone (15 c.c.). Excess of methyl iodide (2·5 c.c.) and anhydrous potassium carbonate (2 g.) were added and the solution kept gently boiling under reflux by means of a water-bath for about twenty-eight hours. Small quantities of methyl iodide were added at intervals in order to make up for

the losses due to evaporation. At the end of this time, the reaction was found to be complete from the absence of colour with ferric chloride. The solution was then filtered and the solvent removed by distillation. The ether ester thus obtained was a liquid insoluble in aqueous sodium hydroxide and it did not give any colour with alcoholic ferric chloride. It was directly employed without further purification.

Method 2.—Karanjic acid (1 g.) was dissolved in acetone (10 c.c.) and excess of methyl iodide (2 c.c.) and anhydrous potassium carbonate (1 g.) were added, and the solution kept gently boiling for about forty-five hours. At the end of this period, the product did not give any colour with ferric chloride. The isolation of the ether-ester was effected as before.

O-Methyl-karanjic-acid.—The liquid ether-ester (2 g.) was treated with 25% aqueous sodium hydroxide (20 c.c.) and the mixture gently boiled on a wire-gauze until the solution just became clear. It was cooled, acidified with dilute hydrochloric acid and the precipitate that was obtained was recrystallised from dilute alcohol. The methyl ether of karanjic acid was thus obtained as colourless elongated rectangular plates melting at 148°. The yield of the pure product was 1·6 g. (Found : C, 62·4; H, 4·4; $-OCH_3$, 16·0; $C_{10}H_8O_4$ requires C, 62·5; H, 4·2; $-OCH_3$, 16·1%.)

O-Methyl-karanjic-acid chloride.—Well dried and powdered methyl karanjic acid (5 g.) was treated with dry carbon tetrachloride (5 c.c.) and finely powdered phosphorus pentachloride (5 g.). The mixture was shaken well and gently heated on a boiling water-bath till no more fumes of hydrogen chloride were evolved and the solution became clear. The hot solution was then decanted from the unused excess of phosphorus pentachloride. The solid was washed with a little more of hot carbon tetrachloride and the washings added to the original solution. On cooling, the acid chloride separated as a thick mass of pale yellow crystals. It was filtered, washed with plenty of dry petroleum ether and finally recrystallised from carbon tetrachloride. The pure substance appeared as clusters of pale yellow needles melting at 72°. (Found: Cl, 16·5; $C_{10}H_7O_3Cl$, requires Cl, 16·9%.)

5-*ω-Methoxy-acetyl*-4-*methoxycoumarone.*—α-γ-Dimethoxy ethyl aceto-acetate was prepared according to the method of Pratt and Robinson.[5]

The ester (1 g.; 1 mol.) was gradually added to finely granulated sodium (0·1 g.; 1 atom) suspended in anhydrous ether (10 c.c.). After about an hour during which the formation of the sodium derivative appeared complete, a solution of the acid chloride (1 g.) in dry ether (15 c.c.) was introduced. A mild reaction started immediately. The mixture was allowed to stand overnight, and was subsequently boiled for about four hours in order to complete

the reaction. After cooling, water was added, the ether layer separated and dried over anhydrous sodium sulphate. On evaporating the solvent, the condensation product was obtained as a liquid which soon solidified. It was mixed with water (8 c.c.) and aqueous potassium hydroxide (9 c.c. of 16% solution) which was added slowly in the course of two hours. The clear solution was then gently boiled for about two hours at the end of which a colourless solid could be seen separating out. The mixture was extracted with ether repeatedly and the ether extract washed with water and evaporated. The solid product thereby obtained readily crystallised from dilute alcohol in the form of colourless rectangular plates melting at 87–88°. It was insoluble in sodium hydroxide and was found to be identical with the sample prepared by methylating 5-ω-methoxyacetyl-4-hydroxy-coumarone described below; the mixed melting point was undepressed.

Methylation of 5-ω-*methoxy-acetyl*-4-*hydroxycoumarone.*—The following improved method for the preparation of the ketone was adopted as it was found to give almost quantitative yield. The main difference from the method adopted by Manjunath *et al.*[2] consists in avoiding water in the preparation of alcoholic potash.

Karanjin (1 g.) was treated with methyl alcoholic potash (2 g. in 30 c.c. anhydrous methyl alcohol) and boiled under reflux in a water-bath for about six hours. As much of the alcohol as possible was then removed, the residue dissolved in water and the solution acidified with excess of dilute sulphuric acid. The product was then ether-extracted and the ether solution washed with plenty of 5% sodium bicarbonate solution till no more could be extracted. The solvent was then distilled off and the solid obtained was recrystallised from dilute alcohol. It appeared as colourless needles and rectangular plates, melting at 96° and it was found to be identical in all properties with a specimen obtained by the degradation of karanjin according to the method of Manjunath *et al.*; yield 95%. The yield of karanjic acid was very small.

The hydroxycoumarone (0·5 g.) was dissolved in anhydrous acetone (5 c.c.) and excess of methyl iodide (1 c.c.) and potassium carbonate (1 g.) added. The mixture was kept gently boiling for about 30 hours. Small quantities of methyl iodide were added at intervals. The completion of the methylation was proved by the absence of colour with ferric chloride. After distilling off the solvent, water was added to the mixture, the solid product was filtered and recrystallised from dilute alcohol. Colourless rectangular plates were obtained melting at 87–88°. The yield was almost quantitative. (Found: C, 65·4; H, 5·5; $-OCH_3$, 28·0; $C_{12}H_{12}O_4$ requires C, 65·5; H, 5·5; $-OCH_3$, 28·2%.)

Acetyl-karanjic acid.—Karanjic acid (1 g.) was dissolved in dry pyridine (3 c.c.) and the solution cooled in freezing mixture for about fifteen minutes. Acetyl chloride (2 c.c.) was slowly added drop by drop in the course of half an hour. The mixture was well stirred and after a few minutes poured on to crushed ice. The solid product was filtered, washed with cold water and after drying, recrystallised from chloroform. It was obtained in the form of long colourless needles melting at 157–58°. It gave no colour with ferric chloride in alcoholic solution. Boiling with water or alcohol should be avoided since it produces decomposition. (Found: C, 60·0; H, 3·8; $C_{11}H_8O_5$ requires C, 60·0; H, 3·6%.)

5-*ω*-*Methoxy-acetyl*-4-*hydroxy-coumarone.*—Well dried acetyl-karanjic acid (2 g.) was mixed with carbon tetrachloride (3 c.c.) and finely powdered phosphorus pentachloride (2 g.). The mixture was heated on a boiling water-bath till the evolution of hydrogen chloride fumes was over and the solution became clear. The hot solution was decanted from the excess of unused phosphorus pentachloride and distilled in order to remove as much of the carbon tetrachloride as possible. A light brown liquid of the acid chloride was thus obtained and it solidified on cooling in ice. It was, however, found to be a liquid at the laboratory temperature and was directly used for further condensation after being washed with petroleum ether, in order to remove carbon tetrachloride and phosphorus oxychloride.

Ethyl-*α*-*γ*-dimethoxyacetoacetate (2 g.; 2 mols.) was gradually added to sodium powder (0·22 g.; 2 atoms) suspended in anhydrous ether (30 c.c.) and shaken. After about an hour a solution of the acid chloride (1 g.; 1 mol.) in dry ether (15 c.c.) was introduced causing a mild reaction. The mixture was kept overnight, and gently boiled for about four hours in order to complete the reaction. After distilling off the ether, the product was treated with 10% methyl alcoholic potash (10 c.c.) and the mixture kept gently boiling for about three hours. As much of the alcohol as possible was then distilled off, and the residue treated with excess of dilute sulphuric acid. The solid product was extracted with ether and the ether solution was washed with aqueous sodium bicarbonate in order to remove any karanjic acid that might have been formed. On evaporating the ether solution, the pure ketone was obtained and it was recrystallised from dilute alcohol. It appeared in the form of rectangular plates and needles melting at 96–97°. It gave a bright violet colour with alcoholic ferric chloride and agreed in all respects with an authentic sample of 5-*ω*-methoxy-acetyl-4-hydroxycoumarone. The mixed melting point was undepressed. (Found: C, 64·0; H, 5·3; $-OCH_3$, 14·7; $C_{11}H_{10}O_4$ requires C, 64; H, 4·9; $-OCH_3$, 15·1%.) When the substance was heated with benzoic anhydride and sodium benzoate at 180° for 6 hours karanjin was obtained in good yield.

Our thanks are due to Dr. S. Rangaswami of the Pharmaceutical Laboratory for the supply of karanjin and to Mr. G. V. L. Narasimha Murthy for the microanalyses.

Summary

The methyl ether of karanjic acid has been converted into 5-ω-methoxyacetyl-4-methoxycoumarone which is found to be identical with the methyl ether of the ketone obtained by the hydrolysis of karanjin with alkali. Following a similar procedure 5-ω-methoxyacetyl-4-hydroxycoumarone has been synthesised from karanjic acid and this yields karanjin when condensed with benzoic anhydride and sodium benzoate. Thus all the stages in the complete synthesis of karanjin have been accomplished.

REFERENCES

1. Limaye .. *Abs. Ind. Sci. Cong.*, 1925, 118 and 1926, 151; *Rasayanam*, 1936, 1–14; and 1937, 119.
2. Manjunath, Seetharamaiah and Siddappa *Ber.*, 1939, **72**, 93.
3. Rangaswami and Seshadri *Proc. Ind. Acad. Sci.* (A), 1939, **9**, 259–64.
4. Reichstein .. *Helv. Chim. Acta.*, 1933, **8**, 126.
5. Pratt and Robinson .. *J. C. S.*, 1925, 168.

PHOTOELECTRIC EFFICIENCY OF FERROMAGNETIC METALS AT DIFFERENT TEMPERATURES IN THE SOFT X-RAY REGION

By Dr. S. Ramachandra Rao
and
Mr. K. S. Sankarasubba Iyer
(*Department of Physics, Annamalai University, Annamalainagar*)

Received March 7, 1941

1. *Introduction*

Richardson and Bazzoni (1921) first showed that photoelectrons liberated from a metal when irradiated with X-rays may be used for the detection and intensity measurement of soft X-rays. In fact they found it possible to detect the K-rays of carbon by the photoelectric method. The substance under investigation was bombarded with electrons in a highly evacuated quartz tube. The soft X-radiation produced passed between two parallel plates of a condenser to be freed from ions and electrons. The filtered radiation was received on a metal plate from which the emitted photoelectrons were collected by a shield. The relative soft X-ray emissivities of different metals could be measured by the photoelectric current, maintaining the bombarding electron current for soft X-ray excitation constant.

Similar observations were made at the same time by Hughes (1922), Kurth (1921), Holweck (1922) and Mohler and Foote (1921).

There have been three directions in which work on soft X-rays and photoelectrons from metals has progressed. Several investigators have adapted the photoelectric method for the study of soft X-ray critical potentials. The photoelectric current divided by the thermionic current is plotted against the potential difference maintained between the cathode and the soft X-ray target. At certain voltages an increase in the soft X-ray excitation takes place. This increase is associated with the excitation of characteristic X-rays. The potentials at which increased excitation is observed are known as critical potentials. The critical potentials of a large number of metals were found by the photoelectric method by Thomas (1925), Compton and Thomas (1926), Richardson and Andrews (1930), Richardson and Rao (1930), Richardson and Chalklin (1926, 1928 *a* and *b*), Andrews, Davies and Horton (1926, 1928) and Davies and Horton (1926). Carbon, nickel, iron, cobalt, tungsten and copper have been studied in detail. Richardson

and Rao (1930) showed that when the ratio of the photoelectric current to the thermionic current is plotted against the applied potential and if large intervals of potentials are chosen, most of the inflexions are smoothed out. A few critical values still remain and these could be associated with the Bohr terms of the atom concerned. The general trend of the curves is thus found to be governed by the X-ray level structure of the element. But the detailed inflexions should be due to other causes.

The efficiency of soft X-ray excitation from metallic elements was studied by Richardson and Robertson (1927 and 1929) and Davies (1928). Richardson and Robertson measured the relative soft X-ray emissivities of fourteen elements by the photoelectric method under various exciting voltages up to 500. They found further that in contrast to the behaviour of ordinary X-rays for which the efficiency is proportional to the atomic number, the soft X-ray efficiency was found to be a periodic function of the atomic number. They showed that the soft X-ray efficiency also depended on the applied potential in the region within 6,000 volts. Nakaya (1929) continued the investigations of Richardson and Robertson paying special attention to the state of the surface of the metals, like the polishing of the surface and the state of degassing of the photoelectric plate. He discovered that under ideal conditions the soft X-ray efficiency increases steadily with the applied potential, rapidly at first and more slowly later and finally tends to reach apparently a saturation value. Rao (1935) has drawn attention to this result of Nakaya and explained the saturation effect as being due to the increased depth at which photoelectrons are liberated at higher potentials and to the consequent absorption of the low velocity photoelectrons.

A third direction in which work has been accomplished is the problem of the photoelectric efficiency of metals in the soft X-ray region. Davies (1928) studied the photoelectric efficiency of nickel, iron, copper and cobalt detectors. The work was greatly extended by Bandopadhyaya (1928) who excited soft X-rays from a copper anticathode and studied the photoelectric efficiency of eleven elements. He took the precaution of degassing both the anticathode and the photoelectric detector.

We shall next consider the velocity distribution of the photoelectrons produced by soft X-rays since this study has a direct bearing on the present investigation. This problem was studied in detail by Rudberg (1929). He used a special method of magnetic analysis to find the velocities of the photoelectrons. Curves were given for the emission from silver, copper, aluminium and carbon. The bombarding voltage was 700 volts, and the anticathode used was arc carbon. The soft X-rays generated were allowed

to fall on one of the metals to be investigated and the velocities of the photoelectrons were determined by magnetic analysis. Rudberg's investigations led him to the discovery of the existence of two groups of electrons in the photoelectric emission. One group of electrons had low energy, mostly of the order of a few volts and scarcely exceeding 20 volts. These electrons accounted for 80% of the total photoelectric current. The second group consisted of fast electrons. This group was found to contribute only a small per cent. to the total emission. It was distributed over the whole region but there was concentration in the part between 200 and 280 volts.

Subsequent investigations of Rudberg (1930) on the study of secondary electron emission showed the presence of three groups of electrons in the secondary emission caused by the bombardment of metals with primary electrons. The first group contained those electrons which were returned with the same velocity as the primary. Those electrons which undergo inelastic collisions with the orbital and structure electrons, and are hence returned with some loss of energy constitute the second group. The slow secondary electrons fall within the third group. Rao (1933) showed that the efficiency of the second and third groups is small at low temperatures but increases rapidly as the potential is raised.

Richardson (1928 and 1930) drew attention to the similarity of the phenomena of soft X-ray excitation and secondary electron emission. He suggested that when a metal surface is bombarded with electrons, the first act is the excitation of a structure electron by the primary which is returned as part of the high energy group of secondaries. When the excited structure electrons return to the ground state, the low energy secondary electrons and soft X-rays result as a consequence. Richardson's explanation accounts for the presence of a large number of slow photoelectrons when a metal surface is irradiated with soft X-rays and for the large yield of slow electrons in the secondary emission.

Tartakowsky and Kudrjawzewa (1932) reported the observation that the secondary electron current from nickel shows a sudden decrease in value at the Curie point of nickel. Their apparatus consisted of a nickel plate which was heated for degassing by a tungsten filament fixed on one side. The primary electrons were incident on the other side. Part of the secondary emission fell into a Faraday chamber and was measured by an electrometer.

The results of the foregoing observers were considered by Treloar and Landon (1938). These authors have observed that no significance can be

attached to the results of Tartakowsky and Kudrjawzewa because of the following uncertainties in their experimental arrangement:

(1) Constancy of the angular distribution of the emitted electrons.

(2) Constancy of the energy distribution of the emitted secondaries.

(3) Constancy of potentials on the glass walls.

(4) Absence of stray magnetic fields due to the current in the filament used to heat the target.

It is obvious that these conditions were not satisfied in the experiments under review. Tartakowsky and Kudrjawzewa (1932) found that at an applied potential of 30 volts, the secondary electron current increased when the temperature of nickel was raised from 150° C. to 350° C. and an abrupt fall was obtained at 350° C., the Curie point of nickel. A continuous rise of the secondary current was thereafter noticed. The secondary emission from a copper target was found to increase linearly with temperature, for which observation there is no theoretical or other experimental support.

Hayakawa (1933) reported similar observations with iron, cobalt and nickel. His method of studying the secondary emission was similar to that adopted by Rao (1930 *a*). He studied the transformations of metals by the abrupt changes in the secondary current as the temperature of the target was steadily raised. The secondary coefficient showed large variations at temperatures corresponding to the Curie point in the case of nickel and to transformation points in the cases of cobalt and iron. Hayakawa interpreted these results in the light of Richardson's (1930) theory of structure electrons. Treloar and Landon (1938) have drawn attention to the existence of several discrepancies in the results of Hayakawa (1933).

Specific attention to the inherent difficulties present in the conclusions of Hayakawa and of Tartakowsky and Kudrjawzewa was drawn by Rao (1937) who did not observe any sudden alterations in the excitation of soft X-rays and the emission of photoelectrons from nickel in the neighbourhood of the Curie point. Attention has already been drawn to the work of Rudberg (1930) on the similarity of the phenomena of secondary electron emission and photoelectric emission from metals by soft X-rays. If any anomaly is noted in the secondary electron current for nickel at the Curie point, one would expect a similar variation in the photoelectric emission. But such has not been found to be the case with respect to nickel in the range below 400° C.

Treloar and Landon (1938) investigated the secondary emission from nickel, cobalt and iron. They obtained no sudden changes at the

transformation or the Curie points. Varadachary (1940) very recently showed that the secondary coefficient of nickel is constant within 1% in the temperature range 30° C. to 450° C. He took special precautions to degas the target thoroughly. His conclusions were confirmed by the investigations of Wooldridge (1940) who found very small changes (less than 1 per cent.) in the secondary coefficient when the temperature of a ferromagnetic material was raised above the Curie point. There is therefore a large mass of experimental data which do not support the possibility of the existence of any abrupt variation of the secondary coefficient when the temperature of a ferromagnetic metal is just raised above the Curie point.

Except for the investigation of Rao (1937) on the photoelectric emission from nickel produced by soft X-rays there has been no other study of the temperature variation of the photoelectric emission. The purpose of the present investigation is to study how the photoelectric emissions of nickel, cobalt and iron vary with temperature when these metals are bombarded with soft X-rays. The temperature range studied was 30° C. to about 1,000° C.

To ensure identical conditions, targets of cobalt, iron and nickel were enclosed together so that they could all be bombarded simultaneously and studied under the same conditions of heat treatment. Special attention was paid to the degassing of the metals, since it has become increasingly recognised in recent years that the thoroughness of degassing greatly influences the ejection of slow electrons from metals (see for example Warnecke, 1936).

2. *Experimental*

(*a*) *Electron Tube.*—The experimental tube is illustrated in Fig. 1. It was made of pyrex by the Scientific Instrument Company of Allahabad. It consists of two vertical arms connected by a horizontal tube. One of the vertical arms has a side tube A for connection to the high vacuum equipment. The arm B consists of a shield S_1 of plate copper, which could be earth connected. The target T made of nickel, used for the production of soft X-rays was mounted on a vertical support and could be rotated in position by magnetic device. The vertical rod on which the target T was fixed had soft iron pieces fixed horizontally. With the aid of a strong horse-shoe magnet these soft iron pieces could be rotated round and thus the target T could be rotated to any desired position. A tungsten filament F_1 was arranged in the position shown in Fig. 1 by leads from the upper cover of the arm B. This filament consisted of four turns of tungsten wire of s.w.g. 38 each turn having a diameter of about three millimetres. The spiral became white hot when a current of about 2·8 amperes was passed through it.

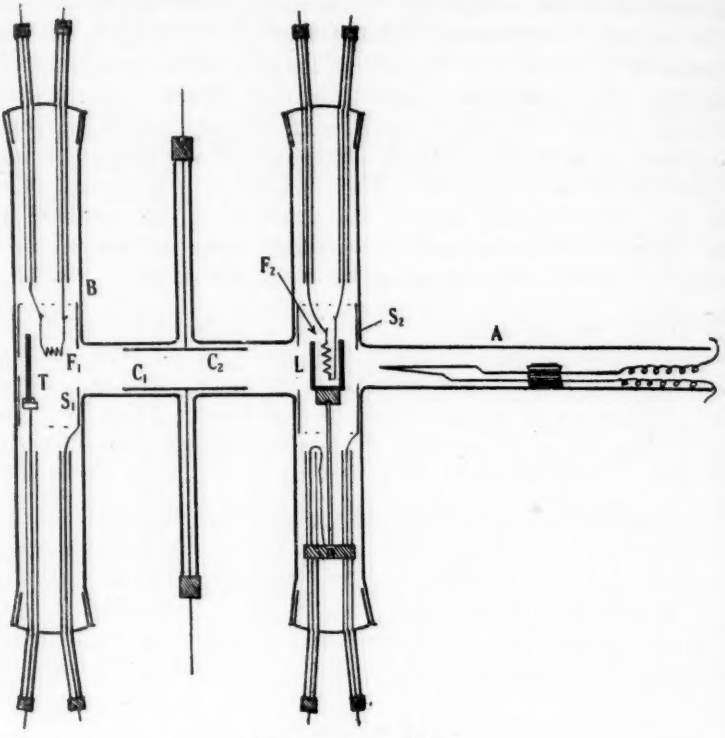

FIG. 1. Electron Tube

During degassing, one of the faces of the target T was turned towards the filament F_1, while during the experiment the other polished face was directed towards the filament. This device prevented deposition of tungsten on that face of the nickel from which soft X-rays were produced. The investigations of Richardson and Chalklin (1926) have shown how the intensity of soft X-ray emission is modified by tungsten deposit.

The soft X-rays produced from the target T passed through an aperture 1 cm. in diameter made in the shield S_1 and then through the condenser plates C_1 and C_2, which were raised to $+36$ volts and -130 volts respectively. All positive and negative ions or electrons were absorbed by these condenser plates. These potentials were found to be more than sufficient to filter off the ions and the electrons diffusing out of the arm B. The filtered radiations were then incident on one of the photoelectric plates mounted in a lantern-like structure.

(*b*) *Lantern.*—The four photoelectric targets used in this investigation were made of iron, cobalt, nickel and copper. The samples of metals used were pure specimens obtained in plate form from Johnson Mathey, London. Each of these targets was cut from metal plate about a millimetre in thickness and was two centimetres long and one centimetre broad. The plates were polished with emery paper of gradually increasing fineness. The finishing of the polishing was done with emery paper, No. 000.

The four metal pieces were mounted into a frame-work to make up a lantern (Fig. 2). This structure was mounted on a support which could be rotated with the aid of a magnetic device explained earlier. Thus any desired metal face could be turned to receive the soft X-rays proceeding along the space between the condenser plates.

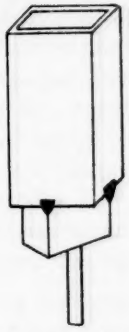

FIG. 2. Lantern

The degassing of the targets was made with a tungsten filament containing six turns of tungsten wire s.w.g. 38, each turn having a diameter of about three millimetres. The spirals were within the hollow space inside the lantern structure. During the degassing operation, the targets were made almost white hot by electron bombardment. But the target faces could be kept clean from tungsten deposits because of the special procedure adopted in enclosing these spirals within the hollow space of the lantern. A shield S_2 made of sheet copper was fixed around the lantern. It had a circular aperture of diamter 1 cm. facing the horizontal tube containing C_1 and C_2. This shield was maintained at a potential of about +50 volts. This potential was found to be more than sufficient to draw all the photoelectrons that were emitted from a target.

All the joints and seals were made with tightly fitting brass caps and some quantity of Bank of England hard sealing wax. Such joints were

found to be perfectly air-tight and the pressure inside the tube may be lowered to values of the order of 10^{-7} cm. without difficulty.

(*c*) *High Vacuum Equipment.*—The high vacuum equipment consisted of a Cenco Hyvac pump and a Cenco three-stage mercury diffusion pump. The low pressures attained were measured with a McLeod gauge. Pressures of the order of 10^{-6} mm. could be measured accurately. Pressures lower than this value were detected by the sticking tendency of the mercury at the top of the capillary tube as the cistern was slightly lowered from its top position. A large glass aspirator half-filled with dry fused calcium chloride was placed next to the backing pump. A rough gauge consisted of a closed U-tube gave the approximate value of the backing pressure. Between the mercury diffusion pump and the electron tube there were two glass traps. One of these contained thermally treated cocoanut charcoal. Both the traps were surrounded by a mixture of solid carbon dioxide snow and methyl alcohol. Temperature in the neighbourhood of $-90°$ C. could be obtained by this method. The traps condensed any vapours present inside and the residual gases issuing from the heated metals and the walls of the containing tubes. The connection for the McLeod gauge was taken between the two traps. Thus the passage of mercury vapour into the electron tube was efficiently prevented by this arrangement. A tube containing phosphorus pentoxide was connected to the McLeod gauge and it served efficiently to absorb the slightest trace of water vapour present inside.

On the high vacuum side stop-cocks having a centimetre bore were used. Except for a short length of pressure tubing used to connect the Hyvac pump, no other rubber connections were used. The glass connections to the diffusion pump were made with the aid of conical ground joints fitting snugly into ground metal joints. Cenco grease was used for these glass-metal joints.

To increase the efficiency of the pumping outfit, all the glass tubes on the high vacuum side had diameters of about 1·8 cm.

(*d*) *Electrical Connections.*—A sketch of the electrical connections adopted is shown in Fig. 3. The currents for the filaments F_1 and F_2 were taken from high capacity storage batteries. The currents were read on ammeters connected in the filament circuits. With the aid of rheostats, the currents were regulated not only to prevent the blowing up of the filaments but also to get any desired thermionic currents. One terminal of each filament was earth connected. The shield S_1 surrounding the target T was also earth connected.

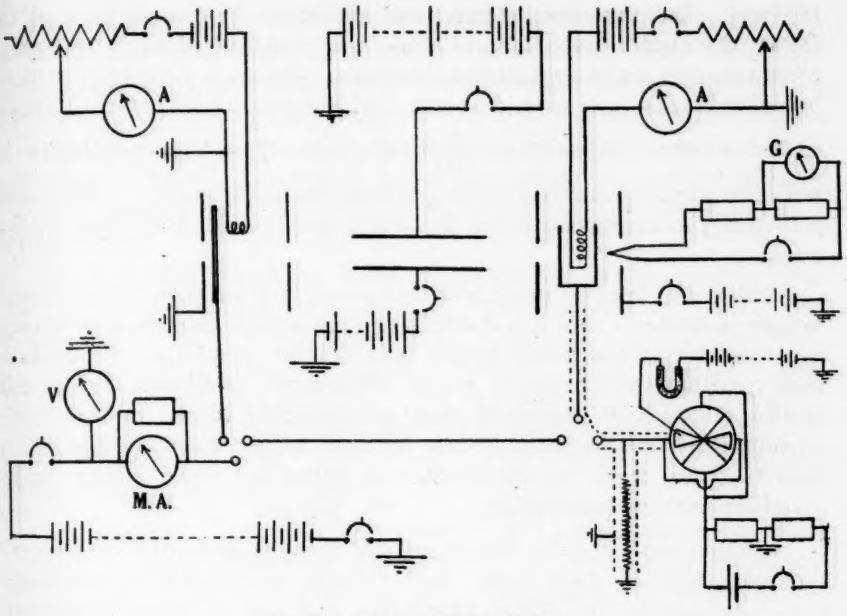

FIG. 3. Electrical Connections

The potentials of -130 volts and $+36$ volts required for the condenser plates were taken from a battery of Estralea dry cells each of which gave 4·5 volts. This battery was earth connected suitably in the middle to give the required potentials on the condenser plates.

The shield S_2 which attracts photoelectrons liberated when filtered soft X-rays fall on one of the metal pieces of the lantern L, was maintained at $+54$ volts with a battery of 12 dry cells. The lantern L could be connected either to a high potential source or to one pair of quadrants of a quadrant electrometer. A leak consisting of a high resistance of the order of 10^{11} ohms was connected between the lantern and the electrometer.

(*e*) *High Resistance.*—Since photoelectric currents to be measured are of the order of 10^{-11} ampere, it is essential to make the high resistance have a value of about 10^{11} ohms. Wire resistances of such high values are out of the question. Grid leaks used for radio work do not have resistances more than 10^8 ohms. Different types of resistances are usually made to have such large values.

Campbell (1912) showed that resistances of values ranging from about 10^8 ohms to about 10^{12} ohms could be constructed with Xylol-methyl alcohol

mixtures. These are easy to make and are known by Campbell's work to follow the Ohm's law. Two of these were constructed using soft glass containers with sealed-in platinum electrodes. The great difficulty with these liquid resistances was a residual and variable polarisation which is found to be sometimes as much as $\frac{1}{200}$th of a volt. This large polarisation is bound to affect the accuracy of the photoelectric measurements. After some preliminary measurements it was decided to give up using such liquid resistances.

Indian ink lines on paper and lead pencil lines on paper may be used as high resistances. But it is doubtful how far such resistances tend to keep a constant value and follow Ohm's law. Various conducting glasses have been tried but these have not proved satisfactory. Andrews, Davies and Horton (1928) used resistances made of conducting glasses in their work on soft X-ray emission from different metals. Hughes and DuBridge (1932) state that they tried various conducting glasses but could seldom make a resistor without polarisation.

Another method is to deposit metallic films by sputtering or evaporation on quartz or glass rods. Such resistors are found to be completely free from polarisation, follow Ohm's law and have a small temperature coefficient. It was decided to make high resistances by depositing lampblack on a quartz rod. Such resistances have been used for photoelectric measurements by Richardson and Chalklin (1926) and Richardson and Rao (1930).

The high resistance employed consisted of a quartz rod of about 4 mm. diameter and 10 cm. long fitted with brass cups at the ends. The quartz rod was smoked lightly and uniformly in the smoky flame of a batswing burner. Electrical connections to the caps were ensured by smearing the cap ends with Indian ink. The quartz rod was enclosed in an outer glass tube, the leads being of platinum wire. A side tube connected to the glass tube contained a small quantity of phosphorus pentoxide. With the aid of a side tube, the space inside was thoroughly evacuated with a pump and the connecting tube was sealed. The smoked quartz rod was thus placed in a vacuum chamber free from water vapour. Such a resistance was found to keep steady for a considerable length of time. Its resistance was found to be nearly 10^{11} ohms by the leakage method using a quadrant electrometer.

(*f*) *Quadrant Electrometer.*—The quadrant electrometer used was one of the Dolezalek pattern obtained from Messrs. Pye and Co. The suspension wire was made of phosphor bronze. The light aluminium vane was raised

to a potential of about 110 volts using a battery of 25 dry cells. The sensitiveness of the quadrant electrometer was determined with a potentiometer arrangement consisting of two resistance boxes and an accumulator. The quadrant electrometer gave a sensitiveness of 600 divisions per volt.

The entire lead from the photoelctric target to the quadrant electrometer was taken through a surrounding metal tube which was earth-connected. The high resistance was also fixed inside a large tin box which was also earth-connected.

(*g*) *Bombarding Potential.*—Bombarding of the targets by electrons from the filaments was necessary for degassing. The potential required for this bombarding was taken from a battery made of Dagenite 2-volt accumulators. The bombarding potential was usually 450 volts. This potential was measured by an electrostatic voltmeter. The accumulators could be connected in four blocks of about 112 volts each and could be charged from a DC generator giving 120 volts. Special care was taken to see that the accumulators were in proper condition.

The bombarding current was measured with a milliammeter having a sensitiveness of 1 milliampere per division. To measure the thermionic current used for the production of soft X-rays from the target T, the milliammeter was suitably shunted to increase its sensitiveness to 0·012 milliampere per division. With the aid of appropriate switches the milliammeter could be included on the side of the target T or on the side of the lantern L.

(*h*) *Degassing.*—The degassing of the target T and the photoelectric plates constituting the lantern L was effected by electronic bombardment. The temperatures reached by the targets during bombardment were about 1,000° C.

The general procedure adopted was as follows: A preliminary pressure of about 10^{-6} mm. was first obtained. The traps were surrounded by carbon dioxide snow and methyl alcohol contained in thermos flasks. The tungsten filaments were glowed till they appeared white hot. The pyrex tube and the metal parts inside were heated by a burner with the sealing wax joints cooled with cotton wads drenched with iced water. A large amount of gas was liberated by this process. Frequently the stop-cock next to the electron tube was closed and the traps were rendered free from the gas they had absorbed. This was accomplished by removing the cooling flask and gently warming the charcoal with a burner.

This operation was continued till very little gas was evolved. Next the targets were heavily bombarded with the traps in the cooling mixture. The

targets were thus raised to temperatures not less than 1,000° C. This bombarding was continued till the evolution of gas practically ceased.

Before observations were taken the nickel target T and the lantern plates were heated by electronic bombardment for a specific length of time. Then observations were taken. The results showed that such uniform treatment yields results which could be reproduced to within 1·5 per cent.

(*i*) *Measurement of the Temperature of the Lantern.*—The temperatures to which the photoelectric plates were raised were determined with a thermocouple made of a platinum wire and a wire containing 90% platinum and 10% rhodium. The thermoelectric current was measured with a sensitive mirror galvanometer G. This thermojunction has been studied in detail by the National Bureau of Standards (U.S.A.) and the electromotive forces at different temperatures are given in Kaye and Laby's Tables of Physical and Chemical Constants. Knowing the values of the appropriate resistances introduced in the circuit, the deflection of the galvanometer could be expressed directly in terms of the excess of temperature of the thermoelectric junction over that of the atmosphere. In fact a division on the scale of the galvanometer represented an excess of 5° on the centigrade scale. The wires constituting the thermojunction were taken out by suitable leads through the wax joint between the electron tube and the high vacuum equipment. The junction could be made to touch one of the lantern plates or could be withdrawn to some distance. This was effected by a magnetic device, the control from outside being with the aid of a powerful horse-shoe magnet.

(*j*) *Method of Measuring Photoelectric Efficiency.*—After the degassing operations, a potential of 400 volts was maintained between the target T and the filament F_1. The thermionic current (i_f) was measured with the milliammeter. The soft X-rays falling over one of the photoelectric targets give rise to photoelectrons. These photoelectrons leave the lantern L and are attracted to the shield S_2. The lantern L becomes positively charged. Let i_f be the photoelectric current. If R be the magnitude of the quartz resistance the upper end of this resistance is raised to a potential equal to $i_f R$ since the lower end is earth-connected.

This potential $i_f R$ is applied to one pair of quadrants of the electrometer. The deflection of the spot of light is obtained. If D is the deflection of the spot of light and k the sensitiveness of the electrometer in volts per division, it follows that $kD = i_f R$. Hence $i_f = \frac{kD}{R}$. The photoelectric current i is thus found to be directly proportional to the deflection D.

To use the electrometer at its full sensitiveness and yet secure a reasonably large photoelectric current, the opposite pair of quadrants were raised to a suitable potential with the aid of a potentiometer outfit shown in Fig. 3. The spot of light was brought close to its initial position by applying an almost equal and opposing potential to the opposite pair of quadrants with the potentiometer arrangement. Knowing the magnitude of the opposing potential and the deflection read on the scale it was possible to calculate the true deflection D which could correspond to the photoelectric current i_f. In this investigation these deflections were found to be nearly 600 divisions on the scale. This would correspond to an applied potential of about 1 volt. The high resistance being nearly 10^{11} ohms, the photoelectric current works to the order of 10^{-11} of an ampere.

The thermionic current between T and F_1 was maintained uniformly at 0·24 milliampere whenever the photoelectric current was measured. A direct comparison of the deflections of the electrometer gave the relative photoelectric efficiencies.

The investigations at high temperatures were carried out by raising the temperature of the lantern to the required value and switching over almost immediately to the photoelectric measurements.

A typical method of determining the photoelectric efficiency was to start a stop-clock and determine the reading of the spot of light at fixed time intervals. On drawing a graph and extrapolating, the efficiency at the starting time and hence at the temperature required could be determined. Since the photoelectric efficiency was practically independent of temperature (except in the case of iron) in the range 30° to 1,000° C. the movement of the spot of light was within a very restricted range, as the temperature of the photoelectric target decreased slowly.

Some Corrections on the Soft X-Ray Side.—To the applied potential to which the soft X-ray target was raised, some corrections are necessary. First the ends of the hot wire cathode are cooler than the middle and practically all the electrons come from the hottest part. The middle third of the filament may be taken to be the source of electrons. The drop along the filament was nearly 6 volts. This would involve a correction of about 3 volts to be subtracted from the reading of the voltmeter since the voltmeter was connected to the negative end of the filament. There may be an uncertainty of about a volt in this correction.

An addition has to be made for the initial emission velocity of the electrons. This velocity is distributed according to Maxwell's law. Taking into account the average velocity of emission, Richardson and Chalklin

calculated a correction of $+0{\cdot}391$ volt when the temperature of the filament is 2,000° C.

They have also considered the work necessary to drag an electron out of the hot cathode. This correction works to about $+4{\cdot}9$ volts. The net correction is hence nearly $2{\cdot}3$ volts. The applied potential for the soft X-ray target relative to electrons emitted from the filament may thus be given as $402{\cdot}3$ volts.

3. Results

In drawing general conclusions from the resutls obtained with iron, cobalt and nickel it should be remembered that the results were recorded on several days spread over a period of about 5 to 6 months. However carefully degassing operations are carried out, perfect identity of the surface condition of the targets is most unlikely. Each observation of the photoelectric efficiency at any particular temperature is the average of several readings which agree to within $1{\cdot}5\%$. In a scrutiny of the results, attention should necessarily be focussed on systematic variations of the photoelectric current as the temperature of the target concerned is gradually raised.

After an examination of all the four metals chosen at different high temperatures, nickel was taken up for special study. The Curie point of nickel is well known to be about 358° C. Hence the temperature range from 290° to 404° C. was carefully and thoroughly investigated.

Table I shows the comparative photoelectric efficiencies of iron, cobalt, nickel and copper at different temperatures. At each temperature the photoelectric efficiency of copper is taken to be 1.

TABLE I

Temperature °C.	Iron	Cobalt	Nickel	Copper
950	0·97	1·16	1·12	1·00
893	0·93	1·16	1·12	1·00
853	0·89	1·09	1·09	1·00
788	0·97	1·08	1·06	1·00
723	1·01	1·19	1·17	1·00
480	0·99	1·02	1·14	1·00
30	1·00	1·08	1·14	1·00

Before proceeding to discuss the conclusions of these observations the photoelectric efficiencies of copper at different temperatures will be

presented. Table II gives the deflection on the electrometer scale for copper estimated at different temperatures.

TABLE II

Temperature	Electrometer deflection
°C.	cm.
950	61·9
893	61·9
853	63·6
788	62·2
723	59·7
480	62·6
30	63·0

It will be observed that with the exception of the observation at 723° C. there is close agreement between the other values. It is tempting to suggest the slight decrease in the deflections at 893° C. and 950° C. as being probably due to a better state of degassing. The deflection of 59·7 cm. observed at 723° C. for copper is probably an erratic observation because the corresponding values for iron, cobalt, and nickel given in Table I are slightly larger than the neighbouring data.

Table III gives the photoelectric efficiency of nickel in the properly degassed state at different temperatures in the neighbourhood of the Curie point.

TABLE III

Temperature °C.	Photoelectric efficiency in terms of this value at 30 °C.
594	1·007
404	1·004
385	0·983
364	0·993
348	0·997
330	1·004
290	0·992
30	1·000

Since the temperature range was restricted it is likely that almost uniform degassing conditions were obtainable. An examination of the above results shows that the photoelectric efficiency of nickel is constant to within 1·3% in the temperature range 290° to 594° C.

Fig. 4 shows the graph between the photoelectric efficiency of nickel in terms of the photoelectric efficiency at 30° C. plotted against the temperature of the target. It is clear that the curve is a straight line passing evenly among the points, this straight line being parallel to the temperature axis. It may be safely concluded that the photoelectric efficiency does not show

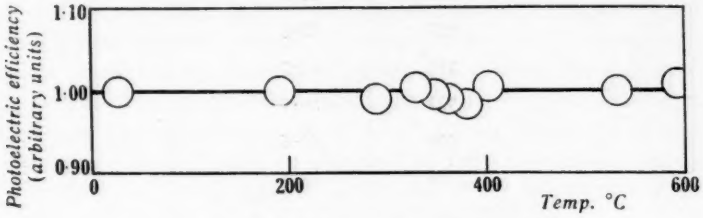

FIG. 4. Graph for Ni at Low Temperature

any abrupt variation in the neighbourhood of 358° C. This observation is in close agreement with the conclusions of Rao (1937). Further the photoelectric efficiency of copper when exposed to soft X-radiation was found by him to be independent of temperature in the range 30° to 500° C.

The photoelectric efficiencies of iron, cobalt, and nickel at different temperatures may next be considered. Fig. 5 shows the graph wherein the

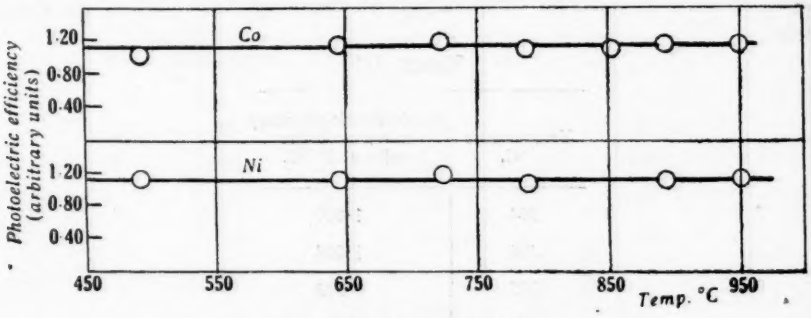

FIG. 5. Graphs for Ni and Co

relative photoelectric efficiencies of cobalt and nickel are plotted against temperature. The values obtained for cobalt and nickel show that in these two cases the photoelectric efficiency may be taken to be independent of

temperature within the limits of experimental error. In any case systematic variations are not noticeable.

The case of iron however seems to stand in a slightly different position. Up to about 770° C. the value of the photoelectric efficiency may be taken to be nearly constant but after 770° C. there appears to be a drop in the value of the photoelectric efficiency and a subsequent gradual rise from 880° C. to about 950° C. It may be mentioned here that three different crystal forms of iron are known. The α and β forms of iron both have a body-centred cubic structure but with different lattice constants. On the other hand the γ form is a face-centred cubic. At temperatures within 768° C., iron exists in the α state. The transition from α to β iron occurs at 768° C. and the transition from β to γ occurs at 910° C.

A similar type of transformation takes place in the case of cobalt at 850° C., at which point there is a transition from the hexagonal close-packed structure to the face-centred cubic lattice. An observation of Table I shows that the crystal transformation in the case of cobalt is not accompanied by a change in the photoelectric efficiency. In the case of iron however it is likely that a rapid change occurs at the transition points corresponding to the α–β and the β–γ forms. This peculiar behaviour of iron will be taken up for special discussion in the next section.

4. *Discussion*

It is necessary to draw attention at the outset to the important point that photoelectrons are produced in the first few atomic layers of the photoelectric target when these are bombarded with soft X-rays. Bandopadhyaya (1928) found that soft X-rays generated at an applied potential of 350 volts fall to 0·6% after transmission through $1 \cdot 36 \times 10^{-5}$ cm. of gold and to 0·1% by transmission through $7 \cdot 9 \times 10^{-5}$ cm. of aluminium. Assuming the edge length of the face-centred cube of gold crystal to be about 4 A, (Clark 1932) the film of gold used above contains 340 lattice layers. In the case of aluminium there would be 1975 lattice layers. It may be shown that by far the larger number of electrons come from the first few layers. This shows that the photoelectron produced by the absorption of a quantum has a very small probability of undergoing a fresh inelastic encounter and ejecting another photoelectron.

Rudberg (1928) found that a double thickness of gold leaf transmitted 1% of the radiation. This gives an absorption coefficient $2 \cdot 9 \times 10^{5}$ cm.$^{-1}$ as compared with the value $5 \cdot 3 \times 10^{6}$ cm.$^{-1}$ for 500 volt electrons calculated by Rudberg from the value of Becker (1927) for nickel.

It is interesting to compare these values for 500 volt soft X-rays with the coefficient for the ultra-violet light. Partzsch and Hallwachs (1913) calculated a value $10 \cdot 3 \times 10^5$ cm.$^{-1}$ for the absorption coefficient of gold leaf for ultra-violet light from the experimental observations of Rubens and Ladenberg (1907). The absorption coefficient found by Rudberg (1928) for gold was the outcome of some preliminary tests. Hence although great accuracy need not be attached to his method, it is clear that the order of value of the absorption coefficient in the 500 volt region is about the same as in the ultra-violet region.

There is another point of resemblance between the two regions under consideration. For hard X-rays, absorption of X-rays may be regarded almost as a photoelectric phenomenon. But with soft X-rays theoretical and experimental considerations show that the efficiency of production of photoelectrons by soft X-rays is low. This is probably due to the absorption of the electrons within the metal. But definite evidence towards this conclusion is lacking. Gudden (1928) has drawn attention to the low efficiency of ultra-violet light.

These similarities lead one naturally to expect some resemblance between the photoelectric properties due to soft X-rays and the ultra-violet light.

We shall next consider the remarkable conclusions of Rudberg who analysed the velocity of the photoelectrons produced by soft X-rays, using a magnetic deflection method. He generated soft X-rays from an anode of arc carbon at an applied potential of 700 volts. The soft X-rays were filtered from ions and electrons by a trapping device and were then incident on the photoelectric target, which was cylindrical in shape. The velocity of the photoelectrons emitted was analysed by the magnetic deviation method. Curves were obtained for the emission from silver, copper, aluminium and carbon and for a transparent silver film deposited on a quartz rod.

In all these cases, the emission was constituted of a group of electrons with energies amounting mostly to only a few volts and a much less prominent group having energies in the region 200–280 volts. Whereas the first group depended on the surface condition, the second group was not so dependent. Rudberg has accounted for the second group satisfactorily by assuming that it consists of primary electrons produced by the K_α radiation of carbon. Thibaud (1927) using a grating method obtained the value 275 volts for this radiation.

There were no electrons with velocities above 300 volts although the soft X-ray tube voltage was 700 volts. The first group of electrons is

according to Rudberg the result of encounters with some of the primary electrons and the atoms. Secondary electrons are emitted and these constitute the first group. The energies of the group of photoelectrons do not amount to more than a few volts.

Rudberg showed that these slow electrons which form a very large percentage of the photoelectrons emitted were not the result of emission due to relatively long wavelength radiations by testing the soft X-rays with a fluorite window transparent down to 1200 A. The photoelectric emission after transmission of the incident radiation through the fluorite was 1/600th of the emission, when the radiation was allowed to fall directly on the target.

These important conclusions of Rudberg that a large percentage of the photoelectrons produced by soft X-rays have velocities which correspond to just a few volts lead naturally to the significance of the photoelectric threshold in such emission. In the emission of photoelectrons when metal surfaces are irradiated with light, the photoelectric threshold plays an important rôle. The same threshold is found to play an equally important part in photoelectric emission due to soft X-rays.

Perhaps no single equation in physical science has played a greater part in the development of theoretical knowledge and experimental technique than the fundamental law of photoelectricity first stated by Einstein (1906, 1907). Consider a monochromatic radiation of frequency ν incident on matter. The velocity v of the photoelectron emitted is given by the equation,

$$\tfrac{1}{2} mv^2 = h\nu - w$$

where h is Planck's Constant and w is the work which the electron has to do in passing through the illuminated surface. On this basis, the whole of the energy $h\nu$ of the quantum is absorbed and reappears as the energy of the photoelectron.

If V is the retarding potential which stops the emission of the photoelectron

$$e\mathrm{V} = h\nu - w.$$

A graph drawn between V and ν gives a straight line. Richardson and Compton (1912) and Compton (1912) were among the first to verify this conclusion of Einstein. The brilliant work of Millikan (1916) led to an accurate and extensive study of the photoelectric effect in its relation to the equation of Einstein. His determination of the Planck's Constant h from such measurement gave a value which is probably accurate to 0·5%. Other workers (for an account, please see Hughes and DuBridge, 1932, pp. 24–26)

have adduced a large amount of experimental evidence in favour of the Einstein equation.

If in this equation, we write $w = h\nu_0$ it becomes

$$\tfrac{1}{2} mv^2 = h(\nu - \nu_0).$$

This equation leads to the important conclusion that a photoelectron is liberated only when ν is greater than ν_0. This frequency ν_0 is known as the photoelectric threshold. Its value for any metal may be determined from the graph between the retarding potential V which just stops emission and the incident frequency ν. On extrapolation, it will be found that V becomes zero at a particular value of ν which is the threshold value. Thus the most important parameter referring to the nature of the surface itself is its photoelectric threshold.

Let us consider soft X-rays generated by a bombarding potential of 400 volts. This corresponds to a minimum wavelength of about 31 A. When this radiation containing wave lengths from 31 A and extending almost up to the ultra-violet falls on a metal target, it may be shown that the intensity of the radiation is directly proportional to the number of photoelectrons produced. Of course Einstein's relation suggests this, for, every quantum of radiation should release one photoelectron. But many investigators (Hughes and DuBridge, 1932, pp. 30–32) have shown that while such a one-to-one relation does not obtain in the emitted photoelectric beam, a proportionality however between the intensity of radiation and the photoelectric current is observed. Special mention may be made of the investigations of Ives (1917) and of Ives, Dushman and Karrer (1916).

Richardson (1912, 1912 *a* and *b*) showed that the number N of photoelectrons ejected by ultra-violet light per unit intensity can be expressed as

$$N = C(\nu - \nu_0)/\nu^3$$

where C is a constant, ν is the frequency of the incident light and ν_0 the photoelectric threshold. This equation has been confirmed by the experiments of Roy (1926).

Richardson and Chalklin (1926) and Miss Laird (1927) showed that the energy in a beam of soft X-rays is proportional to the square of the voltage. This property is similar to what is obtained with hard X-rays and shows that the energy in a beam of soft X-rays is also approximately linearly distributed between the different frequencies according to

$$I_\nu d\nu = K(\nu_l - \nu)\, d\nu$$

where K is a constant, I_ν the intensity of radiation for frequency ν, and ν_l the high frequency limit imposed by the voltage V on the tube.

The total number of photoelectrons liberated is given by

$$N = CK \int_{\nu_0}^{\nu_l} (\nu_l - \nu)(\nu - \nu_0)\, \nu^{-3}\, d\nu$$

When the applied voltage is 400 V and the work function is about 5 volts, it is easy to see that ν_i is much greater than ν_0. The integral therefore gives

$$N = \tfrac{1}{2}\, CK\, \nu_l / \nu_0$$

and since

$$h\nu_l = eV$$

$$N = \tfrac{1}{2}\, CK\, eV/h\, \nu_0$$

This development is made on the lines adopted by Bandopadhyaya (1928).

This relation is of special interest since it is adapted for photoelectric emission by soft X-rays.

One important deduction, namely, that the number of photoelectrons varies as V the applied potential for the production of soft X-rays has been confirmed by the experimental investigations of a large number of workers in soft X-rays. This confirmation is true in the restricted range within 7 or 8 hundred volts. That complications occur at higher potentials and the linear relation is no longer true is shown by the investigations of Richardson and Robertson (1929) and Nakaya (1929).

The other important deduction is that the number of photoelectrons emitted varies inversely as the photoelectric threshold value. Any small variation of this threshold is bound to affect the number of photoelectrons profoundly.

We shall next consider the observations made with each of the four metals studied. It may be mentioned that all the measurements were made with the targets degassed as thoroughly as possible.

Iron.—This metal is remarkable for its very large intensity of magnetization. Its Curie point is 770° ± 5° C. (Stoner, 1934, p. 384). When iron is heated, the transition from the α to the β crystalline form occurs at 768° C. which coincides with the Curie point of iron. The β variety is transformed into the γ variety at 910° C.

Fig. 6 shows the changes in the photoelectric sensitivity generally followed by iron when irradiated by mercury arc. The results were obtained by Cardwell (1928 and 1929). The iron was in the form of a strip which was heated by the passage of electricity through it. Temperatures much higher than 950° C. (melting point of iron = 1527° C.) could not be investigated

since the metal will begin to emit thermions because of the temperature. It is seen that there is a sudden change of slope at both crystal transformations. The change of slope at 475 ± 50° C. occurring at the point B in Fig. 6

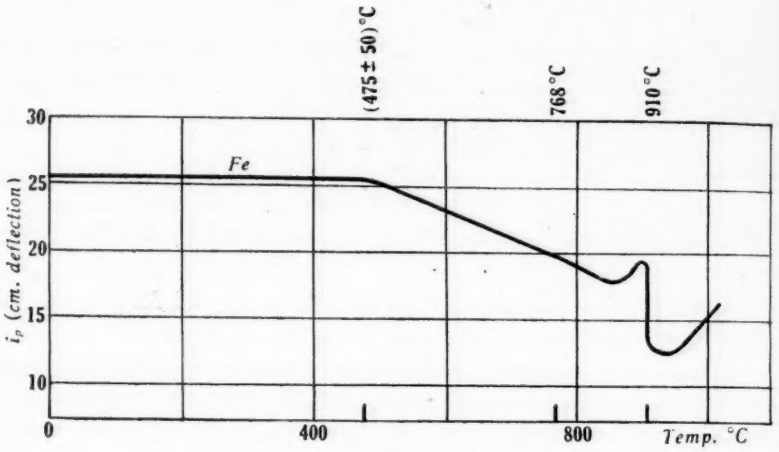

FIG. 6. Graph—Changes of photoelectric sensitivity of iron when irradiated by mercury arc—by Cardwell

is rather puzzling and the cause seems to be obscure. The change at the β–γ transformation is very striking.

Goetz (1923 and 1925) and Seiliger (1926) found a change of thermionic emission of samples of iron when passing through a crystal modification.

But experiments could not establish definitely whether the change was accompanied by a change in the threshold.

Let us examine the other properties of iron before drawing any general conclusions. Fig. 7 shows how the thermal conductivity of iron varies with

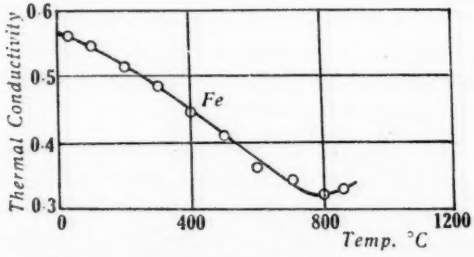

FIG. 7. Graph—Thermal conductivity of iron with temperature

temperature. The data are taken from *International Critical Tables* (Vol. V, p. 221). It will be observed that a slight alteration in slope may be detected at the Curie temperature. At 475° C. there is no change of slope.

The intensity of magnetization is well known to drop rapidly at the Curie point to almost zero. The specific heat of iron also shows a sudden decrease at the Curie point. This decrease is 6·8 per gram atom (Stoner, 1934, p. 373). Klinkhardt (1927) found that a small *decrease* of specific heat of 1·5 calories per gram atom is also obtained at about 900° C. during the β–γ transformation.

These interesting properties do not have any other common feature except that sudden changes occur at the transformation points. But the direction of the change is not the same in all cases.

If we now examine the photoelectric efficiency curve for iron at different temperatures, we observe that the efficiency is constant between 30° C. and about 770° C. At this temperature the efficiency begins to decrease. But at about 880° C. the efficiency increases gradually again. This temperature (880° C.) may be taken to coincide approximately with the β–γ transformation temperature.

It is apparent from the above considerations that there should be a change in the threshold at 770° C. and 880° C. There should be an increase in the threshold at 770° C. and a decrease at 880° C.

Soft X-ray data are thus able to suggest the possibility of changes in the threshold value at the two transition temperatures.

Attention should be drawn here to the fact that the photoelectric efficiency curve for iron shown in Fig. 8 is quite different in every detail from

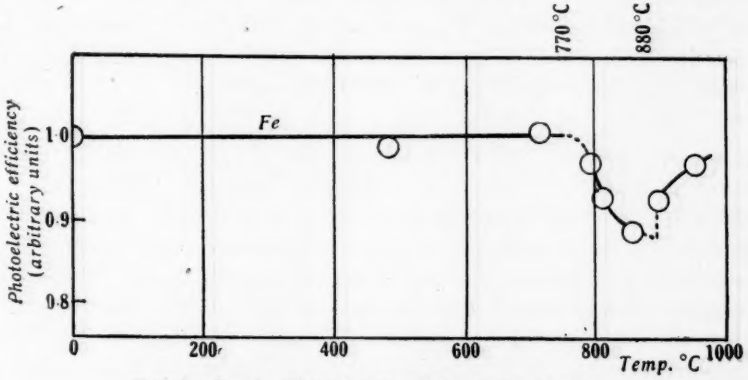

FIG. 8. Graph—Photoelectric efficiency curve for iron

the secondary electron curve of Hayakawa (1933) at different temperatures. Attention has already been drawn to the fact that the investigations of Treloar and Landon (1938) and Varadachary (1940) show that there is no temperature variation of the secondary electron coefficient in the case of iron, cobalt and nickel when the temperatures exceed the transformation and Curie points.

The fact that a change of slope occurs in the photoelectric efficiency curve and not in the secondary electron curve when these are plotted against temperature must be due to the fact that the small variation of the threshold must affect the former and not the latter. A simple calculation shows that a change of the work function from 4·7 volts to 5·2 volts when the iron passes from the α to the β form is enough to explain the observed change. But the secondary electron emission will not be altered by this small change in the work function.

Cobalt.—The Curie point of cobalt is (1120 ± 20)° (Stoner, 1934, p. 384). When the present investigation was started, it was the aim to study the variation of the photoelectric current in the neighbourhood of this point. But experimental conditions would not permit the raising of the temperature to values higher than about 950° C.

Cobalt is however interesting from other points of view. A transformation takes place at 850° C. when possibly the hexagonal close-packed structure becomes face-centred cubic lattice. This transition temperature depends on the purity of the specimen.

Cardwell (1928, 1929) studied the photoelectric sensitivity of cobalt and found a sudden increase in the emission at the transformation temperature 850° C.

Considering the variation of specific heat, the measurements for cobalt are relatively scanty and lacking in precision. But there seems to be so far no definite evidence showing a change of specific heat at 850° C. A large decrease however is noted at the Curie temperature.

The photoelectric efficiency curve for soft X-rays shows no variation with temperature in the range 30° to 950° C. No change of slope is observed at 850° C. Cardwell (Hughesand DuBridge, 1932, p. 65) found the work functions of outgassed cobalt to be 4·25 ± 0·08 volts and 4·12 + 0·04 volts for the hexagonal and face-centred cubic forms. Applying the corrections it is likely that the values are very nearly equal. This explains the absence of any change of slope at 850° C. in the graph between the photoelectric efficiency and temperature. Treloar and Landon (1938) found no change in the secondary emission from cobalt when its temperature was raised from room temperature to about 1,200° C.

Nickel.—This metal is remarkable because of the fact its magnetic Curie point has the low value of (358 ± 2)° C. (Stoner, 1934, p. 384).

Fig. 9 shows the variation of the thermal conductivity with temperature. It is found that the thermal conductivity decreases at first and increases

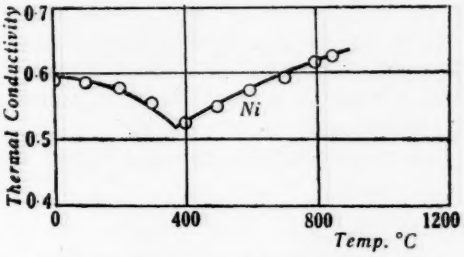

FIG. 9. Graph—Nickel—Thermal conductivity with temperature

again when the metal is raised above the Curie point. The transition at the Curie temperature appears quite sharp. The data for the graph have been taken from the *International Critical Tables* (Vol. V, p. 221).

The specific heat of nickel has been studied with great thoroughness by Lapp (1929). He found for a specimen of Mond nickel that the specific heat decreased from 0·1577 at 353·5° C. to 0·125 at 360·5° C. Thereafter the specific heat rose very slowly to the value of 0·129 at 460° C.

There appears to have been so far no experimental investigation on the photoelectric sensitivity of nickel when its temperature is raised much higher than the Curie point.

Treloar and Landon (1938) and Varadachary (1940) found no change in the secondary emission from nickel in the temperature range 30° to 450° C. Rao (1937) investigated the photoelectric emission from outgassed nickel exposed to soft X-rays and found that the emission was constant when the Curie point was passed. The present investigation leads to the same conclusion. This result shows that the photoelectric threshold does not alter in value when the Curie temperature is passed.

Copper.—It has not been possible to trace in the extensive literature on the subject any investigation on the variation of the photoelectric sensitivity of solid copper with temperature. But the work of Goetz (1927, 1927 *a*) indicates that the sensitivity is constant in the range from the room temperature until the melting point (1085° C.) is reached.

The present research shows that the photoelectric emission remains constant in the entire range from 30° C. to 950° C.

Copper was one of the targets used since it was desirable to have a standard for the measurements on the ferromagnetic metals.

5. *Summary*

Soft X-rays produced from a thoroughly outgassed target of nickel were filtered from ions and electrons by a condenser arrangement and were then made to fall on one of four metal plates fitted into a lantern structure. These four metal targets were of iron, cobalt, nickel and copper. The frame-work could be rotated by a magnetic arrangement and each of the targets could be brought successively for the incidence of soft X-rays. The entire lantern structure was thoroughly degassed before measurements were made.

The photoelectrons produced were attracted to an external shield. Measurement of this current was made by connecting the lantern to a quadrant electrometer and introducing between them a leak made of smoked quartz having a resistance of about 10^{10} ohms.

The experiments were carried out at different temperatures of the target ranging from 30° C. to 950° C. The pressure of the residual gas inside was much lower than 10^{-6} mm. of mercury.

The photoelectric sensitivity of iron for soft X-rays was found to be constant up to about 780° C. The value decreases by about 10% in the range 780° C. to about 900° C. and therafter shows a rise. Attention is drawn to parallel investigations of the photoelectric sensitivity of iron at different temperatures when irradiated with ultra-violet light. The change in the sensitivity when α iron passes into the β iron indicates that probably such a transformation is accompanied by a change in the photoelectric threshold.

Cobalt and nickel have constant values for their photoelectric sensitivity in the range from 30° C. to 950° C. This fact leads to the conclusion that the photoelectric threshold is unaltered when the hexagonal close-packed structure passes into the face-centred cubic structure at 850° C. No change of sensitivity occurs at 358° C., the Curie point of nickel. This observation confirms the result of Rao on nickel.

Reference is made to the work of Rudberg who has shown that in the photoelectric yield from a metal produced by soft X-rays, by far the larger part contains electrons having velocities corresponding to the order of a few volts. A small part of the yield was characteristic of the energy of the Bohr radiation of the carbon emitter which was used. The photoelectric effect due to soft X-rays was similar more to the effect with the ultra-violet light than to the effect produced by hard X-rays. Following

Bandopadhyaya a theoretical derivation has been made of the number of photoelectrons emitted from a target when soft X-rays corresponding to a given applied potential are incident. The significance of the photoelectric threshold in controlling the photoelectric yield is briefly outlined.

BIBLIOGRAPHY

Andrews, Davies and Horton — *Proc. Roy. Soc.* (A), 1926, **110**, 64.
———— .. *Ibid.* (A), 1928, **117**, 649.
Bandopadhyaya .. *Ibid.* (A), 1928, **120**, 2, 46, 78.
Becker .. *Ann. der Phys.*, 1927, **84**, 779.
Campbell .. *Phil. Mag.*, 1912, **23**, 68.
Cardwell .. *Proc. Nat. Acad. Sci.*, 1928, **14**, 439.
———— .. *Ibid.*, 1929, **15**, 544.
Clark .. *Applied Electricity*, 1932, 237.
Compton .. *Phil. Mag.*, 1912, **23**, 579.
——— and Thomas .. *Phys. Rev.*, 1926, **28**, 601.
Davies .. *Proc. Roy. Soc.* (A), 1928, **119**, 543.
——— and Horton .. *Phil. Mag.*, 1926, **2**, 1253.
Einstein .. *Ann. der Phys.*, 1906, **17**, 132.
———— .. *Ibid.*, 1907, **20**, 199.
Goetz .. *Phys. Zeits.*, 1923, **24**, 377.
———— .. *Ibid.*, 1925, **26**, 206.
———— .. *Zeits. f. Phys.*, 1927, **42**, 329.
———— .. *Ibid.*, 1927 *a*, **43**, 531.
Gudden .. *Handbuch der Physik*, 1928, **13**, 103.
Hayakawa .. *Sci. Rep. Tohoku. Univ.*, 1933, **22**, 934.
Holweck .. *Ann. Chim. Phys.*, 1922, **17**, 5.
Hughes .. *Phil. Mag.*, 1922, **43**, 145.
——— and DuBridge .. *Photoelectric Phenomena*, 1932, 442.
Ives .. *Astrophys. Jour.*, 1917, **46**, 241.
———, Dushman and Karrer — *Ibid.*, 1916, **43**, 9.
Klinkhardt .. *Ann. der Phys.*, 1927, **84**, 167.
Kurth .. *Phys. Rev.*, 1921, **18**, 461.
Laird (Miss) .. *Ibid.*, 1927, **29**, 41.
Lapp .. *Ann. de Phys.*, 1929, **12**, 442.
Millikan .. *Phys. Rev.*, 1916, **7**, 362.
Mohler and Foote .. *Sci. Paper Bur.*, Stand, 1921, 425.
Nakaya .. *Proc. Roy. Soc.* (A), 1929, **124**, 616.
Partzsch and Hallwachs .. *Ann. der Phys.*, 1913, **41**, 247.
Rao .. *Proc. Roy. Soc.* (A), 1930 *a*, **128**, 41 and 57.
———— .. *Ibid.* (A), 1933, **139**, 436.
———— .. *Annamalai University Journal*, 1935.
———— .. *Proc. Roy. Soc.* (A), 1937, **159**, 283.

Richardson .. *Phys. Rev.*, 1912, **34,** 119.

———— .. *Phil. Mag.*, 1912 *a*, **23,** 615.

———— .. *Ibid.*, 1912 *b*, **24,** 570.

———— .. *Proc. Roy. Soc.* (A), 1928, **119,** 531.

———— .. *Ibid.* (A), 1930, **128,** 63.

——— and Andrews .. *Ibid.* (A), 1930, **128,** 1.

——— and Bazzoni .. *Phil. Mag.*, 1921, **42,** 1015.

——— and Chalklin .. *Proc. Roy. Soc.* (A), 1926, **110,** 247.

———— .. *Ibid.* (A), 1928 *a*, **119,** 60.

———— .. *Ibid.* (A), 1928 *b*, **12,** 218.

——— and Compton .. *Phil. Mag.*, 1912, **24,** 575.

——— and Rao .. *Proc. Roy. Soc.* (A), 1930, **128,** 16, 37.

——— and Robertson .. *Ibid.* (A), 1927, **115,** 280.

———— .. *Ibid.* (A), 1929, **124,** 188.

Roy .. *Ibid.* (A), 1926, **112,** 509.

Rubens and Landsburg .. *Verh. Dent. Phys. Ges.*, 1907, **9,** 749.

Rudberg .. *Proc. Roy. Soc.* (A), 1928, **121,** 385.

———— .. *K. svenska Vetensk. Akad. Handl.*, 1929, **7,** 1.
This contains a complete list of references up to 1929.

———— .. *Proc. Roy. Soc.* (A), 1930, **127,** 111.

Seiliger .. *Zeits. f. Phys.*, 1926, **38,** 443.

Stoner .. *Magnetism and Matter*, 1934, **373.**

Tartakowsky and Kudrjawzewa *Z. Phys.*, 1932, **75,** 137.

Thibaud .. *Jour. de Physique*, 1927.

Thomas *Phys. Rev.*, 1925, **25,** 322.

Treloar and Landon .. *Proc. Phys. Soc.*, 1938, **50,** 625.

Varadachary .. *Proc. Ind. Acad. Sci.*, 1940, **12,** 381.

Warnecke .. *Jour. de Phys.*, 1936, **7,** 270.

Woolridge .. *Phys. Rev.*, 1940, **58,** 316.

DEPOLARISATION OF LIGHT SCATTERED BY LIQUIDS

By K. Sunanda Bai

(From the Department of Physics, Indian Institute of Science, Bangalore)

Received April 16, 1941

(Communicated by Sir C. V. Raman, Kt., F.R.S., N.L.)

1. *Introduction*

The theories of light scattering in liquids outlined by Raman (1922), Ramanathan (1923), Gans (1924) and others assume that the scattering arises from two causes, namely, (1) fluctuations of density caused by the thermal movements of the molecules and (2) fluctuations of anisotropy caused by their random orientations. These two types of scattering are distinguished by the fact that while the 'density' scattering is completely polarised the 'anisotropic' scattering is depolarised to the extent of 6/7. The resultant depolarisation of the scattered light depends upon the relative magnitudes of these two types of scattering.

Experimental determinations of the depolarisation of scattered light have been made by several investigators for many liquids by the well-known Cornu method. In general it has been observed that the degree of depolarisation is considerably higher for the liquid than for the corresponding vapour and that it depends on the optical anisotropy of the molecule. It has also been shown by Ramanathan (1923) that with increase of temperature the value of depolarisation diminishes. Expressions have been given by Ramanathan (1927) and Cabannes (1929) connecting the observed depolarisation ρ with the optical anisotropy δ of the molecules. For gases $\rho_{gas} = \frac{6\,\delta^2_{gas}}{5+7\,\delta^2_{gas}}$ and for liquids $\rho_{liq.} = \frac{6\,\delta^2_{liq.}}{\frac{5RT\beta\nu}{N} + 7\,\delta^2_{liq.}}$ where R, T, β, N and ν are respectively gas constant, absolute temperature, compressibility, Avagadro's number and number of molecules per c.c. The large increase in the depolarisation for the liquid is thus accounted for by its lower compressibility and higher density at ordinary temperatures. However, the optical anisotropy of the molecules calculated from the depolarisation in the vapour state has been observed to be higher than that from the depolarisation of the liquid (Raman and Krishnan, 1928). This discrepancy is sought to be explained by Raman and Krishnan (1928) on the assumption that the *external polarisation field* surrounding the molecule is not of the Lorentz-Lorenz type but

anisotropic. It is evident that a correct interpretation of the depolarisation of the scattered light by a liquid in terms of the molecular anisotropy would give us important information regarding the nature of the liquid state itself.

Since the discovery of the Raman effect in 1928, the spectrograph has been increasingly used for the investigation of the scattered radiation and it has given us a deeper insight into the nature of diffusion of light by material media. It is now known that the scattering arises as a result of the modulation of the incident radiation by the translatory, rotatory and vibratory movements of the molecules of which the medium is composed. The frequency of the scattered radiation arising from molecular vibrations is always different from that of the incident light and its contribution to the total intensity of scattering is small in gases and liquids. It can also be assumed that in liquids as well as in gases there is no phase-relationship between the vibrations of different molecules. The rotations of the molecules on the other hand give rise to radiations whose frequency is in the neighbourhood of the incident ray itself. In general a part of the rotational scattering has the same frequency as the incident radiation and the rest falls on either side in an asymmetrical fashion. The middle part is called the Q branch and those on either side the P and the R branches. In the case of gaseous molecules of low moment of inertia like H_2, O_2 and N_2, the P and R branches appear as discrete lines. In the liquid state with the exception of H_2, these lines are not resolved and appear as 'wings' on either side of the Rayleigh line. The intensity of the wing is comparable to that of the unmodified line itself. Theoretically if the rotations of the molecules in a liquid are complete and uninfluenced by the presence of neighbouring molecules, the wing should possess a well-defined maximum round about 20 cm.$^{-1}$ corresponding to a frequency ν_m in the expression $\frac{1}{2} I (2\pi\nu_m)^2 = \frac{kT}{2}$, where $k = 1 \cdot 372 \times 10^{-16}$ ergs, T = absolute temperature, and I = the moment of inertia and an extension of about 70 cm.$^{-1}$ Experimentally however it has been observed by Raman and Krishnan (1928), Cabannes and Daure (1928), Bhagavantam and Rao (1934), Rousset (1935), and Weiler (1935) that the intensity of the wing is a maximum at the Rayleigh line itself and falls off rapidly up to 20 cm.$^{-1}$ and afterwards slowly up to 130 cm.$^{-1}$ This discord with the theory has led to an interpretation that the wing in liquids has an origin different from molecular rotations [Cabannes and Rocard (1929), Gross and Vuks (1936)]. Further, this wing is observed to be depolarised to an extent of 6/7, as we should expect if it were due to orientation scattering. It would be interesting to find out what fraction of the depolarised scattering falls on the unmodified line itself. It is also not known to what extent the

rotations of molecules in liquids are restricted and whether any phase-relationship exists between the rotations of neighbouring molecules.

The translatory movements of molecules are responsible for the 'density' scattering. It was suggested by Brillouin (1922) that the density scattering should exhibit Doppler components if the movements of molecules are coherent. That the Rayleigh radiation by liquids gives rise to two completely polarised Doppler-shifted components was demonstrated by Gross (1930), Ramm (1934), Rao (1934) and Raman and Venkateswaran (1938) by their interferometric studies of light scattered by liquids. In addition to the two Brillouin components a partially polarised central component and a continuum throughout the pattern is also observed by Raman and Venkateswaran.* In investigations with the ordinary spectrograph these three components appear together as an unresolved line at the position of the incident frequency.

The depolarisation of the scattered light measured non-spectroscopically is the mean of the depolarisation due to all these causes. It is now obvious that if the spectrum of the scattered light is observed with a broad slit on the instrument the unmodified line would include the whole of the 'wing' and the three components of which the unshifted line is composed. As the slit of the spectroscope is narrowed down, more and more of the wing will be excluded and the depolarisation will diminish. The form of the curve showing the variation of depolarisation with slit width will depend on the distribution of intensity in the wing and the intensity and extent of polarisation of the central line. It is also clear that the lowest value corresponding to the narrowest slit witdth will depend on the resolving power of the spectrograph used.

Investigations on the above lines have been undertaken by Ranganadham (1932, 1933), Rousset (1935), and Saxena (1938). Ranganadham has observed the depolarisation of the scattered light with wide and narrow slit widths for several liquids and has shown that the narrow slit value is smaller than the broad slit value, but always finite. Rousset on the other hand, comes to the conclusion that in the case of two out of four liquids studied by him the narrow slit value tends to zero. On the basis of a careful study of four liquids Saxena has on the contrary demonstrated that the narrow slit value is always finite and tends to be high for viscous liquids.

It is obvious that the depolarisation factor for the limiting slit width is an important physical constant for the liquid under the specified conditions, inasmuch as it together with the depolarisation of the total scattering,

* Unpublished work.

leads to the determination of the fraction of the anisotropic scattering which falls on the unmodified line. A knowledge of the rate of diminution of depolarisation with slit width would further give us important information regarding the distribution of intensity in the wing. Hence in the present paper an extensive investigation of the problem has been undertaken for a large number of liquids and for a wide range of temperatures.

2. *Experimental Arrangements*

The importance of using a spectrograph of high resolving power for the investigation of the depolarisation of the transversely scattered light by liquids was first stressed by Ranganadham. Using a Fuess spectrograph of resolving power 25,000 and a double-image prism he separated out the vertical and the horizontal components of the scattered light and compared the ratio of their intensities by varying the time of exposure and making use of Schwarzchild's formula, and also by the method based upon intensity marks. Rousset has discussed the possible errors in the measurement of the depolarisation ratio of the scattered light by means of a double-image prism and a spectrograph. In his investigations he has used a two-prism glass spectrograph having a dispersion of 20 A.U./mm. in the 4,358 A.U. region and a theoretical resolving power of 50,000. The focal length of the collimator was 67 cm. and that of the camera 47 cm. The scattered light was limited by an aperture of 4 mm. He eliminated the error due to oblique reflection on the prisms of the spectrograph by using a quarter-wave plate just in front of the slit. The light from a mercury arc was condensed by means of a lens having a small aperture ratio thus limiting the convergence error to about 1%. For the measurement of the depolarisation ratio he compared the density of the image due to the horizontal component to that due to the vertical component reduced to the same magnitude by varying the time of exposure. If the image of the horizontal component is obtained in time T, and that of the vertical component in time γ T, then ρ is given by the formula $\rho = \gamma^n$ (n = coefficient of Schwarzchild).

Saxena used a large Littrow glass spectrograph of Hilger (E 349) of aperture $\frac{F}{7}$, the diameter of the camera objective being 127 mm. The dispersive system was equivalent to three 60° prisms of dense flint glass of face 15·2 cm. and height 11·7 cm. It had a theoretical resolving power of 75,000 and a dispersion of 11 A.U./mm. in the 4,358 A.U. region. He determined the depolarisation ratio by placing a nicol after the double-image prism in the path of the scattered light and turning it degree by degree till equality between the horizontal and vertical components was

obtained. The photographic plate was used only as a detector. If θ be the angle through which the nicol is turned from the horizontal or the vertical position to bring the two components to equality then we have $H \cos^2 \theta = V \sin^2 \theta$ or $\frac{H}{V} = \rho = \tan^2 \theta$. This method is more accurate than Rousset's as it is independent of the laws of blackening of the photographic plate.

The experimental technique adopted in the present investigation is illustrated in Fig. 1. Light from a pyrex mercury arc S was concentrated

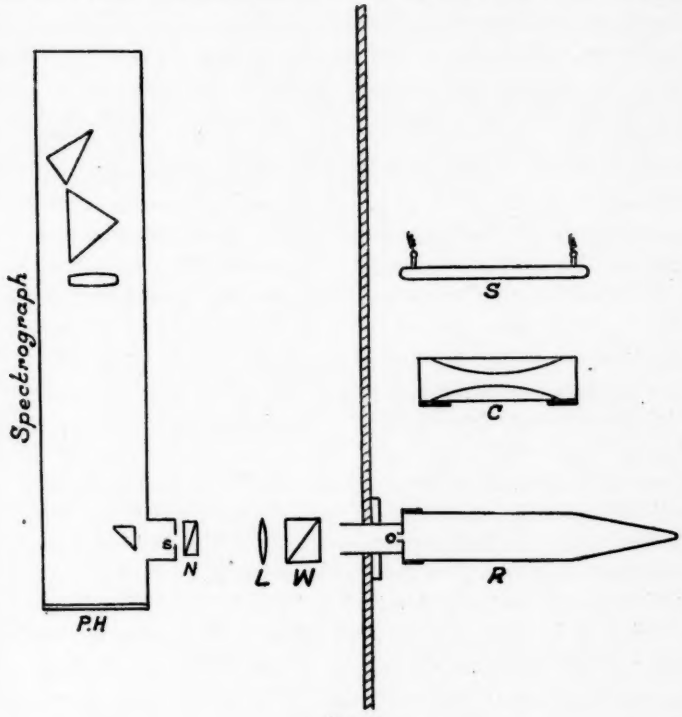

FIG. 1

by means of a condenser C (aperture 4″) on the Raman tube R. The condenser was placed at a distance of one foot from the tube so that the convergence error $\frac{\theta^2}{2}$ (θ being the semi-angle of convergence) was 1·3%. The scattered light was taken through a small axial hole O of diameter 2 mm. on a blackened brass cap fixed to the observation end of the experimental tube. A double-image prism W of quartz (aperture 1½″) was placed

in the path of the scattered beam and the two images thus formed were focussed on the slit of the spectrograph by a lens L of focal length 7 cm. The spectrograph was the same as that used by Saxena. A nicol N was placed in front of the slits for the measurement of the relative intensities of the components. The axes of the Raman tube, the focussing lens and the spectrograph were carefully aligned so that the full apertures of the collimating lens and the prisms were illuminated, thus ensuring that the maximum resolving power of the instrument was made use of.

About 18 liquids having widely different physical properties and different degrees of depolarisation were chosen for investigation. These liquids were pure Kahlbaum's chemicals further purified several times by slow distillation in vacuum till they were rendered completely dust-free. The liquid was contained in a Raman tube of diameter 3 cm. and length 20 cm. to one side of which was fused a strain-free glass plate, the other end being drawn out into a horn. The horn was painted with black paint which gave a perfect ground for the scattered light. The light emerging from the condenser illuminated only 10 cm. of the experimental tube. For investigations at higher temperatures the tube was surrounded by a cylindrical electric furnace whose temperature could be controlled by varying the current in the heating coils.

Saxena's method for the measurement of depolarisation ratio was found to be too laborious, especially for the study of a large number of liquids. Hence in the present investigation a modification of his method which is no less accurate was employed. The nicol N was rotated in order to bring the two components to approximate equality as judged visually and then the small difference in the intensities of the horizontal and vertical components was measured microphotometrically. For this purpose the two components were recorded with moderate intensity so as to fall on the straight line portion of the density-log·intensity curve, and on the same plate a series of intensity marks were taken with varying slit widths using as source a 6-volt bulb run by means of storage batteries. Density-log. intensity curves were drawn for the 4,358 A.U. region of the plate and from these curves the small difference in the intensities of the two components was determined. This factor multiplied by $\tan^2\theta$ where θ is the angle through which the nicol is turned, gives the depolarisation ratio. The measurements of depolarisation were made for slit widths ranging from 2,000 μ to 10 μ. Slit widths greater than 2,000 μ were not employed as the illumination on the slit tends to deviate very much from uniformity. It may be remarked that with a resolving power of 75,000 for the spectrograph, lines nearly 0·3 cm.$^{-1}$ apart could be just resolved in the 4,358 A.U.

region. As the Brillouin components in liquids are diplaced from the central component by about 0·25 cm.$^{-1}$ the spectrograph used in the present investigation is capable of just excluding the wing beyond these components. The narrow slit width of 10 μ corresponding to a half slit width of 0·29 cm.$^{-1}$ is also very near to this theoretical limit of resolution.

Results and their Discussion

The liquids studied in the present investigation may be classified as follows:

Class I.—Those having high depolarisation and high viscosity: tetraline, formic acid, acetic acid, isobutyric acid, nitrobenzene and ethyl lactate.

Class II.—Those having high depolarisation and low viscosity: benzene, dichlorobenzene, carbon disulphide and bromoform.

Class III.—Those having low depolarisation and high viscosity: glycol and cyclohexanol.

Class IV.—Those having low depolarisation and low viscosity: chloroform, ethyl ether, ethyl alcohol, methyl acetate, acetone and carbon tetrachloride. In the case of liquids of classes I and II for which the depolarisation is very high, the measurements could be made with great accuracy. For liquids of classes III and IV for which the deplorisation is low, the percentage error is probably high, especially because the convergence error of 1·3% becomes comparable with the percentage of depolarisation itself. However it may be mentioned that for carbon tetrachloride for which accurate determinations of depolarisation have been made by Rousset (1935) the values obtained here, namely, 5·2% and 1·3% for the broad and narrow slit widths respectively compare very favourably with the values of 5·1% and 1% given by the latter. From the graphs which follow it may be seen that the points for various slit widths also fall on a smooth curve showing that the accidental errors in measurement cannot be very great.

Table I gives the depolarisation ratios obtained for various liquids at slit widths ranging from 1,000 μ to 10 μ. The last column gives the depolarisation observed for the totally scattered light non-spectroscopically by the previous authors, and it may be noticed that they agree well with the corresponding value for a half slit width of 29 cm.$^{-1}$ showing thereby that the intensity of the wing beyond this limit is negligible. Graphs are drawn (Figs. 2–6) with half slit values expressed in wave numbers as abscissæ and the observed depolarisation as ordinates. In Fig. 2 the curves for benzene at two temperatures, namely, 30° C. and 80° C. are given along with that of Saxena. The close identity of the curve given by the latter and

TABLE I

No.	Liquids*	$\nu = 29$	$\nu = 14{\cdot}5$	$\nu = 5{\cdot}8$	$\nu = 2{\cdot}9$	$\nu = 1{\cdot}45$	$\nu = {\cdot}73$	$\nu = {\cdot}29$ cm.$^{-1}$	ρ
1	Tetraline (30° C.)	·535	·525	·50	·485	·470	·460	·455	
	(150° C.)	·34	·31	·26	·23	·21	·19	·18	
	(220° C.)	·286	·256	·20	·17	·155	·140	·133	
2	Formic acid (30° C.) ..	·525	·515	·49	·475	·455	·45	·445	·53
	(95° C.) ..	·44	·41	·32	·25	·20	·168	·14	
3	Acetic acid (30° C.) ..	·40	·385	·354	·334	·312	·30	·293	·42
	(110° C.) ..	·35	·314	·234	·175	·133	·107	·094	
4	*Iso*-butyric acid (30° C.) ..	·347	·325	·267	·234	·194	·174	·161	
	(145° C.) ..	·273	·230	·164	·122	·094	·075	·065	
5	Nitrobenzene (20° C.) ..	·68	·67	·63	·61	·58	·565	·550	·72
	(200° C.) ..	·572	·53	·42	·35	·28	·235	·193	
6	Ethyl lactate (30° C.) ..	·248	·236	·202	·174	·154	·143	·138	
7	Benzene (30° C.)	·43	·39	·30	·24	·187	·155	·138	·44
	(78° C.)	·39	·34	·24	·175	·128	·094	·074	·40
8	Dichlorobenzene (85° C.) ..	·55	·52	·46	·41	·375	·35	·335	
9	Carbon disulphide (20° C.) ..	·625	·60	·53	·45	·41	·365	·33	·62
10	Bromoform (30° C)	·29	·235	·225	·19	·168	·158	·145	
11	Glycol (30° C.)	·064	·063	·059	·052	·047	·045	·043	
12	Cyclohexanol (30° C.) ..	·082	·081	·076	·072	·070	·068	·067	
	(158° C.) ..	·057	·053	·045	·041	·039	·037	·036	

	(158° C.) ..	·057	·053	·045	·041	·039	·037	·036	
13	Chloroform (20° C.) ..	·17	·144	·098	·067	·039	·03	·028	·21
14	Ethyl ether (20° C.) ..	·074	·067	·048	·04	·033	·029	·028	·08
15	Ethyl alcohol (20° C.) ..	·054	·046	·034	·026	·020	·018	·016	·06
16	Methyl acetate (30° C.) ..	·212	·185	·130	·094	·069	·054	·046	
17	Acetone (20° C.)	·20	..	..	..	..	..	·06	..
18	Carbon tetrachloride (30° C.)	·052	..	..	..	..	..	·013	·055

*4,358 A. U. was used as the exciting line for all liquids except for nitrobenzene for which 5,461 A. U. was employed.

TABLE II

No.	Liquids	K. S. Bai		Ranganadham		C_Q	Viscosity
		ρ_0 (unmodified	ρ_∞ (Total)	ρ_0	ρ_∞		
1	Tetraline (30° C.) ..	·45	·54			·65	
	(150° C.)	·18	·34			·40	
	,, (220° C.)	·13	·28			·37	
2	Formic acid (30° C.)	·44	·53	·53	·55	·64	$·01804_{20}$°c.
	(95° C.)	·12	·45			·147	
3	Acetic acid (30° C.)	·28	·40	·395	·41	·552	$·01219_{20}$°c.
	(110° C.)	·08	·36			·143	
4	*Iso*-butyric acid (30° C.)	·15	·35			·31	$·01318_{20}$°c.
	(145° C.)	·06	·29			·147	
5	Nitrobenzene (20° C.)	·54	·68			·443	·02
	(200° C.)	·18	·59			·153	
6	Ethyl lactate (30° C).	·13	·25			·432	
7	Benzene (30° C.)	·12	·44	·20	·41	·153	$·00649_{20}$°c.
	(78° C.) ..	·065	·41			·089	
8	Dichlorobenzene (86° C.)	·30	·56			·287	
9	Carbon disulphide (20° C.)	·30	·63	·33	·64	·195	$·00367_{20}$°c.
10	Bromoform (30° C.)	·14	·30			·364	
11	Glycol (30° C.) ..	·042	·064			·638	$·218_0$° c.
12	Cyclohexanol (30° C.)	·066	·085			·757	
	(158° C.	·034	·06			·55	
13	Chloroform (20° C.)	·025	·175	·06	·19	·117	$·00564_{20}$°c.
14	Ethyl ether (20° C.)	·026	·081	·055	·08	·30	00234_{20}°c.
15	Ethyl alcohol (20° C.)	·015	·054	·03	·055	·264	$·0099_{30}$°c.
16	Methyl acetate (20° C.)	·04	·22			·178	$·00478_0$°c.
17	Acetone (20° C.) ..	·06	·20	·09	·21	·247	$·0033_{20}$°c.
18	Carbon tetrachloride (30° C.)	·013	·052	·012	·039	·24	$·0096_{20}$°c.
19*	Phenol (84° C.) ..	·40	·64		·70	·296	$·127_{18·3}$°c.
	(23° C.)	·53	·70	·53	·75	·36	
20	Benzo-phenone ..	·66	·75	·66		·86	
21	Glycerine ..	·30	·33	·30	·33	·87	$8·30_{20·3}$°c.

* The data for the liquids 19, 20 and 21 are taken from Saxena's paper.

the present one at the room temperature gives a check of the experimental method employed. In Table II the limiting slit values ρ_0 and the broad slit values ρ_∞ are collected together for various liquids. Columns *four* and *five* contain corresponding values obtained by Ranganadham with a Fuess spectrograph. It may be noticed that in almost all cases the broad slit values of Ranganadham are nearly the same as those given here, but his narrow slit values are relatively higher. This is evidently due to

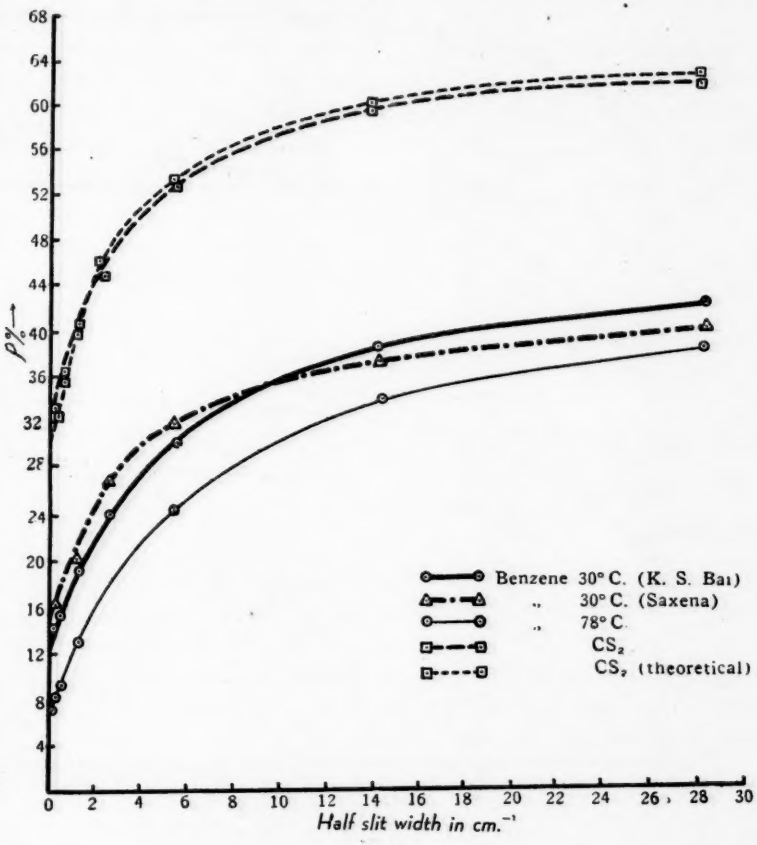

FIG. 2

the insufficient resolving power of the spectrograph used by him. Both Ranganadham and Saxena have noticed that for liquids like salol and glycerine in spite of the fact that the depolarisation ratio is high there is practically no variation in the depolarisation with slit width. In the

present investigation only small variations have been observed for viscous liquids like tetraline, formic acid, acetic acid, nitrobenzene, glycol and cylcohexanol. On raising the temperature of these liquids and thereby increasing their fluidity the difference between the broad and narrow slit values tends to be of the same order as for mobile liquids. It may be generally

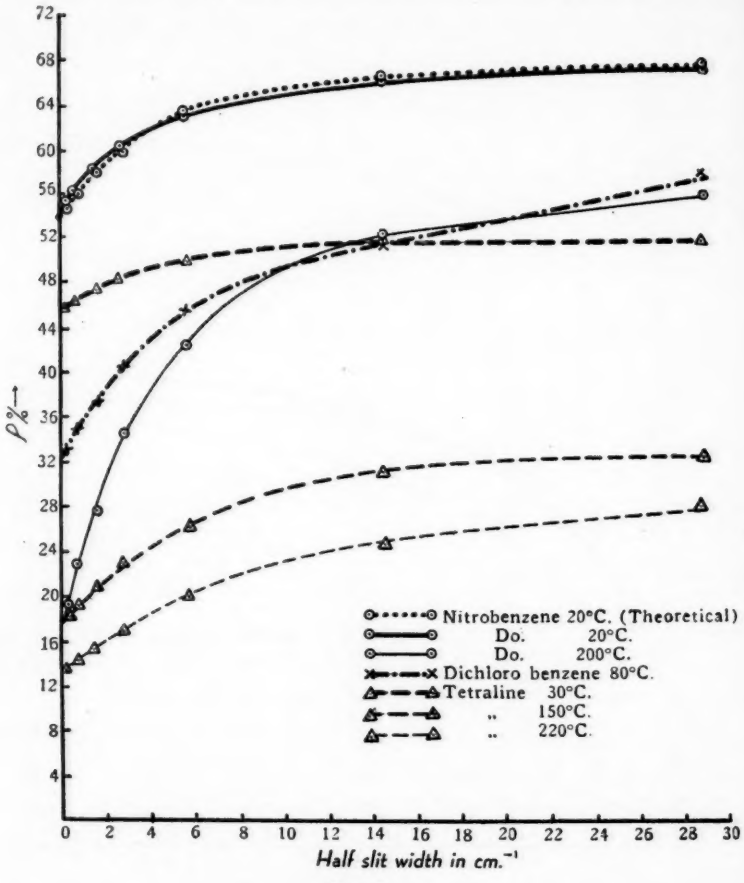

FIG. 3

stated that for all the liquids studied the curve is nearly horizontal up to about 10 cm.$^{-1}$ and below this falls off rapidly. The depolarisation of the unmodified line given by the point of intersection of the curve with the Y-axis is always finite for all liquids. The turning point of the curve depends very much on the depolarisation and the viscosity of the liquid. For liquids of

classes I and III it is about 6 cm.$^{-1}$ and for those of classes II and IV it is about 15 cm.$^{-1}$ If the temperature is raised sufficiently high the former liquids behave like those of the latter class. These results indicate that most of the intensity of the wing is concentrated in the region between zero and 15 cm.$^{-1}$ for mobile liquids and the extent of this region diminishes with increase of viscosity.

4. *Ratio of Intensity of the Q Branch to the Total Intensity of the Wing*

From the experimental data for ρ_0 and ρ_∞ we have calculated the fraction of the intensity of the wing which falls on the unmodified line without making any assumption regarding the intensity of density scattering. Thus if I_Q and I_R are the intensities of the Q branch and of the total anisotropic scattering

$$\rho_0 = \frac{\frac{6}{13} I_Q}{I_D + \frac{7}{13} I_Q}$$

and

$$\rho_\infty = \frac{\frac{6}{13} I_R}{I_D + \frac{7}{13} I_R}$$

where I_D is the intensity of polarised scattering in the liquid. Eliminating I_D from these two equations we get

$$C_Q = \frac{I_Q}{I_R} = \frac{\rho_0 (6 - 7\rho_\infty)}{\rho_\infty (6 - 7\rho_0)} \qquad (1)$$

The value of C_Q, *viz.*, the ratio of the intensity of the Q branch to the total intensity of the wing, is calculated for all the liquids studied and entered in column six of Table II.

Based on the assumption that in liquids all the molecules have complete freedom for rotation Placzek and Teller (1933) have derived for polyatomic molecules having an axis of symmetry of the order more than two, the following expression for C_Q:

$$C_Q = \frac{1}{8}\left[\left(2 + \frac{21}{\beta} + \frac{27}{\beta^2}\right) - \left(\frac{12}{\beta} + \frac{27}{\beta^2}\right)\sqrt{1+\beta}\ \text{arc}\ \frac{\sinh \sqrt{\beta}}{\sqrt{\beta}}\right] \qquad (2)$$

where β is given by $\frac{C}{A} = \frac{1}{1+\beta}$, C and A being the principal moments of inertia of the molecules. Table III gives the values of C_Q calculated from

TABLE III

Liquid	C/A	C_Q from Eq. (2)	C_Q from Eq. (1)
Benzene ..	2	·254	·154
Carbon disulphide ..	0	·25	·194
Carbon tetrachloride ..	1	·20	·238

the above formula and those calculated from the values of ρ_0 and ρ_∞ obtained in the present investigation. The disagreement between these two values shows that the assumption of complete freedom of rotation for molecules in a liquid is not valid. The minimum value of C_Q given by Placzek and Teller is 0·17 whereas, as may be seen from Table II, in some cases C_Q is very much lower than this value. Further, according to the same

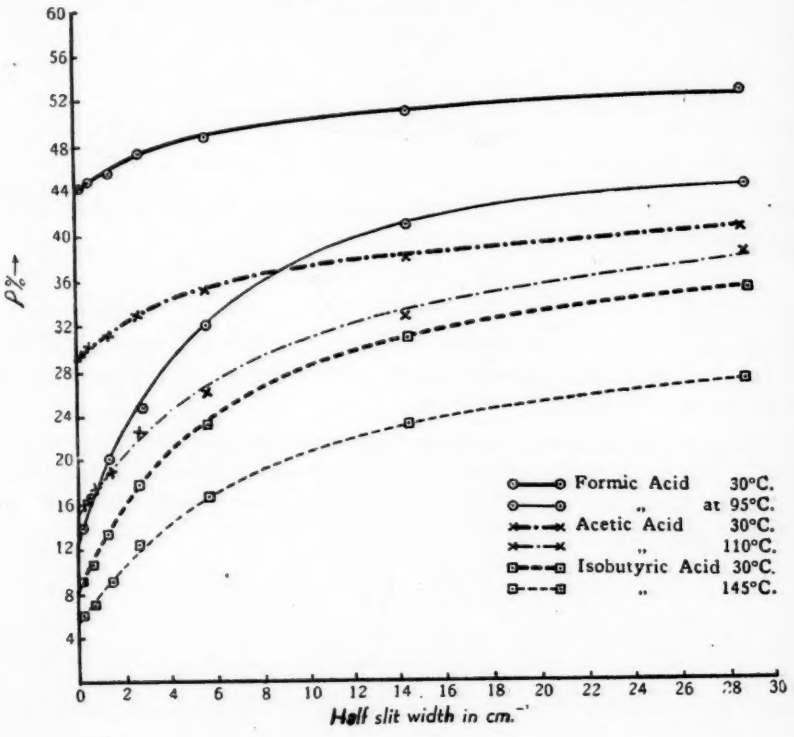

FIG. 4

authors the ratio C_Q as well as the total intensity of anisotropic scattering is independent of temperature. On the contrary in the case of liquids studied here, an increase of temperature always lowers the value of C_Q. These deviations from theoretical expectations are no doubt intimately connected with the nature of the rotational movements of molecules in the liquid and their mutual interaction. A close examination of C_Q for various liquids also shows that it depends very much on the fluidity of the liquid. For cyclohexanol, glycol, tetraline and formic acid which possess high viscosity it is about 0·7. It falls off rapidly with rise of temperature. As we approach the boiling point, C_Q assumes a value lower than 0·15 for fatty acids and aromatic compounds. For ethyl ether and ethyl alcohol which possess very low viscosity C_Q is nearly 0·25 which is what we should expect if the molecular rotations are complete.

5. *Distribution of Intensity in the Wing in Liquids*

Manneback (1930) has theoretically worked out the spectral distribution of intensity of the rotational scattering for diatomic molecules and later, the treatment has been extended to polyatomic molecules by Placzek and Teller (1933). In general, the rotational scattering consists of an unmodified part (Q branch) and modified parts on either side (P and R branches). The intensity of the P and R branches has a maximum round about 20 cm.$^{-1}$ depending on the moment of inertia of the molecules beyond which it falls off exponentially till it reaches a zero value at about 70 cm.$^{-1}$ That in the case of liquids the continuous spectrum on either side of the Rayleigh line does not possess such a maximum and further shows an extension much more than could be expected from the theory was established by several authors already referred to.

In the last section we have already seen that the fraction of the total intensity falling on the Q branch is very much influenced by the mutual interaction of molecules in the liquid. Since the molecules are closely packed the frequency of intermolecular collision becomes great and causes a broadening of the rotational lines. This is responsible for the disappearance of the quantised nature of the rotational scattering in liquids as well as in gases under high pressure (Bhagavantam, 1931). It is also possible that the intensity maximum of the P and R branches may shift to smaller frequency due to the same cause. Rousset (1935) has, however, observed that in four typical liquids he could not discover any maximum up to 7·5 cm.$^{-1}$ This is confirmed by our observations on benzene examined by a three-meter spectrograph having a dispersion of 2 A.U./mm. in the 4,358 A.U. region. In order to investigate whether any maximum

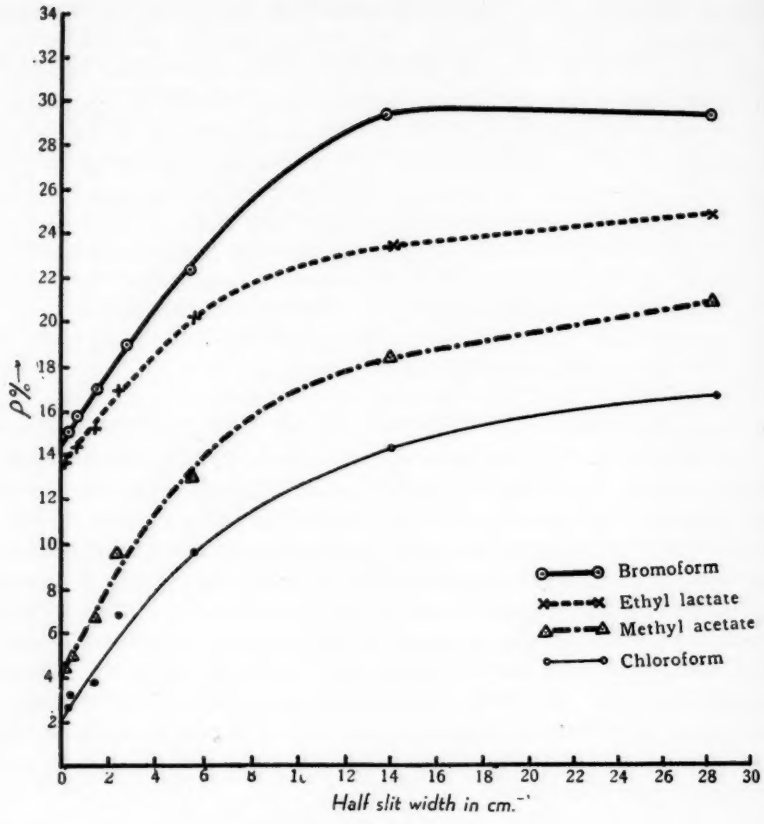

FIG. 5

exists below this limit the spectrum of benzene and chloroform have been studied with a Fabry-Perot interferometer having plate distances of 1 mm. and 5 mm., the distance between consecutive rings of the interference pattern being 5 cm.$^{-1}$ and 1·66 cm.$^{-1}$ No maximum was observed in the pattern except those due to density scattering. It is therefore reasonable to assume that the intensity of the wing in liquids has a maximum at the Rayleigh line and falls off exponentially with increasing wave number shift on either side. Thus if we neglect the small difference in the intensities of the P and R branches we may represent the intensity of the wing over a small element dx at any point x from the origin by $d\,\mathrm{I}_x = \frac{\mathrm{C}}{2}\, e^{-kx} dx$, where C and k are constants characteristic of the liquid under the specified conditions. The

total intensity of the P and R branches of the wing is then given by $2\int_0^\infty \frac{C}{2}e^{-kx}\,dx = \frac{C}{k}$ and the intensity up to ν cm.$^{-1}$ by $I_\nu = \frac{C}{k}(1-e^{-k\nu})$. It is thus evident that

$$C_Q = \frac{I_Q}{I_Q + \frac{C}{k}}.$$

Hence the depolarisation for any slit width ν is given by

$$\rho_\nu = \frac{\frac{6}{13}I_Q + \frac{6}{13}\frac{c}{k}(1-e^{-k\nu})}{I_D + \frac{7}{13}I_Q + \frac{7}{13}\frac{C}{k}(1-e^{-k\nu})},$$

$$\therefore = \frac{x - 6e^{-k\nu}}{y - 7e^{-k\nu}},$$

where x is written for $6/(1-C_Q)$ and y is a constant whose magnitude depends on the density scattering as well as the ratio of the Q branch to the total orientation scattering. This is the same as the empirical formula given by Saxena. The constants x, y and k are calculated for sixteen liquids for which the variation of depolarisation with slit width is known. x and y are obtained from the wide and narrow slit values of ρ and k is deduced by the method of successive approximations till the theoretical values of depolarisation for various slit widths agree with the observed data. These values of the constants x, y and k are given in Table IV. In all cases, the theoretical curve drawn with the given values of the constant follow closely the experimental curve as is illustrated for two typical liquids, carbon disulphide in Fig. 2 and nitrobenzene in Fig. 3. This agreement clearly shows that for all liquids examined the assumption that the intensity distribution is exponential is valid.

The Constants x *and* y.—No special significance could be attached to the variation of the constant y from liquid to liquid as it depends on the absolute intensities of different types of scattering about which we know very little at present. The constant x is given by the factor $\frac{6}{1-C_Q}$ and therefore, as in the case of C_Q, it depends on the viscosity of the liquid. As may be seen from Table IV, increase of temperature lowers the value of this constant which is in agreement with the observations made on C_Q in the previous section.

The Constant k.—An examination of the value of k for various liquids shows that its magnitude depends very much on the liquid fluidity. For

TABLE IV

No.	Liquids	x	y	k
1	Tetraline (30° C.)	17·9	33·2	·16
	(150° C.)	10·1	29·6	·11
	(220° C.)	9	30	·08
2	Formic acid (30° C.)	17·2	32·5	·14
	(95° C.)	7·04	15·6	·11
3	Acetic acid (30° C.)	13·46	33·7	·16
	(110° C.) ..	6·99	19·4	·10
4	*Iso*-butyric acid (30° C.)	8·7	24·8	·12
	(145° C.) ..	7·04	24·2	·08
5	Nitrobenzene (20° C.)	10·8	15·9	·14
	(200° C.)	6·8	11·6	·08
6	Ethyl lactate (30° C.)	10·6	42·5	·13
7	Benzene (30° C.)	7·1	16·1	0·1
	(78° C.)	6·6	16·1	·08
8	Dichloro benzene (85° C.) ..	8·4	15	·12
9	Carbon disulphide (20° C.) ..	7·4	11·8	·12
10	Bromoform (30° C.)	9·4	31·3	·11
11	Glycol (30° C.)	16·1	247	·16
12	Cyclohexanol (30° C.)	23·6	277	·14
	,, (158° C.)	14·4	239	·08
13	Chloroform (20° C.)	6·8	38	·09
14	Ethyl ether (20° C.)	8·6	105	·09
15	Ethyl alcohol (20° C.)	6·9	126	·10
16	Methyl acetate (30° C.)	7·0	31	·10

viscous liquids like glycol, cyclohexanol and tetraline it is as high as 0·16. With increase of temperature it tends to approach a value of ·08 which is the minimum observed for highly mobile liquids. The magnitude of k and its variation with temperature do not show any dependence on the anisotropy of the molecules. Thus an increase of temperature is attended with two distinct changes, namely, that the ratio of the intensity of the Q branch

to the total intensity of the wing is diminished and the constant k which determines the distribution of intensity in the wing is lowered. These results lead us to the following conclusion:—

The relative intensity of the unmodified part to the total rotational scattering in a liquid depends on its viscosity and as the temperature is raised a part of it is released from the Q branch and distributed in the P and R branches appearing with an intensity which is an exponential function of the frequency change.

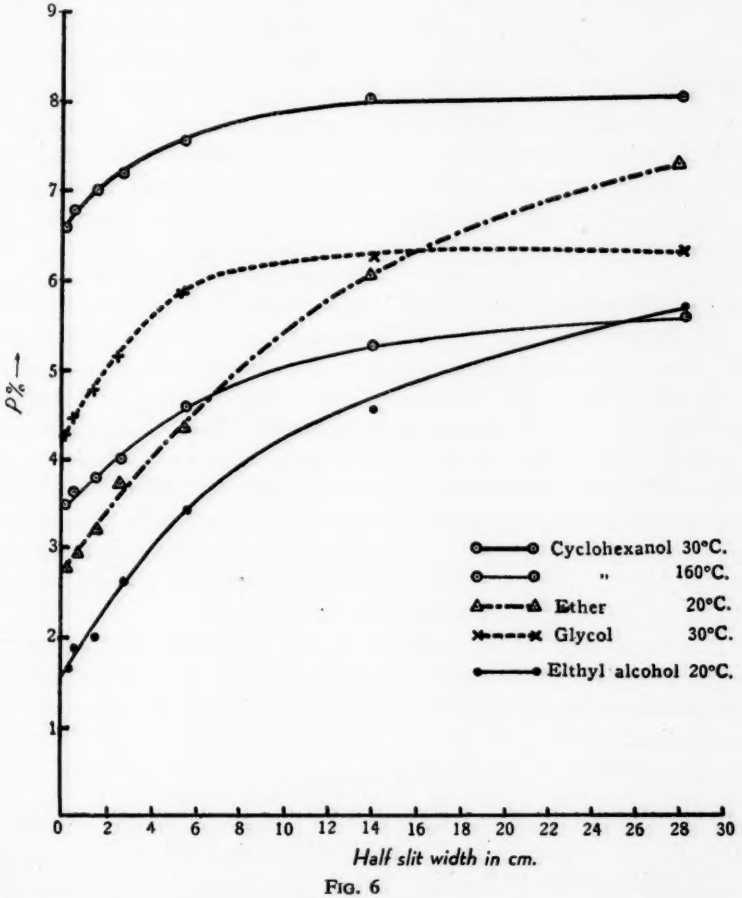

FIG. 6

The foregoing conclusions suggest that the state of aggregation of molecules in a liquid is composite in character. Thus some of the molecules

are free to rotate or oscillate and give rise to the P, Q and R branches, while others are attached to each other somewhat as in a solid. The latter give rise to a Q branch alone. The relative number of the two types of molecules depends on the viscosity of the liquid. For highly viscous liquids like tetraline, glycol, cyclohexanol, etc., the wing accompanying the Rayleigh line is considerably weaker, showing thereby that the solid-like structure predominates. This thesis is supported by the observations of Raman and Venkateswaran (1938) that the velocity of hypersonic waves in glycerine is 2,500 metres per sec. at 20° C. which is considerably higher than the sonic velocity of 1,910 metres/sec., thus indicating that for mechanical disturbances of sufficiently high frequency viscous liquids like glycerine are practically indistinguishable from amorphous solids.

Gross and Vuks (1935) have observed that as the temperature of a liquid is raised the intensity of the wing up to 20 cm.$^{-1}$ is enhanced while no perceptible change could be noticed beyond this region. Recently these observations have been confirmed by Bapayya (1939) but no explanation has so far been offered. From the conclusions arrived at above it is obvious that the observed enhancement of the intensity with increase of temperature is due to the redistribution of the intensity released from the Q branch to the P and R branches. For small changes of temperature we can expect the maximum change in intensity to take place only in the neighbourhood of the Rayleigh line itself. Neither Gross and Vuks nor Bapayya have extended their study to temperatures far removed from the room temperature and therefore we cannot ascertain the exact distribution of this extra intensity in the entire range of the wing. We have also to take into consideration any possible changes in the total intensity of the wing with increase of temperature. Further investigations appear necessary to determine the absolute value and the mode of distribution of the intensity of the rotational scattering in liquids at various temperatures.

In conclusion, I desire to express my grateful thanks to Sir C. V. Raman for his keen interest in the work. Thanks are also due to Dr. C. S. Venkateswaran for his helpful suggestions during the progress of this investigation.

Summary

The depolarisation of scattered light for slit widths ranging from 2,000 μ to 10 μ of a spectrograph of high dispersion and resolving power has been investigated for 18 liquids. Graphs are drawn with half slit width as abscissæ and the observed depolarisation as ordinates. In all cases the curve is nearly horizontal up to about 10 cm.$^{-1}$ below which it falls off rapidly.

Contrary to the conclusions of Rousset, but in agreement with the observations of Ranganadham and Saxena ρ_0, the depolarisation of the unmodified line corresponding to the limiting slit width, is finite for all liquids studied. The difference between ρ_0 and ρ^{∞} is smaller the more viscous the liquid is. With increase of temperature and, consequently, the decrease of viscosity, this difference becomes greater, ρ_0 and ρ_∞ themselves assuming smaller values. In all cases C_Q the ratio of the intensity of the unmodified part of the rotational scattering to the total intensity of the wing, is calculated by using the expression

$$C_Q = \frac{\rho_0 (6 - 7\rho_\infty)}{\rho_\infty (6 - 7\rho_0)}.$$

This ratio shows great dependence on liquid fluidity. It is as high as 0·7 for viscous liquids like cylcohexanol, glycol, tetraline and the fatty acids, and comes down to a value less than ·15 when the liquid is mobile.

Experimental evidence is furnished showing that the wing in liquids starts with maximum intensity at the Rayleigh line itself and falls off exponentially with increasing wave number shift. Representing the intensity of the wing at any point x by $d\mathrm{I}_x = \frac{\mathrm{C}}{2} e^{-kx}$, where C and k are constants, the following expression is deduced for the depolarisation ρ_ν for any slit width of half value ν:

$$\rho_\nu = \frac{x - 6\,e^{-k\nu}}{y - 7\,e^{-k\nu}},$$

where x is a constant given by $\frac{6}{1-C_Q}$ and y depends on the magnitudes of the density and orientation scattering. These constants have been calculated for sixteen liquids. The constant k which depends on the intensity distribution of the P and R branches is lower for mobile than for viscous liquids. From an examination of the variation of C_Q and k with temperature it is concluded that the relative intensity of the unmodified part of rotational scattering in a liquid depends on its viscosity and as the temperature is raised, a part of it is released and re-distributed in the P and R branches as an exponential function of the frequency shift. The effect of temperature on the intensity distribution in the wing observed by Gross and Vuks and also by Bapayya is satisfactorily explained on the basis of the above principle.

REFERENCES

Bapayya, K. .. *Proc. Ind. Acad. Sci.*, 1939, **10**, 253.

Bhagavantam, S., and Rao, A. V. *Ibid.*, 1934, **1**, 419.

———— .. *Ind. J. Phys.*, 1931, **6**, 319.

Brillouin, L. .. *Ann. de Phys.*, 1922, **17**, 88.

Cabannes, J. .. *La Diff. Moleculaire de la lumiere*, Paris, 1929.

——— and Daure, P. .. *Compt. Rend.*, 1928, **186**, 1533.

——— and Rocard, Y. .. *Joyr. de Phys.*, 1929, **10**, 52.

Gans, R. .. *Zeit. f. Phys.*, 1924, **30**, 231.

Gross, E. .. *Nature*, 1930, **18**, 718 ; **126**, 201, 400, 603 ; and 1932, **129**, 722.

——— and Vuks, M., .. *Jour. de Phys.*, 1935, **6**, 457 and 1936, **7**, 114.

Manneback .. *Zeit. f.Phys.*, 1930, **62**, 224.

Placzek and Teller .. *Ibid.*, 1933, **81**, 209.

Ramanathan, K. R. .. *Proc. Ind. Assoc. Cult. Sci.*, 1923, **8**, 1–181.

———— .. *Phy. Rev.*, 1923, **21**, 564.

———— .. *Ind. Jour. Phy.*, 1927, **1**, 413.

Raman, C. V. .. *Molecular Diffraction of Light*, 1922.

——— Krishnan, K. S. .. *Phil. Mag.*, 1928, **5**, 498.

———— .. *Nature*, 1928, **122**, 278.

————Venkateswaran, C. S. *Ibid.*, 1938, **142**, 791 and 1116 and 1939, **143**, 798.

Rao, B. V. R. .. *Proc. Ind. Acad. Sci.*, 1934, **1**, 2161.

Ramm, W. .. *Phys. Zeits.*, 1934, **35**, 111 and 756.

Ranganadham, S. P. .. *Ind. Jour. Phys.*, 1932, **1**, 353.

———— .. *M.Sc. Thesis*, Madras University, 1933.

Rousset, A. .. *D.Sc. Thesis*, Paris University, 1935.

———— .. *Compt. Rend.*, 1936, **202**, 654.

Saxena, B. D. .. *Proc. Ind. Acad. Sci.*, 1938, **8**, 460.

Weiler .. *Ann. Phy.,Lpz.*, 1935, **23**, 493.

CONDENSATION OF MALONANILIC ACID WITH ALDEHYDES

Part IV. With *o*-, *m*- and *p*-Methoxybenzaldehydes: The Influence of a Hydroxy-group

By P. I. Ittyerah and Kantilal C. Pandya

(From the Department of Chemistry, St. John's College, Agra)

Received March 3, 1941

In the condensations of malonic acid with aromatic aldehydes in the presence of a trace of an organic base, attention has already been drawn to the retarding or restricting influence of the hydroxy-group, which, when present on the ring, lowered the yield of the corresponding cinnanic acid derivative.[1] It has also been observed that the yields became quantitative when the hydroxy-group was replaced by the methoxy-[2] or the methylene-dioxy-group.[3] A similar observation is now made regarding condensations with malonanilic acid: in Part II of the present series,[4] the yields obtained from the reactions of malonanilic acid on *o*-, *m*- and *p*-hydroxybenzaldehydes were on the whole significantly low. Of the nine condensations studied, one gave only 18% yield, three gave approximately 33%, one gave 51%, two gave slightly above 60% and only two gave about 80%. The nitrobenzaldehydes on the other hand gave remarkably better yields, some times reaching up to the theoretical (Part III).[5] The present paper describes the condensations with the corresponding methoxybenzaldehydes, which show, as expected, a rise in the yields up to about 92% of the theoretical.

As in so many well-known cases, and also as in the malonic acid condensations, the hydroxy-group represses the activity and the reaction of the aldehyde-group to the greatest extent, as indicated by the yields of the reaction-products, when it is in the ortho-position to the aldehyde.[6]

As in Parts I, II and III, [7, 4, 5] the condensations have been carried out in three different conditions, (i) by Robinson's method as adopted by Ray and collaborators,[8] *i.e.*, the pyridine-piperidine method; (ii) by our pyridine-trace method, and (iii) in the absence of any base. The results are in conformity with those obtained earlier, *i.e.*, the highest yields are obtained with the trace-method ; and secondly, the products are exclusively or mainly the corresponding cinnamanilide, when a base is used, and are exclusively or mainly the corresponding benzylidene-malonanilic acid, when no base is present : in other words, the presence of even a trace of an organic base favours decarboxylation as well as the condensation reaction.

In the case of the methoxybenzaldehydes the condensations have been studied under a greater variety of conditions than usual, different temperatures and periods of heating being employed and different organic bases being also used. Triethanolamine has been used for the first time in these condensations, but the result it gave has not been encouraging.

The condensation of malonanilic acid with *p*-methoxybenzaldehyde (pyridine-piperidine) has already been carried out by Ahluwalia, Haq and Ray,[8] who mention the products but do not state the yields. The condensation by their method is repeated for purposes of comparison of the yields, which are lower than those obtained by the trace-method (*vide* also 7). The *m*- and *o*-methoxybenzaldehydes are condensed with malonanilic acid for the first time and the products are new.

Experimental

Condensation with p-*Methoxybenzaldehyde.*

Without any Base. (p-*Methoxybenzylidene-malonanilic acid and* p-*Methoxycinnamanilide*).—1·4 g. of the aldehyde and 1·8 g. of malonanilic acid (1 : 1 mol.) were mixed and heated in a flask on a water-bath. The whole soon melted to a brown liquid, gradually turned green, and solidified in about 1·5 hours. Heating was continued for 5 hours in all. The flask was then cooled, the product extracted with 10% sodium carbonate solution, and the unreacted aldehyde separated. The alkaline extract, when acidified with concentrated hydrochloric acid, gave a pale green solid, which, on recrystallisation from aqueous alcohol, came out as white needles, melting at 212°. (*p*-Methoxybenzylidenemalonanilic acid, m. 213° dec. Ray and workers,[8] *loc. cit.*)

The acid gave a silver salt, melting with decomposition at 200°. (Ag, Found : 26·67%; $C_{17}H_{13}O_4NAg$ requires 26·79%.) Yield, 1·8 g., *i.e.*, 60% of theory.

In another experiment, the heating was continued for eight hours, which gave the acid as well as some of the decarboxylated cinnamanilide, the total yield being slightly higher (about 70%, made up of 47% acid and 23% anilide).

With Pyridine-Piperidine Mixture.—0·7 g. aldehyde, 0·9 g. malonanilic acid, 2 g. pyridine and 2 drops of piperidine (1 : 1 : 5 : trace) were heated together at 50–60° for one hour, the product allowed to cool, acidulated water added, and the whole kept for some time. The water was then decanted off, the residue was treated with sodium carbonate solution, and the acid and the anilide were separated as above. The acid weighed 0·7 g. (47% of theory) and the anilide 0·4 g. (30·8% of theory), the total yield being about 77·8%.

p-*Methoxy-dibromocinnamanilide.*—The cinnamanilide (m.p. 140°) decolorised both Baeyer's reagent and bromine water. A saturated solution of this in alcohol was made and treated with bromine (two atoms) in alcoho or water: the mixture was thoroughly shaken and kept for about four hours, when a white solid had separated out, which was filtered off and recrystallised from dilute alcohol. It came out in white needles, melting at 180°. (Bromine, Found: 39·08%; $C_{16}H_{14}O_2NBr_2$ requires 38·83%.)

With a Trace of One Base.—Condensations were carried out with a trace of pyridine at diffeent temperatues and for different periods of time. Condensations were also conducted with traces of piperidine, lutidine and triethanolamine respectively : the best yields were found when piperidine in a trace was used. The results are all given in a table below (Table I).

TABLE I

Base	Temperature	Time of heating	Yields %		
			Acid	Anilide	Total
None	Water-bath	5 hours	60	0	60
„	„	8 hours	47	23	70
Pyridine-piperidine ..	50°–60°	1 hour	47	30·8	77·8
Pyridine-trace	Room	1 week	0	0	0
	60°–70°	12 hours	26·7	23	49·7
	Water-bath	5 „	20	46	66
	„	8 „	0	61·5	61·5
	110°–20°	1·5 „	0	77	77
Piperidine-trace	Room	1 week	20	8	28
	Water-bath	5 hrs. or 8	0	92·3	92·3
	110°–20°	1·5 „	0	92·3	92·3
Lutidine-trace	Water-bath	5 „	0	69·2	69·2
	„	8 „	0	84·6	84·6
Triethanolamine-trace ..	„	8 „	13·3	38·4	51·7

Condensation with m-*Methoxybenzaldehyde.*

Without any Base. (m-*Methoxybenzylidine-malonanilic Acid and* m-*Methoxy-cinnamanilide.*).—1·4 g. of the aldehyde and 1·8 g. of the malonanilic acid (1:1 mol.) were heated together on a water-bath for five hours. The reactants soon melted to a clear liquid, a slight effervescence was noticed and

there was a copious evolution of water vapour. After three hours the liquid began to set to a solid green mass. At the end it was extracted as usual. The acid, recrystallised from aqueous alcohol, came out as colourless needles, melting at 182° (dec.), and decolorising Baeyer's reagent and bromine water. (N, Found : 4·86%; $C_{17}H_{14}O_4N$ requires 4·73%.) The acid gave a silver salt, which starts decomposing at 210° and completely decomposes with frothing at 220° (Ag, Found : 26·72%; $C_{17}H_{13}O_4NAg$ requires 26·79%). The *m*-methoxy-cinnamanilide, recrystallised (dilute alcohol), melted at 107° and also decolorised Baeyer's reagent and bromine water (N, Found: 5·3%; $C_{16}H_{14}O_2N$ requires 5·5%). The yields of the acid and the anilide were 1·2 and 0·8 g. respectively. On longer heating the acid diminished, and the anilide increased, the total also being slightly greater. (*Vide* Table II.)

With Bases.—Condensations were carried out as above in the presence of pyridine-piperidine mixture (Ray's method) and of a trace of pyridine, piperidine, lutidine and triethanolamine respectively. The highest yields were obtained with a trace of pyridine. The detailed results are set in Table II below:—

TABLE II

Base	Temperature	Time of heating	Yields %		
			Acid	Anilide	Total
None	Water-bath	5 hours	40	30·8	70·8
	„	8 „	26·7	53·8	80·5
Pyridine-piperidine ..	60°–70°	1 hour	40	23	63
Pyridine-trace ..	Water-bath	5 hours	0	77·5	77·5
	„	8 „	0	92·3	92·3
	120°	2 „	0	77·5	77·5
Lutidine-trace ..	Water-bath	8 „	0	38·4	38·4
Triethanolamine-trace ..	„	8 „	13·3	30·8	44·1

Condensation with o-*Methoxybenzaldehyde.*

Without a Base. (o-*Methoxybenzylidene-malonanilic Acid and o-Methoxy-cinnamanilide*).—Condensations were carried out as before. A greenish solid product came out which by the usual treatment gave (i) the acid, colourless flat crystals, melting at 228°, which was the acid (N, Found: 4·86%; $C_{17}H_{14}O_4N$ requires 4·73%); (ii) the anilide came out as colourless needles, melting at 164° (N, Found: 5·72%; $C_{16}H_{14}O_2N$ requires 5·55%). Both the

products were crystallised from dilute alcohol, and decolorised bromine water as well as Baeyer's reagent. As can be seen from Table III below, the total yield was good, 70%, which increased to about 74% on longer heating.

With Base.—With pyridine-piperidine, the yield was about the same, 63%, in one hour's heating, but on account of the shorter time of heating, the acid was about twice as much as the anilide.

A trace of pyridine or of piperidine gave still better yields, up to about 85%, though requiring longer heating-time. Lutidine and triethanolamine, in a trace, gave lesser yields even with full eight hours' heating.

TABLE III

Base	Temperature	Time of heating	Yields %		
			Acid	Anilide	Total
None	Water-bath	5 hours	47	23	70
	„	8 „	26·7	46·1	73·8
Pyridine-piperidine ..	60–70°	1 hour	40	23	63
Pyridine-trace	60–70°	12 hours	6·8	61·5	68·3
	Water-bath	8 „	0	84·6	84·6
	110–20°	2·5 „	0	77	77
Piperidine-trace	Water-bath	8 „	0	77	77
	110–20°	2·5 „	0	84·6	84·6
Lutidine-trace	Water-bath	8 „	0	38·4	38·4
Triethanolamine-trace ..	„	8 „	13·3	38·4	51·7

The following table (Table IV) gives consolidated figures of the maximum yields, of the acids, of the anilides and of the total, obtained respectively from the three hydroxy-benzaldehydes and the three methylated benzaldehydes. (The former figures are taken from the results already published[4].)

In every case the maximum yield of the acid was obtained when no base or any other condensing agent was used, and so also the highest anilide-yield was obtained when only pyridine or sometimes piperidine was used in a trace. Except in the case of *m*-hydroxybenzylidene-malonanilic acid, the yields are decidedly superior when the hydroxy-group is changed to the methoxy.

TABLE IV

Aldehyde	Acid	Anilide	Total
o-Hydroxy-benzaldehyde	0·0	37·8	37·8
o-Methoxy- „ ..	47·0	84·6	84·6
m-Hydroxy- „	51·8	79·6	79·6
m-Methoxy- „	40·0	92·3	92·3
p-Hydroxy- „	18·0	79·6	79·6
p-Methoxy- „ ..	60·0	92·3	92·3

The authors' thanks are due to the Government of the United Provinces for the award of a Research Scholarship to one of us (P.I.) which has enabled him to take part in this work.

REFERENCES

1. Pandya and Sodhi .. *Proc. Ind. Acad. Sci.*, (A), 1938, **7**, 381, and preceding parts of the series ; also Pandya and Sodhi, (A), 1939, **9**, 511.
2. ———, and Vahidy .. *Ibid.*, A, 1936, **4**, 134 ; 1937, **5**, 437.
3. ———— .. *Ibid.*, A, 1935, **2**, 402.
4. Ittyerah and Pandya .. *Ibid.*, A, 1941, **13**, 119.
5. ———— .. *Ibid.*, A, 1941, **13**, 122.
6. Khan, Kurien and Pandya .. *Ibid.*, 1935, **1**, 440 ; Pandya and Vahidy, *Ibid.*, 1936, **4**, 141, 144.
7. Mehra and Pandya .. *Ibid.*, 1938, **7**, 369.
8. Ahluwalia, Haq and Ray .. *J.C.S.*, 1931, 2059.

351-41.—Printed at The Bangalore Press, Bangalore City, by G. Srinivasa Rao, Superintendent and Published by The Indian Academy of Sciences, Bangalore

ERRATA

Vol. XIII, No. 4, *April* 1941.

Page 300, line 8 from the bottom, *instead of* 409 Kg./m.^{3}, *read* 401 Kg./m.^{3}

„ 311, equation (3) *should read*

$$k = 0{\cdot}15\left(\frac{R}{1000}\right)^{1{\cdot}5} + 0{\cdot}04 \qquad (3)$$

„ 311, line 10, 0·4 *should read* 0·04.

„ 311, line 14, 0·2 *should read* 0·02.

„ 313, Table II, heading of column 6, Kg. m.^{3} *should read* Kg./m.^{3}

„ 313, item 20, column 6, 410·5 *should read* 400·5.

„ 315, under References,

line 1, " un " *should read* " und ".

line 2, " 1933 " *should read* " 1923 ".

line 7, " Mitzl d. Fach Aus Holztrasen " *should read* " Mittl. d. Fach. Aus Holzfragen ".